LAPPEENRANTA UNIVERSITY OF TECHNOLOGY
LUT School of Engineering Science
Degree Program of Chemical Engineering

Master's Thesis
2017

Daria Bogatenko

ANALYSIS OF VOLUMETRIC MASS TRANSFER AND OVERALL GAS HOLD-UP IN GAS-LIQUID REACTORS RELATING TO GAS FERMENTATION

Examiner: Professor Tuomas Koiranen
Supervisor: Dmitry Gradov

ABSTRACT

Lappeenranta University of Technology
LUT School of Engineering Science
Degree Program of Chemical Engineering

Daria Bogatenko

Analysis of volumetric mass transfer and overall gas hold-up in gas-liquid reactors relating to gas fermentation

Master's Thesis

2017

67 pages, 44 figures, 4 tables and 5 appendixes

Examiner: Professor Tuomas Koiranen
Supervisor: Dmitry Gradov

Key words: aerobic fermentation, multiphase flow, mixing, gas-liquid reactor, mass transfer, gas hold-up, flooding, bubble size.

The concept of gas fermentation is of great interest nowadays. Flue gases of manufactories can be utilized as a feedstock for production of biofuels, such as ethanol. The process of fermentation involves gas-liquid mixing that is why the specific parameters of these systems were studied.

Volumetric mass transfer, gas hold-up, flooding, bubble size and other parameters make significant effect on gas-liquid mixing system. Also, these parameters are deeply connected to each other and all together form system that provide mixing efficiency. Gas hold-up is in almost linear relation with gas flow rate. However, if bubbles are not well dispersed the increase of gas flow rate can result in decrease of gas-liquid mass transfer.

The thesis was aimed at the comparison of gas-liquid mixing parameters for three reactors at laboratory scale. The conventional air-lift and stirred tank reactors were compared with new reactor OKTOP designed by Outotec company.

Based on achieved experimental results coefficients for the equations of mass transfer, power draw and gas hold-up were determined for all the reactors in studied solutions.

TABLE OF CONTENTS

Acronyms

ALR	Air lift reactor
CMC	Sodium carboxyl methyl cellulose
CTD	Contact time distribution
GHG	Greenhouse gas
MCR	Modular compact rheometer
RSB	Roundtable on Sustainable Biomaterials
RTD	Residence time distribution
STR	Stirred tank reactor

Nomenclature

A	tank cross-sectional area	m^2
a	interfacial area	m^2
C^*	concentration of solute gas in liquid at interface	mol/m^3
C_L	saturation concentration of solute gas in bulk liquid	mol/m^3
C_n	constant, which depends on viscosity	-
$C(t)$	concentration at time moment t	mol/m^3
D	impeller diameter	m
D_L	diffusivity of liquid	m^2/s
d_b	Sauter mean diameter	m
d_0	gas channel diameter	m
E	energy dissipation per unit volume of fluid in reactor	W/m^3
$E(t)$	residence time distribution function	-
$E^*(t)$	bubble residence time distribution function	-
Fl	gas flow number	-
Fr_I	Froude number	-
g	acceleration of gravity	m/s^2
K	consistency index	$Pa \cdot s^n$
K'	constant	-
K_b	bubble regime criterion	-
k_l	mass transfer coefficient	m/s
M	torque	N·m
N	impeller speed	rps
N_{g-l}	overall mass transfer rate of gas through liquid	$mol/m^3 \cdot s$
N_Q	empirical pumping number	-
n	flow index	-
n_0	amount of material at the beginig of the process	mol
Δn	amount of material exiting the reactor	mol
P_0	impeller power draw in non-aerated mixing	W
P_g	impeller power draw in aerated mixing	W
$P_{gas\ supply}$	power of gas supply	W
P_{imp}	power draw of impeller	W
P_{tot}	overall power draw (impeller and gas supply)	W
Δp_{gd}	pressure loss in gas distributor holes	Pa
Δp_{sp}	the static pressure of the gas-liquid mixture	Pa
Q	volumetric gas flow rate	m^3/s
Q_L	liquid mass flow rate	kg/s
S_g	free sectional area with gas fraction	m^2
S_{g-l}	free sectional area with gas-liquid fraction	m^2
Δt	time interval which material spends in the reactor	s
$TIPS$	tip speed	m/s
U_g	superficial gas velocity	m/s
u_g	real gas velocity	m/s
V	liquid volume	m^3
V_d	dead volume	m^3
V_g	gas volume	m^3
V_{g-l}	volume of gas-liquid mixture	m^3

v	flue gas volumetric flow rate	m^3/s
v_g	reduced gas velocity	m/s
β	exponent	-
γ'	average shear rate	1/s
δ	empirical coefficient	-
$\bar{\theta}_h$	average residence time	s
μ	viscosity	Pa·s
μ_{app}	apparent viscosity	Pa·s
ρ_g	density of gas	kg/m^3
ρ_l	density of liquid	kg/m^3
σ	surface tension	N/m
τ_c	circulation time	s
τ_g	gas contact time	s
ϕ	gas hold-up	%

LITERATURE REVIEW

1. Introduction

Emissions of industrial gases to atmosphere lead to various side effects, such as, for example, greenhouse effect. Reduction of these emissions by means of utilization of flue gases is of crucial importance. However, not only the reduction of wastes to atmosphere is of great interest, but also production of biofuels (for example ethanol).

Mixing is a process of turning heterogeneous system into homogeneous one. Examples of mixing application in industry are dissolution of ammonia in water for production of ammonium hydroxide, gas fermentation processes, etc. Selection of optimal reactor of mixing is dictated by many factors such as volumetric mass transfer, gas hold-up, energy consumption and others.

Volumetric mass transfer is an important characteristic of multiphase mixing processes. It defines kinetic of molecular diffusion.

Outotec company designed OKTOP reactor for application in hydrometallurgy. Within FERMATRA project OKTOP is studied on its suitability for aerobic fermentation and compared against conventional reactors. The purpose of this work is the experimental study of multiphase mixing in three gas-liquid contactors, namely OKTOP, air-lift reactor (ALR) and flat-bottom stirred tank reactor (STR) by measuring global parameters characterizing oxygen mass transfer into liquid media. [1]

1.1. Fermentation process

Fermentation is a biochemical processing of organic materials by using microorganisms. The term was earlier referred to anaerobic processes only, but now it is used more generally and includes aerobic processes also. [2]

Fermentation process has found wide application in food, medicine and alcohol production a long time ago. An example of fermentation is a process of glucose conversion into ethanol and CO_2 with yeast as catalysts [2]:

$$C_6H_{12}O_6 \xrightarrow{ferments} CH_3CH_2OH + CO_2 \quad (1)$$

Main product of fermentation process are cells or any useful metabolite. All operations have to be carried out under sterile conditions to prevent contamination of a culture. Cells grow and multiply in reactor by using the nutrient medium. [2]

There are two basic ways of fermentation. In periodical fermentation (closed system), all reagents are loaded before beginning of the process (batch process). When required quantity of product has formed, the process is stopped. Continuous cultivation (open system) is an operation where nutrients are supplied to the solution while dead cells and their products of living are removed. [2]

1.1.1. Anaerobic fermentation

Basically, anaerobic fermentation process is going without oxygen supply. During the technological process, complex chemical organic compounds decompose to CO_2 and CH_4. [3]

Living in the environment where the oxygen is limited, prokaryotes have to get energy by using anaerobic breathing. There are many types of microorganisms suitable for anaerobic fermentation. Selection of microorganisms is based on the analysis of the climate conditions. For example, thermophiles are active at 45 - 70 °C, while mesophylls prefer temperature range of 20 - 40 °C. Thermophilic mode requires high energy supply, therefore mesophilic regime is preferable. The most efficient bioreactors are working in thermophilic mode 43 - 52 °C. [3]

Optimal conditions in living media are important for the anaerobic fermentation process. There are many parameters that have to be controlled such as temperature, keeping of anaerobic conditions, nutrient concentration, pH, the concentration of toxic substances. [3]

1.1.2. Aerobic fermentation

Aerobic fermentation or aerobic respiration is a process taking place with the presence of oxygen. Microorganisms use oxygen for growth and reproduction [4]. The example of aerobic respiration is [5]:

$$\text{glucose} + \text{oxygen} \rightarrow \text{carbon dioxide} + \text{water (+energy)} \tag{2}$$

Aerobic fermentation is a usual process for animal and plant cells. A big part of the reactions is taking place in mitochondria. Ferments affect the reactions as catalysts. Cells prefer using oxygen because it requires less energy. [4]

This way of using energy from aerobic fermentation is widely known in biology and microbiology. Nowadays, aerobic fermentation found its application in acid vinegar, beer, wine, cheese, milk and other production. Also, aerobic fermentation is used in water treatment. [4]

1.1.2.1. Gas fermentation

The process of gas fermentation is natural for the microorganisms which grow using hydrothermal vents gases. This could be the oldest process of the ethanol production. Bacteria C. ljungdahlii and C. autoethanogenum are mainly used in gas fermentation process. [6] LanzaTech company has patented some bacteria of acetogens family. [7]

The energy output of carbon monoxide is higher than of carbon dioxide and hydrogen, but still, the biggest part of the carbon in the reaction is CO_2. [6]

$$6CO + 3H_2O \xrightarrow{ferments} CH_3CH_2OH + 4CO_2 \left(\Delta G^0 = -224.90 \frac{kJ}{mol}\right) \tag{3}$$

As a result, carbon monoxide fermentation process produces CO_2. H_2 usage can lower CO_2 production, but at the expense of Gibbs energy decreased [6]:

$$5CO + H_2 + 2H_2O \xrightarrow{ferments} CH_3CH_2OH + 3CO_2 \left(\Delta G^0 = -204.80 \frac{kJ}{mol}\right) \tag{4}$$

$$4CO + 2H_2 + H_2O \xrightarrow{ferments} CH_3CH_2OH + 2CO_2 \left(\Delta G^0 = -184{,}70 \frac{kJ}{mol}\right) \tag{5}$$

$$3CO + 3H_2 \xrightarrow{ferments} CH_3CH_2OH + CO_2 \left(\Delta G^0 = -164{,}60 \frac{kJ}{mol}\right) \tag{6}$$

By increasing amount of H_2 it is possible to obtain ethanol without CO_2 emission [6]:

$$2CO + 4H_2 \xrightarrow{ferments} CH_3CH_2OH + H_2O \ \left(\Delta G^0 = -144{,}50\frac{kJ}{mol}\right) \tag{7}$$

Also, CO2 is used in gas fermentation in order to achieve ethanol and water [6]:

$$2CO_2 + 6H_2 \xrightarrow{ferments} CH_3CH_2OH + 3H_2O \ \left(\Delta G^0 = -104{,}30\frac{kJ}{mol}\right) \tag{8}$$

This is the conventional way of the gas fermentation technology that is used by different companies all over the world. The main purpose is production of ethanol as a source of renewable energy s in the nearest future. [6]

*1.1.2.2.*Preconditions for using gas fermentation

Solution of global ecological problems takes one of the most important parts of human's life nowadays. Due to rapid growth of industry, a number of sources of carbon dioxide emission significantly has risen. [7]

Industrial gases, such as carbon dioxide and carbon monoxide emitted to atmosphere, can be used for producing different types of organic materials applicable to food, medical, chemical and fuel industry. [7] Application of gas fermentation can reduce harmful emissions to atmosphere, expand the scope of production and increase revenues. [1] Thus, usage of gas fermentation can reduce the impact of greenhouse gas (GHG) to climate. [8]

The fermentation process was of great interest for the commercial scale due to high product selectivity, efficiency and other advantages. INEOS Bio, Coskata and LanzaTech developed demonstration and pilot plants of fermentation process [8]:

1. Coskata technology is American methanol manufacturing company from 2008 to 2015. In 2015, the company originates new Synata Bio, but it has not developed to industrial scale yet. [8]
2. INEOS Bio is a bioenergy company aiming on renewable energy and biofuels produced from low price carbon compounds. The company is novel, but nowadays, due to the

rapid development, it is one of the leading chemical producing companies with annual turnover is around forty billion dollars. [9]

3. LanzaTech has partners in China, USA, UK, Sweden and other countries. They use gas fermentation to refine off-gases coming from steel mill. The company has patented microbes for the transformation of metallurgy gaseous wastes to biofuels. [8]

*1.1.2.3.*Industrial application of gas fermentation

Gas fermentation opens a new way of utilizing industrial gaseous wastes. The base of this process is chemical conversion of off-gases to biofuels, food and chemicals by microorganisms. These microbes act as catalysts of chemical reactions for producing ethanol, acetic acid, methane and others. [10] In Figure 1 a block scheme is presented describing of the gas fermentation process. [7]

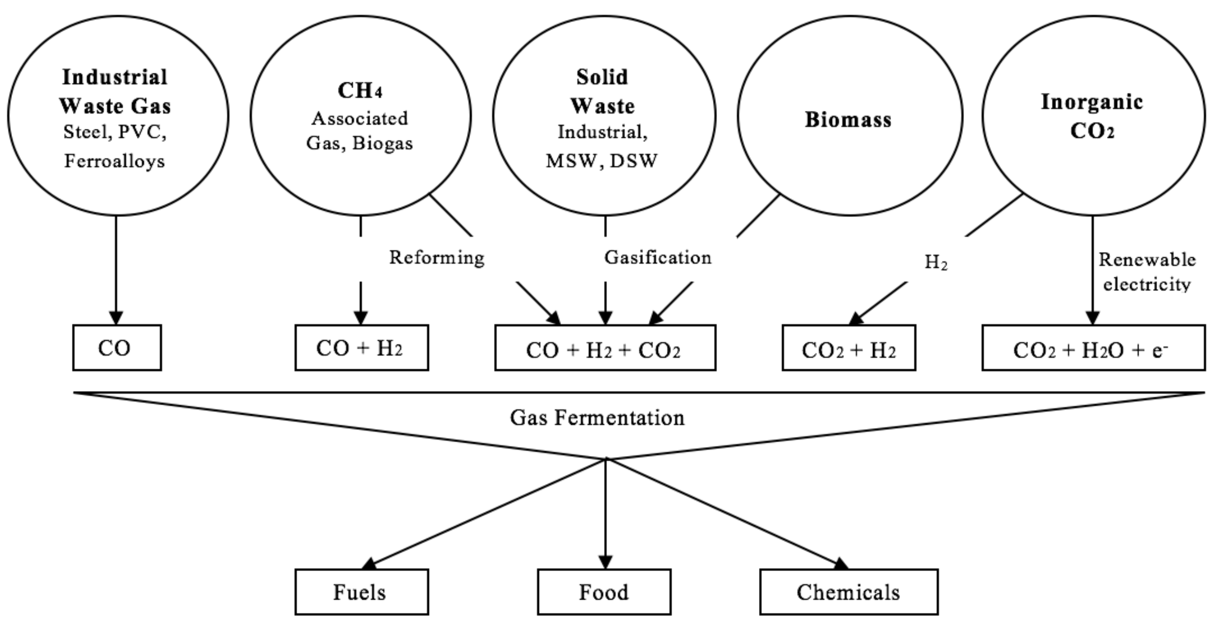

Figure 1. Description of the gas fermentation process. [7]

Gas fermentation can be carried out at various scales [7]:

1. 0.1 - 0.5 mL (Petri dish)
2. ≤ 0.5 L (chemical flask)
3. ≤ 5 - 30 L (laboratory scale mixing reactors)
4. ≥ 100 L (industrial bioreactors)

Commonly, industrial application of fermentation process technology takes place in aerated reactors called fermenters or bioreactors. [7]

Typically, a fermenter is made of stainless steel, as the material does not corrode and it produces no toxic compounds. All the equipment, materials and gases used in fermentation must be sterilized with steam under high pressure. Reactor interior should be smooth and polished with no cracks or indentations where bacteria may collect. [7]

The emissions from manufactories can be compared with gases of hydrothermal vents that is the reason why cells can use industrial waste gases for growing. Commonly used gases in fermentation process are listed below [7]:

1. Carbon dioxide
2. Carbon monoxide
3. Hydrogen
4. Methane
5. Hydrogen sulfide

In Figure 2 the scheme of gas fermentation process is presented.

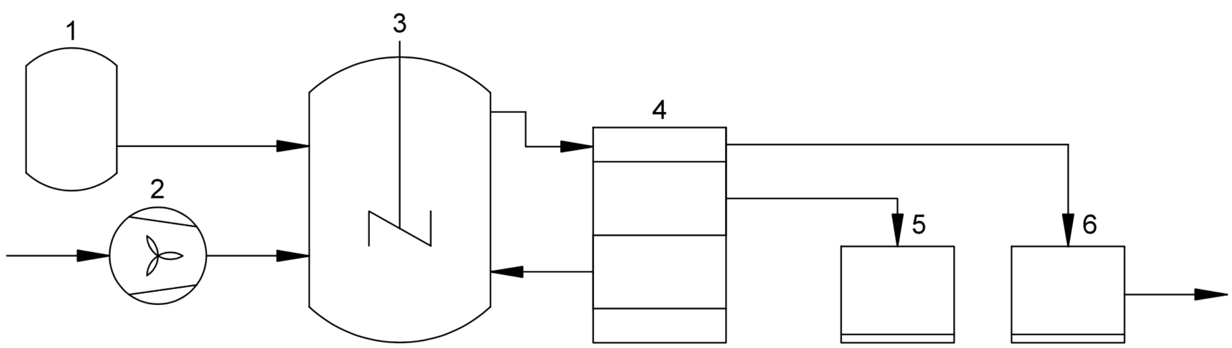

Figure 2. Gas fermentation process.
1 - growth tank; 2 - gas blower; 3 - fermenter; 4 - separator; 5 - refinery collector; 6 - product collector. [7]

The first step of the process is cells (microbes) cultivation in favorable conditions in growth tank 1. Cells need nutrition for growth. When population of cells has grown enough they are transported into fermenter (bioreactor). [7]

Gases are supplied into fermenter through gas blower 2. After bioreactor solution goes to separation column 4 where valuable compound is separated, while microorganisms are returned back into the fermenter. By-product is moved to refinery stage and ready product is collected in tank 6. [7]

2. Reactors for gas fermentation

Effective gas-liquid mixing has to keep mass transfer high at minimum energy supply (chemical reaction, absorption, etc.). [11] Equipment selection depends on the following parameters: fluids properties, reaction rate, operational conditions, flow parameters and costs. [12]

2.1. Bubble column

Bubble column found its usage as multiphase reactors in different types of chemical industry (petrochemical, biochemical). [13] In Figure 3 different types of bubble column are shown.

Main advantages of bubble column are [13]:

1. High mass and heat transfer rate
2. Low maintenance and operating costs
3. Bubble column are very compact reactors
4. Ease of the catalysts usage

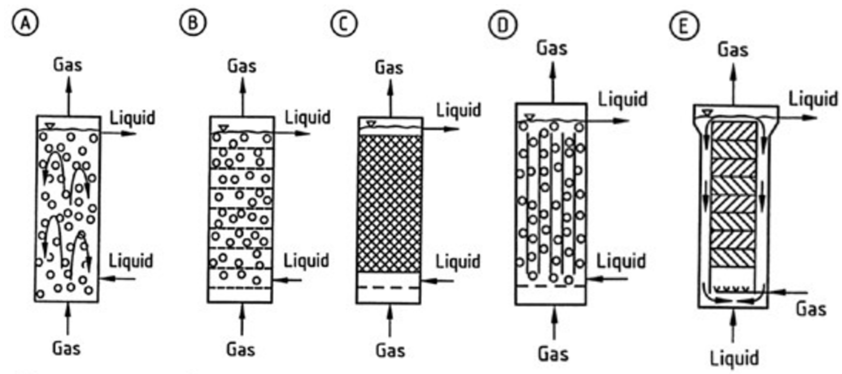

Figure 3. Types of bubble column.

A - simple bubble column; B - cascade bubble column with sieve trays; C - packed bubble column; D - multi shaft bubble column; E - bubble column with static mixers. [14]

Typically, bubble column reactor is of cylindrical form with gas supply mounted in bottom. In chemical and biochemical industry, the reactors are mostly used in fermentation, chlorination, polymerization, water treatment, hydrogenation etc. Bubble column is widely used in production of biofuels. [14]

Also, bubble column is used for scientific research purposes to study fluid and bubble dynamics, gas hold-up, heat and mass transfer. [14]

2.2. Air-lift reactor

ALR and bubble column have different constructive features. For bubble column gas flow is not foamed and the mixing is random. ALR has two different channels for down and up flow. Due to such construction, ALR has circular process that intensify of the reactor's work. [15] Different types of ALR are schematically shown in Figure 4.

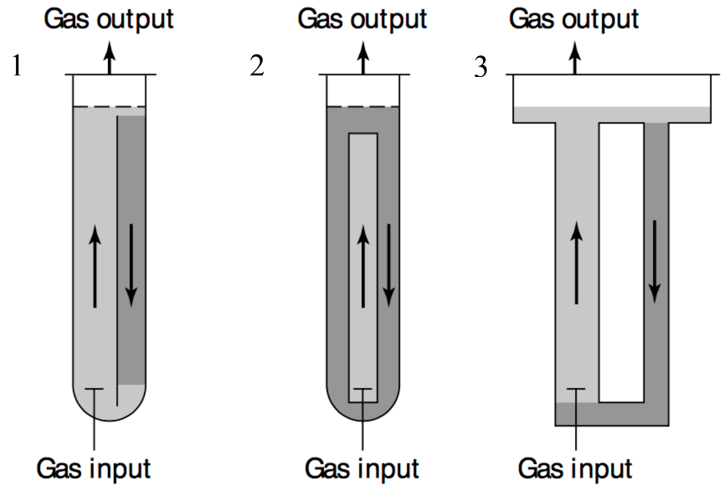

Figure 4. Types of air-lift reactors.

1 - internal-loop split ALR; 2 - internal-loop concentric tube reactor; 3 - external-loop ALR. [15]

ALRs can be schematically divided into four sections where the flow characteristics are different [15]:

1. Riser is the part where gas flow is supplied from the bottom and the motion of the gas-liquid phase is directed upward
2. Downcomer part is parallel to the previous section where gas-liquid recirculation is achieved due to pressure gradient and density difference between the parts
3. Base part of ALR is designed to affects fluids velocity, gas hold-up and solid phase flow
4. Gas separator part includes riser and downcomer. Its construction minimizes gas recirculation through the downcomer. In Figure 5 it is possible to see different types of gas separators

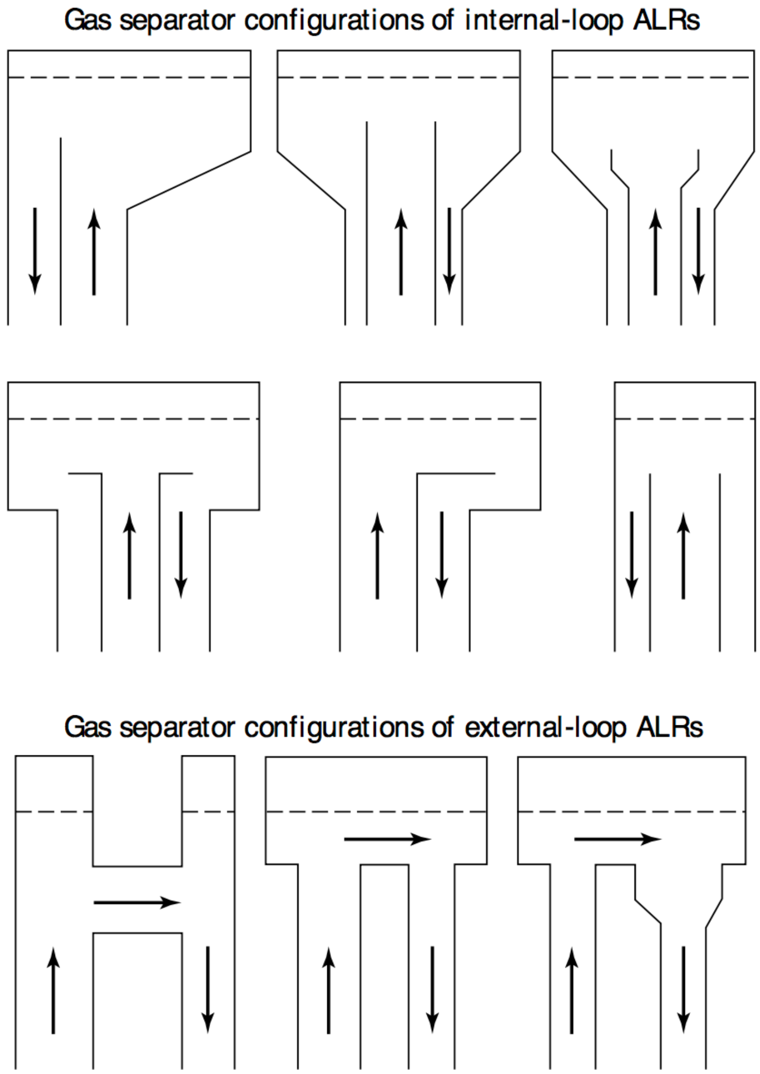

Figure 5. Gas separator types. [15]

Advantages of ALR [16]:

1. Absence of moving parts results in simple design that put risks, maintenance and operational costs to minimum
2. Cleaning and sterilization procedure is easy
3. High mass and heat transfer rate

ALR is used as a fermenter in biochemical industry for cultivation of animals and plants cells, wastewater treatment, treatment of gases containing hazardous compounds. [15]

2.3. *Stirred tank reactor*

Stirred tank reactor is a vessel with an agitator. A typical STR configuration is shown in Figure 6.

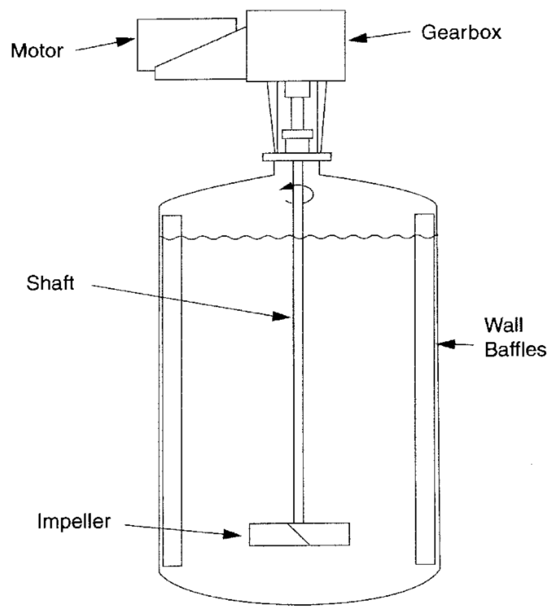

Figure 6. STR with top-entering agitator. [12]

STR with top-entering agitator is a conventional reactor for mixing processes. STRs can be divided into different types according to geometry of impeller, application, flow and sphere of its application. For example, axial flow impellers can be effectively used for solids suspension and liquid blending. In Table 1 impeller types and classes are presented. [12]

Table 1. Classes and types of impellers. [12]

Radial flow	Flat-blade impeller
	Disk turbine (Rushton)
	Hollow-blade turbine (Smith)
Axial flow	Hydrofoils
	Pitched blade turbine
	Propeller
Special	Retreat curve impeller
	Sweptback impeller
	Glass-lined turbines
	Spring impeller
Up/down	Disks
	Circles
	Plate
High shear	Cowles
	Disk
	Bar
	Pointed blade impeller

There are many types and configurations that are used in various applications and in different scales. In Figure 7 one may see some examples of different agitated tanks. [12]

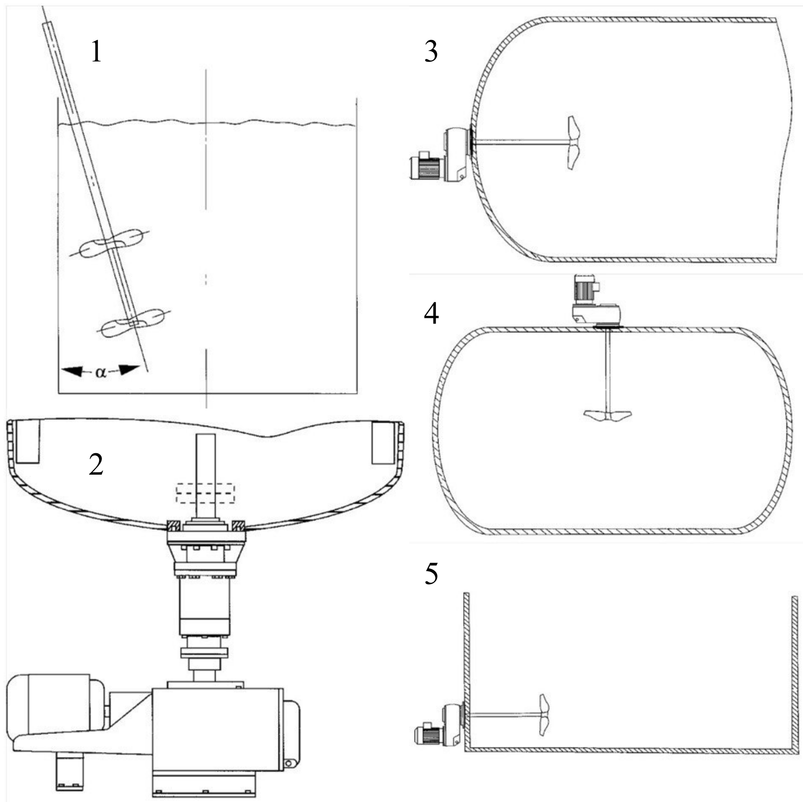

Figure 7. Types of stirred tank reactors.

1 - small-scale angular top-entering mixer; 2 - bottom-entering agitator; 3 - cylindrical horizontal vessel with side-entering mixer; 4 - the cylindrical horizontal vessel with top-entering mixer; 5 - large-scale side entering mixer. [12]

Advantages of STR [17, 18]:

1. Stable operation
2. High-temperature stability
3. High mass and heat transfer rate
4. Easily to-control process

2.4. Pipe mixing

Basically, mixing process takes place in a vessel or tank, but it also can be organized in pipes. Pipe mixing has low energy consumption while mixing rate is high. Therefore, pipe mixing is used for mixing of rapidly decomposed substances. Pipe mixers such as the static mixer, tee, impinging jet, spray nozzle, in-line mechanical, empty pipe or duct, elbows are used in industry. [12]

Advantages of static mixers [12]:

1. Compact equipment
2. Low maintenance and operating cost
3. Low energy consumption only for pumping system
4. Fast mixing process
5. Self-cleaning, cleaning ease (disposable or interchangeable mixers)

2.4.1. Static (motionless) mixers

This type of mixing system does not need energy for mixing due to the absence of the moving parts that consume energy. Beginning of the technology can be found in 1950s. The first commercial company, started the development of the motionless mixers, was Kenics. Nowadays, large number of companies produce static mixers. [12]

Few examples of motionless elements are presented in Figure 8.

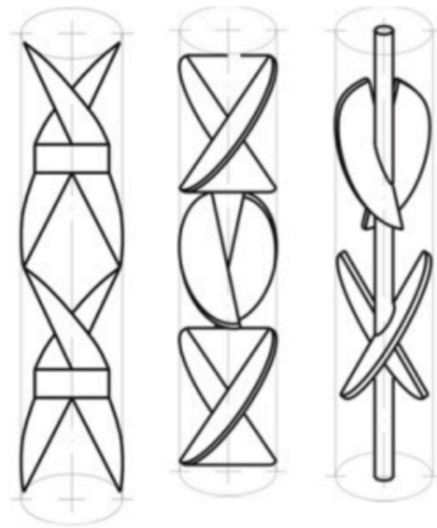

Figure 8. Examples of motionless elements. [19]

Static mixers are effective in gas-liquid mixing. Motionless mixers are usually used in turbulent flows applications. In industry, they are used in extraction, absorption, heat transfer etc. [12]

3. Gas-liquid mixing

3.1. Bubble size

Gas-liquid flow happens with appearance of bubbles, slugs, droplets, ligaments, liquid films and others. Gas-liquid interaction is affected by many forces such as drag, lift etc. and it is accompanied with breakage and coalescence phenomena leading to bubble size distribution change. Flow regimes of gas in liquid are shown in Figure 9. [20]

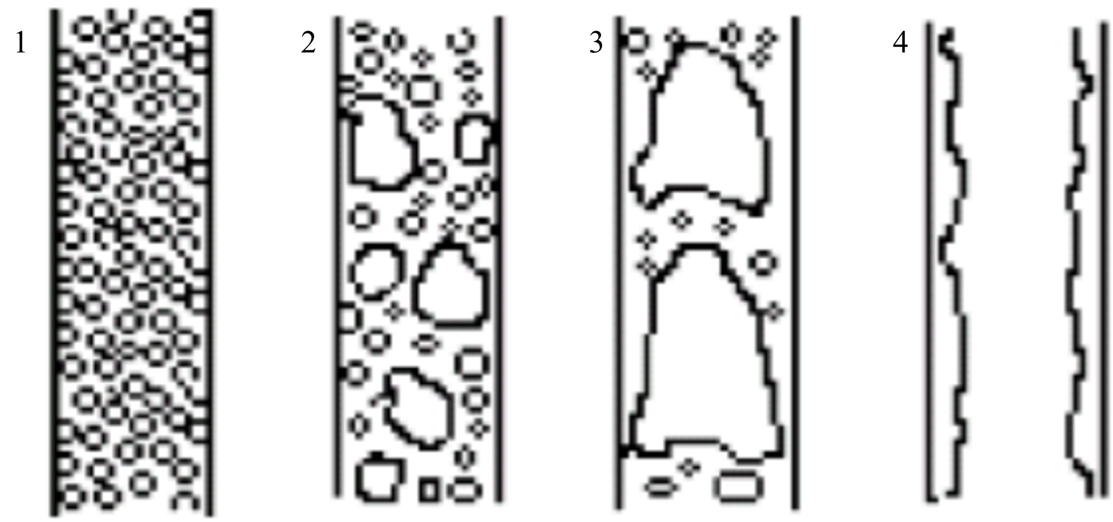

Figure 9. Gas-dispersion into liquid.

1 - homogeneous flow of bubbles; 2 - heterogeneous churn flow; 3 - slug flow; 4 - annual flow. [20]

Gas dispersion into liquid produces bubbles of spherical, ellipsoidal, and more complicated shapes. Flow regime depends on volumetric power draw and gas flow-rate. [20]

3.1.1. Main correlations/equations

3.1.1.1. Air-lift reactor

When gas dispersion is in bubble regime (perfect or imperfect bubbly) bubble size can be determined by diameter of channels in gas sparger, liquid properties and pressure (below 106 Pa pressure has insignificant effect). The following expression can be used to calculate bubble Sauter mean diameter [21]:

$$d_b = d_0 \sqrt[3]{\frac{d_0 \sigma}{(\rho_l - \rho_g) g}}, \qquad (9)$$

where d_b - Sauter mean diameter, m; d_0 - gas channel diameter, m, σ - surface tension, N/m; ρ_l and ρ_g - density of liquid and gas respectively, kg/m^3; g - acceleration of gravity, m/s^2.

3.1.1.2. Stirred tank reactor

Relation between spherical bubble size, gas hold-up and interfacial area at the assumption of constant bubble size is [22]:

$$d_b = \frac{6\varphi V}{a}, \quad (10)$$

where ϕ - gas hold-up, fraction; a - interfacial area, m^2.

The correlation for Sauter mean bubble diameter was developed by Calderbank based on balance between dynamic and interfacial forces during breakup (1956a; 1956b; 1958) [22]:

$$d_{SM} = 4.15\left[\frac{(P_g/V)^{0.4}\rho_l^{0.2}}{\sigma^{0.6}}\right]^{-1}(\varphi)^{0.5} + 0.09 \text{ cm}, \quad (11)$$

where P_g - impeller power draw in aerated mixing, W; V - liquid volume, m^3; the $[(P_g/V)^{0.4}\rho_l^{0.2}]/\sigma^{0.6}$ is in centimeters. This equation is applicable to flows of low Reynolds number and vessel sizes below 100 L. [22]

3.1.2. Measurement methods

Experimental techniques for bubble size distribution measurement are important. As a result, plenty of big numbers of different measurements of bubble size were developed. Optical methods are preferable since they do not affect fluids properties and hydrodynamics. Fast breakage and collision phenomena impose certain demands upon measurement technique. [20]

There are main types of bubble size measurements methods [20]:

1. Optical
2. Acoustical
3. Photographic
4. Bubble trap

Early measurement methods did not include optical and were based on photography, acoustic and bubble traps (mechanical). However, as a result, bubble trap and acoustic methods were found to be of low accuracy. For example, bubble trap technique has a time delay, and it is not suitable for bubble size measurement because the measurement does not count for bubble dissolution. The photographic method has been developed significantly. [23]

4.1.2.1.Photographic method

The typical set-up of bubble size distribution (BSD) measurement by photographic method consists of camera and lighting system directed to object of study. Gas flow is controlled by rotameter. In Figure 10, schematic representation of BSD measuring set-up using the photographic method is shown. [23, 24]

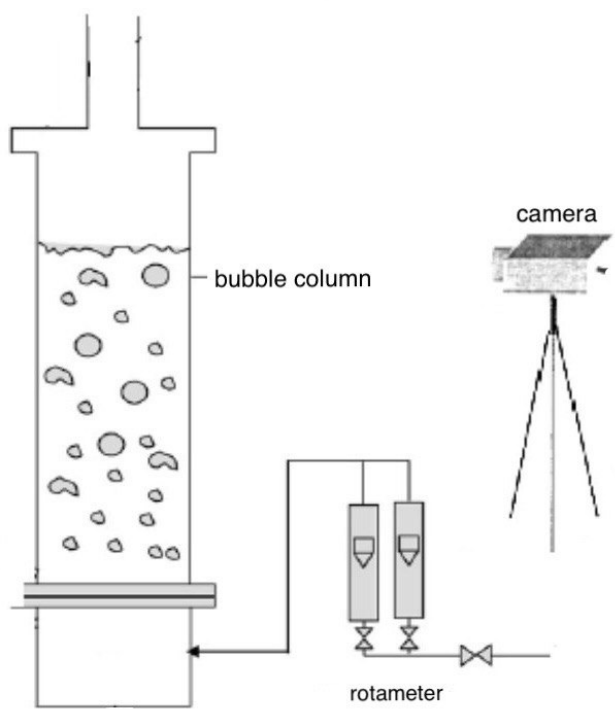

Figure 10. Scheme of photographic method set-up. [23]

Disadvantage of this method is analysis of experimental data. It can be solved by using complicated software for data analysis. However, due to rapid development of the technology the problem is reduced to minimum. [24]

3.2. Gas hold-up (Volume fraction)

Cumulative volume of bubbles in liquid is called gas hold-up. Gas hold-up depends on t physical properties of liquid, bubble break-up, foaming, type and construction of reactor. [25]

Theoretically, a huge can affect positively to the solution as they are used for gas transfer, however high level of gas hold-up can have a side effect. For example, when microorganisms have used all oxygen from bubbles and the bubbles are kept longer in the solution, it may become toxic. [25]

However, gas hold-up is very important parameter connected with hydrodynamics of gas-liquid reactors. Gas hold-up gives information about phases volumetric fraction and, as a result, residence time. Also, gas hold-up and bubble size distribution defines interfacial area. [25]

3.2.1. Main correlations/equations

Gas hold-up is the fraction of gas in gas-liquid mixture, which can be expressed as follows [21]:

$$\varphi = \frac{V_g}{V_{g-l}}, \qquad (12)$$

where V_g - gas volume, m^3; V_{g-l} - volume of gas-liquid mixture, m^3.

*3.2.1.1.*Bubble column

General correlation for the gas hold-up in bubble column is [26]:

$$\varphi = AU_g^B \mu_{app}^C \sigma^D, \qquad (13)$$

where U_g - superficial gas velocity, m/s; μ - viscosity, Pa·s. [26]

3.2.1.2. Stirred tank reactor

Gas hold-up can be found by following equation [22]:

$$\varphi = A\left(\frac{P_g}{V}\right)^B U_g^C \mu_{app}^D \sigma^E \tag{14}$$

3.2.2. Measurement methods

Determination of gas volume fraction can be made using visual methods via measuring of difference between surface levels of non-gassed and gassed solutions.

Usage of ultrasonic radar probe is one of the most exact ways for the gas hold-up detection. Ultrasonic probe is located above liquid surface and it measures the distance to it. But the equipment should be strongly calibrated especially if foams are present.

Slipover technique can be shown as an effective and reliable technique. Gas volume is determined as volume of liquid spilled over. [12]

3.3. Mass transfer

Gas-liquid mass transfer for aerobic fermenters or stirred tank reactors is rate-controlling step. As a result, gas absorption rate becomes important. The liquid k_L and gas k_g side coefficients appear due to the transport description using the film mechanism. Mass transfer of liquid into gas may be disregarded due to low liquid s phase diffusivity. Therefore, mass transfer coefficient k_L is of crucial importance. k_La contains interfacial area a and mass transfer coefficient k_L. [12]

3.3.1. Main correlations/equations

Overall mass transfer rate is expressed as follows [12]:

$$N_{g-l} = k_L aV(C^* - C_L)_{mean} \tag{15}$$

where $N_{g\text{-}l}$ - overall mass transfer rate of gas through liquid, mol/m^3·s; C^* - concentration of solute gas in liquid at interface, mol/m^3; C_L - saturation concentration of solute gas in bulk liquid mol/m^3.

3.3.1.1. Air-lift reactor

The volumetric mass transfer in bubble column can be determined [26]:

$$k_L a = A U_g^B \mu_{app}^C \sigma^D, \tag{16}$$

where μ_{app} - apparent viscosity, Pa·s.

3.3.1.2. Stirred tank reactor

The following correlation generalized and modified by van't Riet for studying how viscosity and surface tension affect mass transfer coefficient [22]:

$$k_L a = A \left(\frac{P_{tot}}{V}\right)^B U_g^C \mu_{app}^D \sigma^E, \tag{17}$$

where P_{tot} - overall power draw (impeller and gas supply), W, that can be calculated using the equation [22]:

$$P_{tot} = P_g + P_{gas\ supply}, \tag{18}$$

where $P_{gas\ supply}$ - power of gas supply, W.

By measuring gas-liquid mass transfer in miljet jelly and glycerol solutions, Yagi and Yoshida in 1975 proposed the correlation for $k_L a$ applicable to Newtonian liquids [22]:

$$\frac{k_L a D^2}{D_L} = A \left(\frac{\rho N D^2}{\mu_{app}}\right)^B \left(\frac{N^2 D}{g}\right)^C \left(\frac{\mu_{app}}{\rho D_L}\right)^D \left(\frac{\mu_{app} U_g}{\sigma}\right)^E \left(\frac{ND}{V_s}\right)^F, \tag{19}$$

where N - impeller speed, rps; D - impeller diameter, m; D_L - diffusivity of liquid, m^2/s.

3.4. Contact time

3.4.1. Liquid circulation time

Bioreactor performance depends on mixing intensity of. For fluctuating environmental conditions study, an important concept is circulation time as, for example, when cell is circulating through the different parts of reactor it can face different condition. Circulation time distribution (CTD*) is an alternative method of characterization of circulation time in stirred vessel. A lot of circulation time equations ca be found in literature, as an example, Middleton (1979) proposed the equation for circulation time quantification in non-aerated systems [12]:

$$\tau_c = 0.5V^{0.5}\frac{1}{N}\left(\frac{T}{D}\right)^3 \qquad (20)$$

3.4.2. Mixing time to residence time distribution

The probability function, describing the time that fluid is in mixed vessel, is residence time distribution. The comparison criterion of different reactors is their difference with ideal models. RTD is an important parameter for the mixing efficiency determination. [12]

The first idea of RTD as a characteristic of chemical reactor was related to MacMullin and Weber. Till 1950 the conception was not intensively used. Professor P.V. Danckwerts (1950) organized main RTD philosophy by the definition of its interests. The other studies were mostly related to his theory. [12]

RTD can be divided into three types [12]:

1. Inlet step function (responses step)
2. In concentration changing time τ_0 ($C_0 \rightarrow C$)
3. Inlet Dirac delta function (pulse responses)

Two types of RTD are shown in Figure 11.

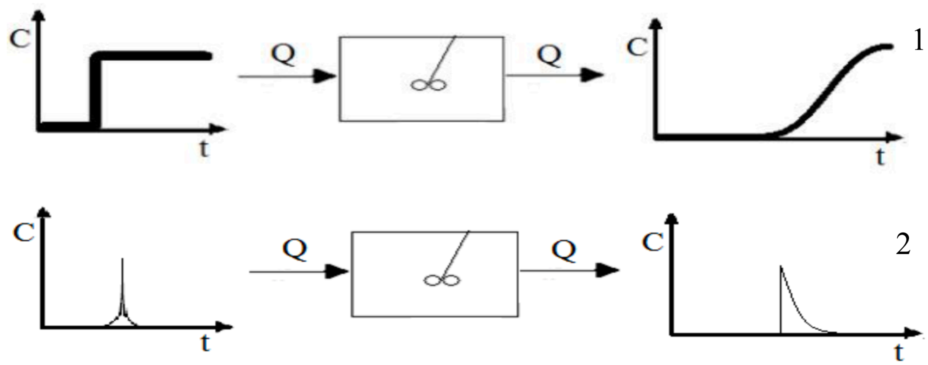

Figure 11. RTD types.

1 - step response; 2 - pulse response. [12]

*3.4.2.1.*Ideal RTD

For the ideal model CSTR is mixed tank where the tracer material is added at once. Accumulation and inflow give outflow as a result. The function of ideal RTD is [12]:

$$E(t) = \frac{C(t)}{\int_0^\infty C(t)} = \frac{e^{-t/\tau}}{\Delta t} \tag{21}$$

E(t) - residence time distribution function.

*3.4.2.2.*Non-ideal RTD

In a real case in CSTR appears dead volume where mixing is not efficient: $V_{tot} = V + V_d$. [12] In Figure 12 it is possible to compare two RTD cases.

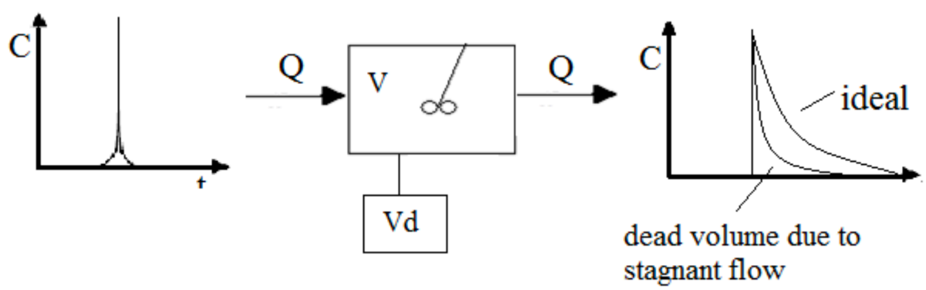

Figure 12. Dead volume appearing in non-ideal RTD [12].

Non-ideal RTD function [12]:

$$E(t) = \frac{e^{-t/\tau} Q}{V_{tot} - V_d}, \quad (22)$$

where V_d - dead volume, m^3.

3.4.3. Gas contact time

Bubble residence time (gas contact time) is the time interval, which bubble spends in a reactor. Bubble size affects contact time. Big bubbles tend to escape reactor faster, while small ones spend stay longer. [27] Gas contact time affects on mass transfer rate, gas hold-up and other important parameters. Average gas residence time defines overall rate of the mixing process it can be determined using the equation [22]:

$$\tau_g = \frac{V_g}{Q}, \quad (23)$$

where τ_g - gas contact time, s; Q –volumetric gas flow rate, m^3/s. [22]

Another way to determine bubble residence time is injection of tracers (inert chemical molecule or atom) to the reaction mixture and measuring of its concentration as the function of time in the effluent gas stream. Tracer is injected at time t = 0. [27]

Amount of tracer at the beginning of the process is n_0. It is injected to reaction mixture in one shot. After measurement, the outlet concentration of tracer its amount is ΔN which is measured at time Δt. Δn the amount of tracer can be determined [27]:

$$\Delta n = C(t) v \Delta t, \quad (24)$$

where v – flue gas volumetric flow rate, m^3/s; Δn - amount of material exiting the reactor, mol; Δt - time interval which material spends in the reactor, s; $C(t)$ - concentration at time moment t, mol/m^3. After the division to n_0 [27]:

$$\frac{\Delta n}{n_0} = \frac{C(t)v}{n_0}\Delta t, \tag{25}$$

where n_0 - amount of material at the beginning of the process, mol; the equation can be transformed [27]:

$$E^*(t) = \frac{C(t)v}{n_0}, \tag{26}$$

where $E^*(t)$ - bubble residence time distribution function. Volumetric flow rate v is usually constant, the function can be [27]:

$$E^*(t) = \frac{C(t)}{\int_0^\infty C(t)dt} \tag{27}$$

3.5. Flooding

The parameter is related only to agitated vessels. Flooding is a flow regime when gas is not dispersed into the liquid. In agitated vessels gas dispersion is an important phenomenon, which determines the size of bubbles and mass transfer. [28] Ways of gas dispersion are shown schematically in Figure 13.

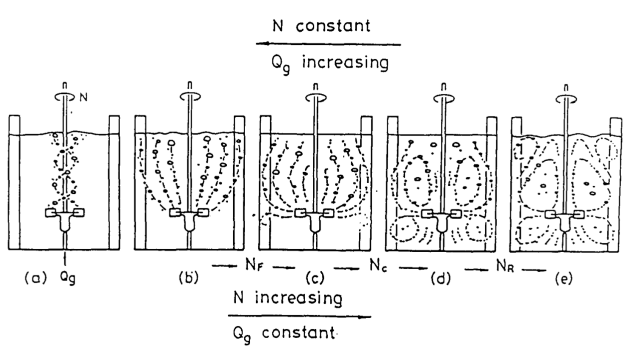

Figure 13. States of gas dispersion.

(a) - no gas dispersion, gas flow is along the impeller axis; (b) - gas dispersion occurs in the upper part of the vessel, bubble column regime; (c) - appearance of minor circulation in lower part; (d) - good gas dispersion; (e) - intensive gas dispersion, appearance of third circulation loop.

Flooding phenomenon in mixed tank can be observed by following agitator power that decreases sharply. Therefore, gas dispersion is not efficient below flooding point where mass transfer and gas hold-up are reduced. [28]

3.5.1. Main equations

The balance of bubbles buoyant pumping and impeller pumping was cited by Smith and Warmoeskerken, and after reduction it is [22]:

$$Fl = \alpha Fr_I, \tag{28}$$

where *Fl* – gas flow number (Q/ND^3); Fr_I - Froude number of impeller (ND^2/g). Before 1985 constant was determined as 0.6, but Smith and Warmoeskerken determined it as 1.2. Here is the correlation successfully applied to check the data of Zwietering (1963) and explain the difference between two values of the coefficient *a* [22]:

$$Fl = \left(\frac{P_g N_p}{P_0 \beta}\right)\left[Fr_I - K' Fr_T \left(\frac{T}{D}\right)\right], \tag{29}$$

where Fr_T - tank Froude number; *K'* - constant; β - exponent. [24]

3.5.2. Measurement methods

Common way for flooding measurement is tracking of power draw curve of impeller power, which was developed by Nienow in 1977. Previous methods were not exact and included physical parameters, which were not crucial while important parameters, such as gas flow rate, were missed. [28]

Power draw of gassed mixing is included into empirical correlations of mass transfer, gas hold-up, interfacial area, for the comparison of reactors with different design and operating costs calculation. Power draw can be also defined as an integral value which depends on impeller flow regime. The regime can be determined by the rotational speed and geometry of the impeller, rheology and other physical properties of liquid and gas flow rate. [22]

Luong and Voleski in 1979 reviewed the correlations for Newtonian liquids and CMC solutions with below 0.2 % by weight:

$$\frac{P_g}{P_0} = A\left(\frac{Q}{ND^3}\right)^B \left(\frac{\rho_L D^3 N^2}{\sigma}\right)^C, \quad (30)$$

where P_0 - impeller power draw in non-aerated mixing, W [22].

4. Process design of the reactors

4.1. Stirred tank reactor design

Standard stirred tanks are designed for low viscosity liquids. The standard flat bottom STR is shown in Figure 14.

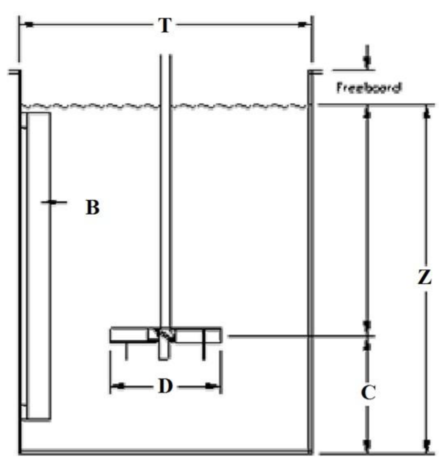

Figure 14. Flat bottom STR.
T - tank diameter; D - impeller diameter; Z - liquid height; B - baffle width; C - impeller. [12]

Geometrical sizes ratios of standard stirred tank are listed below [12]:

1. Impeller diameter to tank diameter: D/T = 1/3
2. Liquid height to tank diameter: Z/T = 1
3. Baffle width to tank diameter: B/T = 1/10 - 1/12
4. Impeller distance from the bottom to tank diameter: C/T = 1/3

4.1.1. Mixing power

Mixing power can be found via impeller power according to the following formulation:

$$P = \rho N_p D^5 N^3, \tag{31}$$

where N_p - impeller power number, which is unique for every impeller type and it is determined empirically in standard stirred tank. Empirical correlations of power number versus Reynolds number for six blade turbines of widely used shapes are presented in Figure 15. [12]

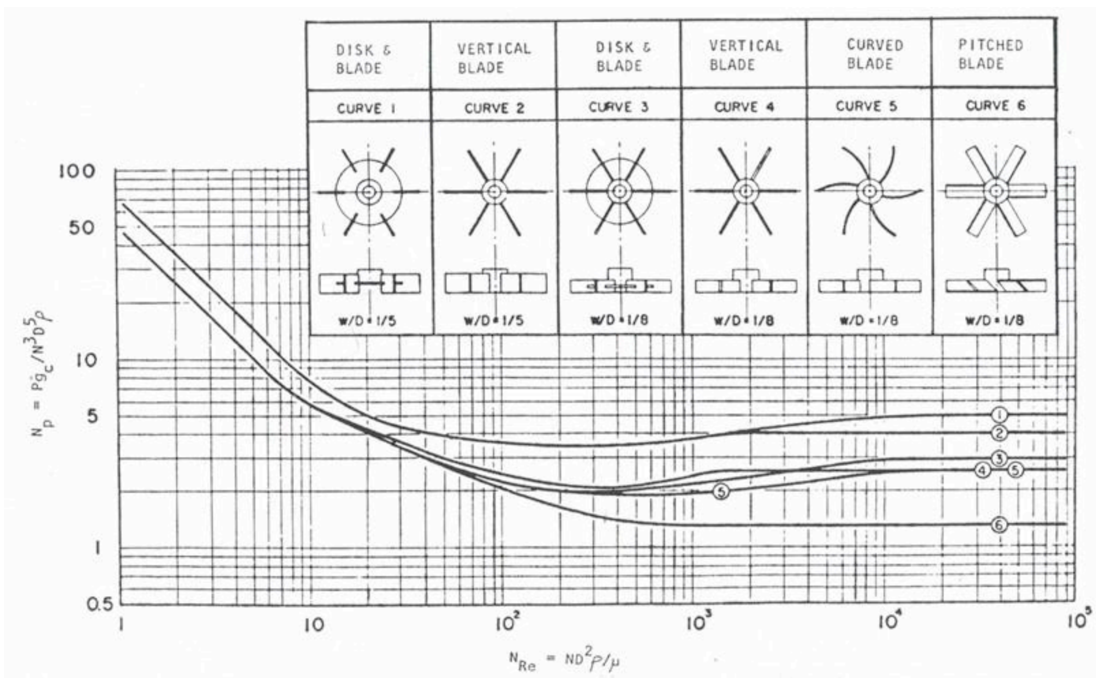

Figure 15. Power number against Reynolds number of some turbine impeller. [29]

Also, mixing power can be calculated via torque:

$$P = 2\pi NM, \tag{32}$$

where M - torque, N·m. [12]

4.1.2. Pumping capacity

Pumping capacity (volumetric gas flow rate) can be determined by the following equation:

$$Q = N_Q N D^3, \tag{33}$$

where N_Q - empirical pumping number, which depends on flow regime, mixer type, a number of impellers and tank geometry (D/T). [12]

4.1.3. Mixing efficiency

Mixing time affects mixing quality and degree of mixedness and can be defined by the equation [12]:

$$\tau_{macro} = C_n \tau_c, \tag{34}$$

where C_n - constant, which depends on viscosity, can be found by the equation [12]:

$$C_n = 0.74\,\mu^{0.244} + 0.00031\mu + 3.7 \tag{35}$$

τ_c - circulation time, s; that also determine the efficiency of mixing process, and is important for preliminary mixing design can be calculated by the equation [12]:

$$\tau_c = \frac{V}{Q} \tag{36}$$

Tip speed is an important design parameter as it determines maximum shear rate which is connected with of mixing power. It is of crucial importance for dispersion processes:

$$TIPS = \pi N D, \tag{37}$$

where *TIPS* - tip speed, m/s; [12]

Specific power input is an important parameter for gas-liquid mixing as it determines the size of micro scaled eddies, is changing in different points of the stirred vessel [12]:

$$\frac{P}{V} = \frac{\rho N_p D^5 N^3}{V} \tag{38}$$

Average fluid velocity is important for mixing processes with high pumping capacity as scaled-up criteria:

$$v_{bulk} = \frac{Q}{A}, \tag{39}$$

where A - tank cross-sectional area, m^2. [12]

4.2. Air-lift reactor design

4.2.1. Main parameters

Liquid volume (non-gaseous):

$$V_L = \frac{Q_L \tau}{\rho}, \tag{40}$$

where Q_L - liquid mass flow rate, kg/s; τ - contact time, s [31].

Gas-liquid mixture density can be determined [31]:

$$\rho_{l-g} = \rho_l(1-\varphi) + \rho_g \varphi \tag{41}$$

When gas is bubbled through liquid, contact surface area F is formed. Analyzing the efficiency of bubbling apparatus, the concept of specific interfacial surface area is usually used [31]:

$$S_V = \frac{F}{V_{l-g}} \tag{42}$$

At the assumption that gas-liquid mixture contains bubbles of spherical shape and constant size interfacial surface area can be expressed as follows [31]:

$$S_V = \frac{6\varphi}{d} \tag{43}$$

The regime of dynamic cellular foam appears when gas velocity in the holes of the gas distributors higher than the speed of free ascent of the bubble ($v_0 > v_{up}$). For water-air system the velocity $v_g = 0.25$ - 0.26 m/s. In openings of sparger of industrial apparatus, gas velocity usually substantially exceeds this value and can reach 10 - 15 m/s. In this case, gas escapes the hole in form of an expanding jet, which is broken up into bubbles of various sizes at some distance from sparger. Resulting gas-liquid mixture has a cellular structure, and height of its layer increases with increasing gas flow. Upper limit of the existence of the regime of dynamic cellular foam is determined by the following condition [31]:

$$K_b = \frac{v_g}{(v_l g)^{1/3}} \leq 18, \tag{44}$$

where K_b - bubble regime criterion [31].

The regime of dynamic non-cellular foam sets at K_b more than 18. A mobile gas-liquid mixture is formed which consists of different-sized gas bubbles of an undefined shape that carry liquid droplets. If ALR has a small diameter (tube), gas rises upwards in form of elongated large bubbles (projectiles) separated by interlayers of liquid with small bubbles. In this case, the bubbling regime is projectile or cork [31].

The rate of energy dissipation per unit volume of fluid in reactor, W/m^3; for ALRs can be calculated [31]:

$$P/V = v_g g \tag{45}$$

Hydraulic resistance can be used to determine changes of flow sharp or direction in ALR under operating conditions can be expressed as [32]:

$$\Delta p = \Delta p_{gd} + \Delta p_{sp} = \zeta_0 \frac{\rho_g v_0^2}{2} + H\rho_l g, \tag{46}$$

where Δp_{gd} - pressure loss in gas distributor holes, Pa; Δp_{sp} - the static pressure of the gas-liquid mixture layer with height H, Pa; ζ_0 is the coefficient of resistance of a one-sided flooded hole. [32] It can be determined by means of empirical correlation presented in Figure 17.

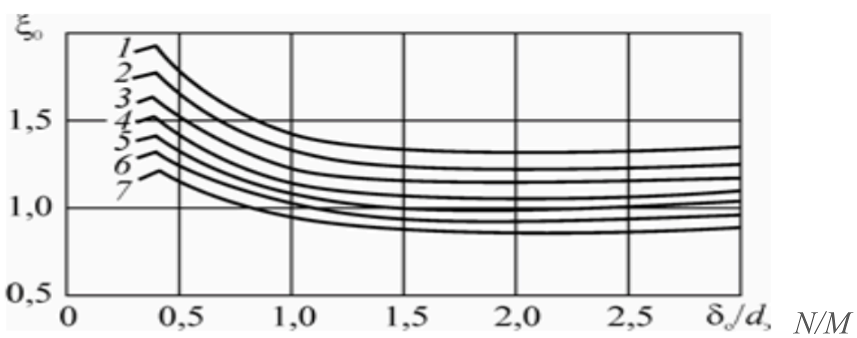

Figure 17. Coefficient of hole resistance at different surface tension:
1 - 0.02; 2 - 0.03; 3 - 0.04; 4 - 0.05; 5 - 0.06; 6 - 0.07; 7 - 0.08. [31]

EXPERIMENTAL PART

5. Aims of the experimental study

The experiments were aimed at the comparison of three commonly used reactors suitable for fermentation. They were OKTOP reactor, air-lift reactor and flat bottomed stirred tank reactor. Volumetric mass transfer, gas hold-up, bubble size distribution and flooding are process parameters describing gas-liquid mixing and they characterize operational unit performance that is to be compared. Also, in the experimental work six solutions were tested: water, ethanol 0.5, 3 and 5 w %, CMC 0.05 and 0.15 w %. The selection of these solutions is dictated by fluid properties variation that might take place in gas fermentation.

5.1. Experimental plan

The experiments were carried out under normal conditions: temperature 20 ºC and atmospheric pressure. Temporal history of dissolved oxygen concentration was used for the analysis of volumetric mass transfer. Air was supplied into the reactors with the following flow rates: 1, 6.5, 10, 18 and 25 L/min. For the stirred vessels, the impeller speed was set as follows: 400, 450, 550 and 650 rpm. For the STR it was decided to omit experiments with ethanol 5 w % solution as the maximum concentration for vital activity of bacteria is 3 % of ethanol and the influence of gas-liquid surface tension on global parameters was tested in OKTOP reactor. The surface tension of the ethanol solutions and water are presented in Table 2.

Table 2. Surface tension water - ethanol. [33]

Ethanol content, w %	σ, mN/m.
0	72.1
0.5	70.56
3	62.87
5	56.71

Also, the viscosity of the CMC solutions was measured as it is non-Newtonian liquid and its viscosity depends on the rate of the impeller. The analysis in detail is presented in chapter 6.2.3. of the thesis. The experimental plan is introduced in Table 3.

Table 3. Experimental plan for studying gas-liquid mixing for different reactor types.

OKTOP reactor, designed by Outotec			
Solution	**Gas flow rate, L/min**	**Impeller speed, rpm**	**Measured value**
Water	1	400	mass transfer
Ethanol 0.5 %	6.5	450	gas hold-up
Ethanol 3 %	10	550	torque
Ethanol 5 %	18	650	bubble size
CMC 0.05 %	25	-	-
CMC 0.15 %	-	-	-
Air-lift reactor			
Water	1	-	mass transfer
Ethanol 0.5 %	6.5	-	gas hold-up
Ethanol 3 %	10	-	bubble size
Ethanol 5 %	18	-	-
CMC 0.05 %	25	-	-
CMC 0.15 %	-	-	-
Stirred tank reactor			
Water	1	400	mass transfer
Ethanol 0.5 %	6.5	450	gas hold-up
Ethanol 3 %	10	550	torque
CMC 0.05 %	18	650	bubble size
CMC 0.15 %	25	-	-

6. Materials and methods

6.1. Reactors used in the analysis

As it was mentioned earlier three reactor types were used for global parameters analysis. The lab scale reactors were of similar volume namely 13.5, 14 and 13 L of OKTOP, ALR and STR respectively. ALR type was an internal-loop concentric tube. STR was equipped with Rushton turbine. The gas was supplied from sparger mounted in bottom of the reactors. Three reactor types are presented in Figure 18.

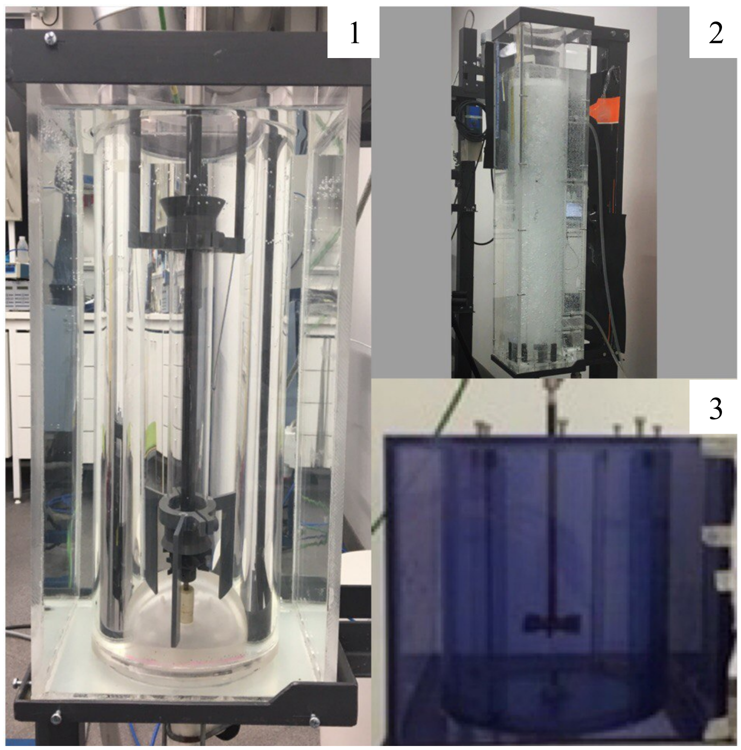

Figure 18. Lab scale reactors used in this work.
1 - OKTOP; 2 - air-lift reactor; 3 - stirred tank reactor.

The stirred reactors were equipped with torque meter in order to get information on power draw. All the reactors were encapsulated into plexyglass prism meant to be filled with a liquid of similar optical transparency to prevent visual distortion for imaging.

6.2. Measurement methods

6.2.1. Mass transfer

Dissolved oxygen meter MARVET BASIC was used to measure mass transfer (Figure 19). The oxygen meter has a probe with membrane. It is immersed in a solution and performs measurement of dissolved oxygen concentration and temperature. Measurements are written every six seconds. In Appendix I one may find the example of the recorded measurements.

Figure 19. MARVET BASIC dissolved oxygen meter.

Before experiment, any measuring device has to be calibrated. MARVET BASIC is designed to be calibrated in oxygen saturated solution as well as in zero-concentration solution. Sodium sulfide of 5 % concentration was used as zero-point solution in the calibrations.

At first, a solution was blown with nitrogen in order to create oxygen free solution. Dissolve oxygen probe was submerged in the area of high mixing intensity to remove analyzed portions of water. Then, air was introduced while temporal history of oxygen concentration change in the solution has been recorded. The example of mass transfer measurement is shown in Figure 20.

Time constant is system response time for increasing oxygen concentration until it reaches value 63.2 %. It was measured in every solution resulting in 9 to 12 s. Mass transfer was calculated in MODEST software using a different time constants of the device to determine uncertainties in k_La measurements. Deviation is increasing when the overall time of the process is decreasing (value of mass transfer becomes higher). Software automatically determines the initial and saturation concentrations of oxygen from the recorded temporal history.

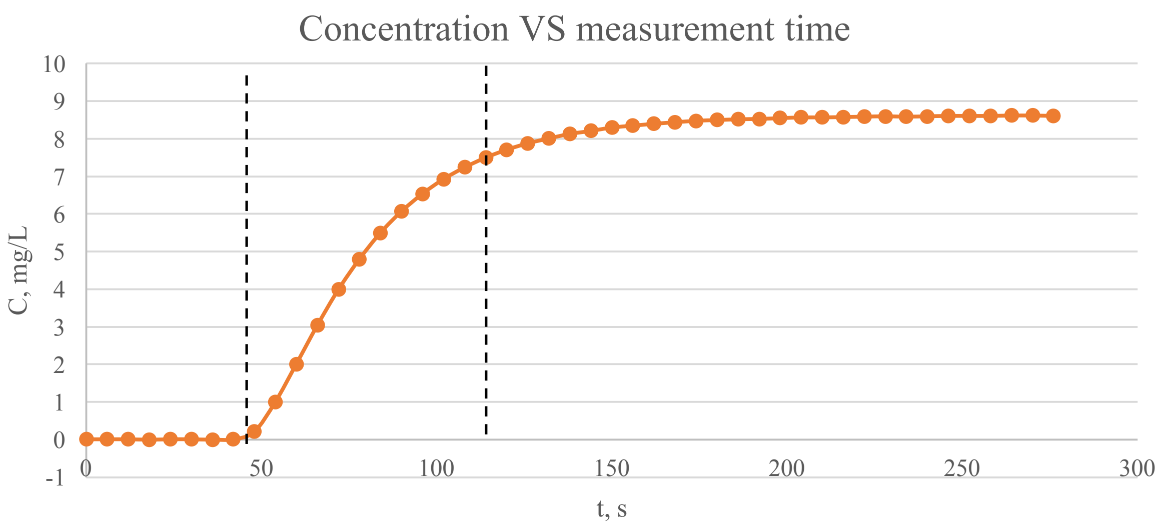

Figure 20. Temporal history of oxygen concentration change.

6.2.2. Bubble size

For bubble size detection photographic method was used, which was discussed earlier in 3.1.2.1. A measuring ruler was attached to the transparent walls of all reactors. Twenty photos were taken at every set of operational conditions. In Figure 21 the examples of photos are presented.

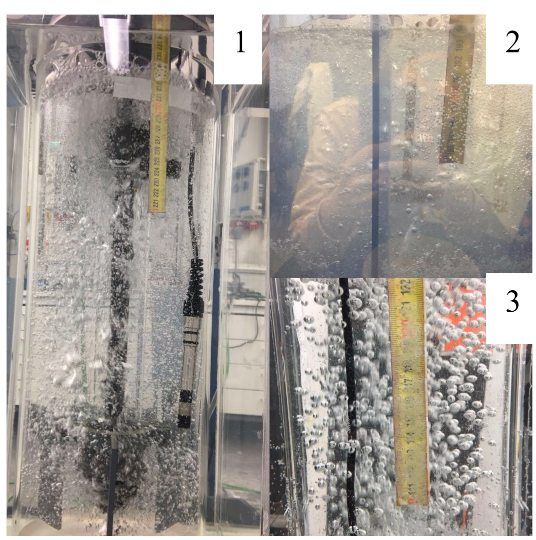

Figure 21. Photos for bubble size measurement.
1 - OKTOP reactor; 2 - STR; 3 - ALR.

Minimum and maximum sizes of bubbles were determined using photographs. In Appendix I the example of bubble size table is presented.

6.2.3. Power draw

Power draw has been determined based on measured torque in stirred vessels. MAGTROL torque-meter was used. The device is shown in Figure 22.

Figure 22. MAGTROL on shaft torque-meter, model TM 206.

The torque was measured to determine power draw of mixing. The flooding phenomenon is discussed in chapter 3.5. of the thesis. Due to the shaft swinging the torque read outs were slightly fluctuating. An example of measured data is shown in Appendix I.

6.2.4. Gas hold-up measurement

Surface level difference method was used to determine gas hold-up in all the reactors. Surface level was determined by a ruler attached to the reactors wall. Fluctuations of liquid level were taken into account by tracking minimum and maximum values of liquid height recorded. Deviation was determined by measurement of the average level using the ruler. An example of gas hold-up measurement is shown in Appendix I.

6.2.5. Viscosity analysis of CMC solutions

Value of shear rate in stirred reactor can be of wide range, therefore apparent viscosity becomes an important parameter in mixing of non-Newtonian liquids. Rheological analysis of CMC solutions was made using modular compact rheometer of Anton Paar company, MCR 302. The rheometer is presented in Figure 23.

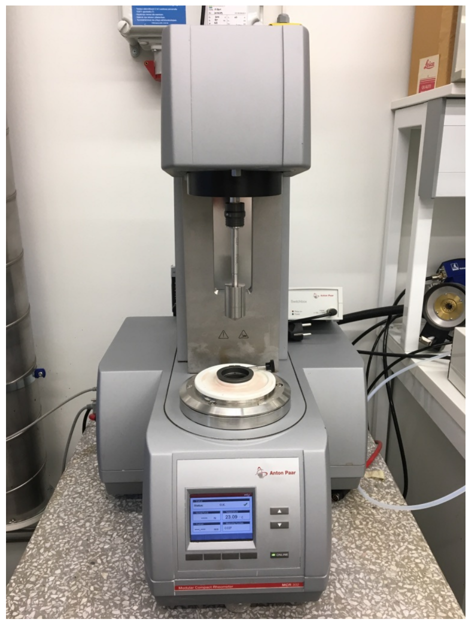

Figure 23. Anton Paar, modular compact rheometer, MCR 302.

The conical rotator was used in rheological tests. And a CMC solution sample of 100 mL was analyzed. Shear stress was measured in the following range 1 to 300 1/s of shear stress. Example of experimental data of rheometer is presented in Appendix I.

7. Results and discussions

7.1. Viscosity analysis

The main point of the analysis is to define viscosity for different impeller speed in stirred vessels and for air lift reactor. Figure 24 presents the dependence of logarithm of viscosity on logarithm of share rate of rheometer cone for two CMC solutions.

The parameters n and K, which can be determined from the graph, are used for the equation by which can be calculated shear rate. The rate determines the viscosity of CMC solutions in the reactors. The tables of the calculations are presented in Appendix V.

Mean shear rate in ALR:

$$\gamma' = \left(\frac{1}{K} g\rho U_{gas}\right)^{\frac{1}{n+1}} \tag{44}$$

where *γ'* - average shear rate, 1/s; *n* - flow index; *K* - consistency index, Pa·s^n. Indexes can be determined by the log (μ) VS log (N) graph.

Mean shear rate in STR:

$$\gamma' = \left(\frac{1}{K}\frac{P_{tot}}{V}\right)^{\frac{1}{n+1}} \tag{45}$$

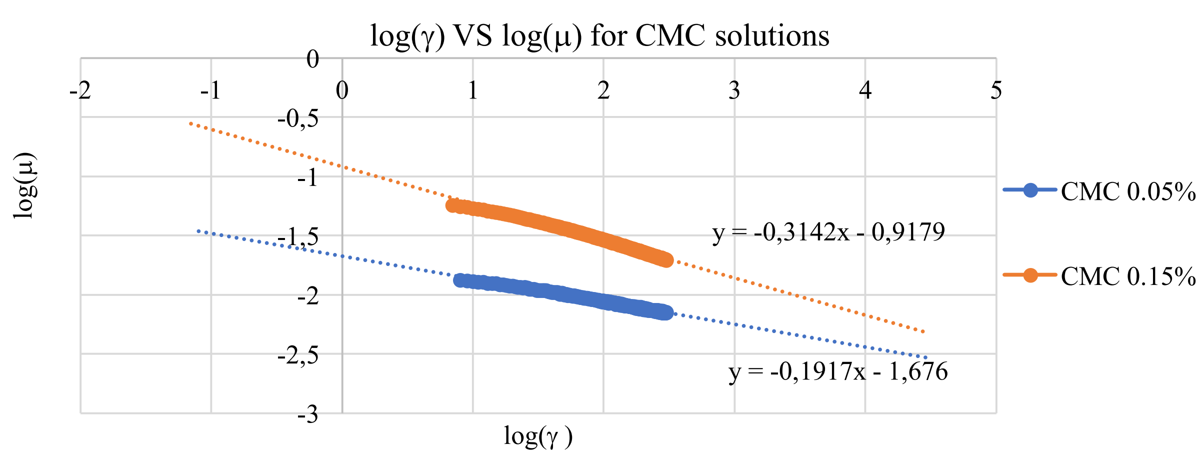

Figure 24. Viscosity analysis for CMC solutions.

Coefficients n and K determined for CMC solutions are listed in Table 4.

Table 4. CMC solutions coefficients.

n, -	K, Pa·s^n
CMC 0.05 %	
0.8083	0.211
CMC 0.15 %	
0.6858	0.12

7.2. Flooding experiments for OKTOP and STR

All the experimental data is presented in Appendix II. The minimum point on the power-graph corresponds to the reactor flooding point at the impeller rotation speed. The flooding point affects the mass transfer coefficient. It is considered, that after flooding the mixing is not effective. For OKTOP reactor and STR flooding in air-water system is presented in Figures 25 and 26 respectively the rest flooding graphs are presented in Appendix III. As it can be seen from the graphs the fact about the flooding mentioned earlier is confirmed. Mixing power for the reactors was determined as non-gaseous power draw per volume of the reactor. Calculations examples are listed in Appendix IV.

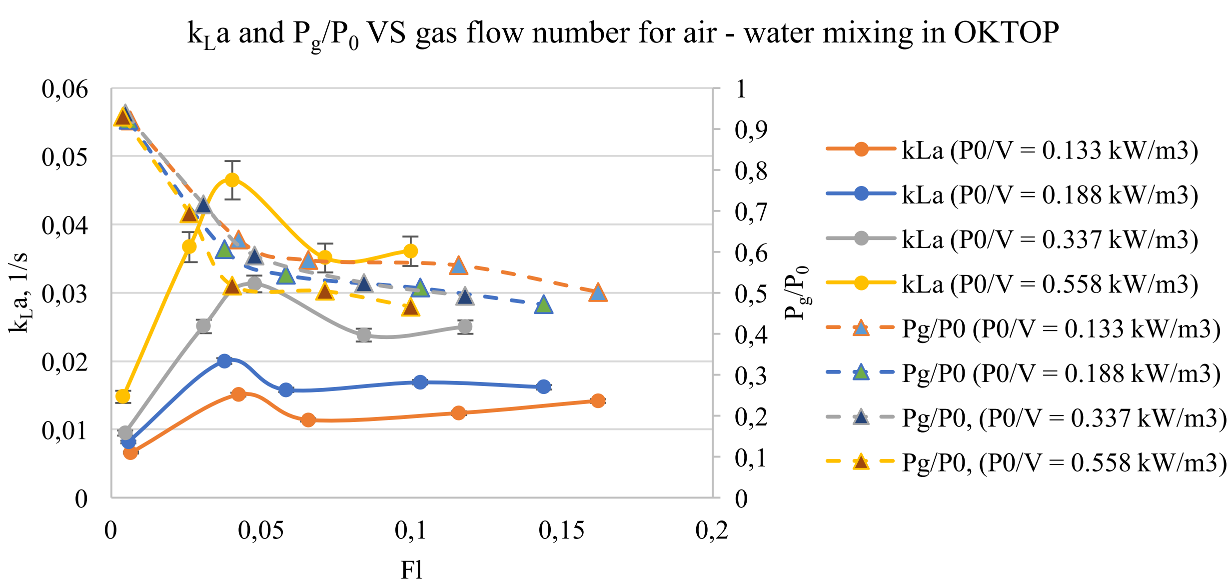

Figure 25. Flooding for air - water mixing in OKTOP.

In Figure 25, it can be seen that the maximum values of the mixing power 0.133 and 0.188 kW/m^3 can be reached with gas flow rate 6.5 L/min. The optimal gas flow rate at power 0.337 and 0.558 kW/m^3 is 10 L/min.

Intreval between values of gas flow rates was quite large, due to this the maximum of the graph cannot be determined exactly. That is why the highest value is determined as maximum.

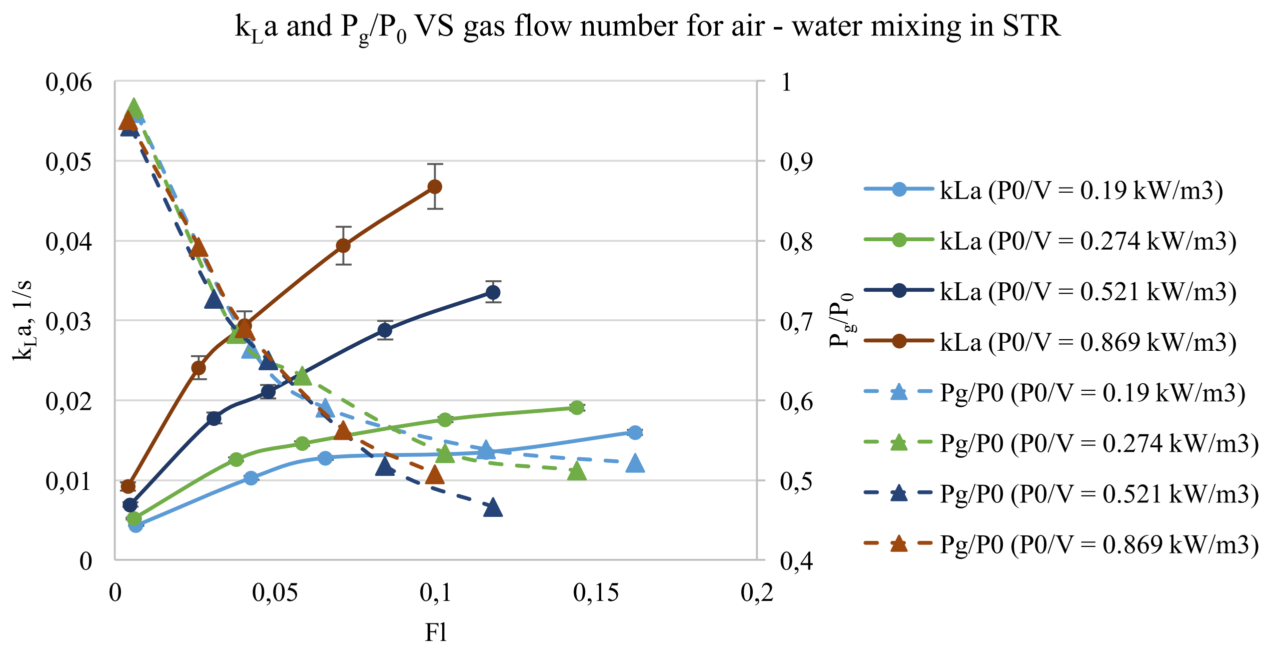

Figure 26. Flooding for air - water mixing in STR.

It is interesting to note the main differences between STR and OKTOP line graphs, that for STR it has no minimum points of power draw and, as a result, no maximum for the value of mass transfer coefficient.

7.3. Comparison of the reactors in k_La VS gas flow rate axes

After analyzing of all the experimental data, it is possible to compare them in k_La VS gas flow rate graphs. In such manner, it is possible to compare the maximum values of the mass transfer coefficients in the reactors. The comparison of the reactors is presented in Figures 27 - 32.

7.3.1. Water

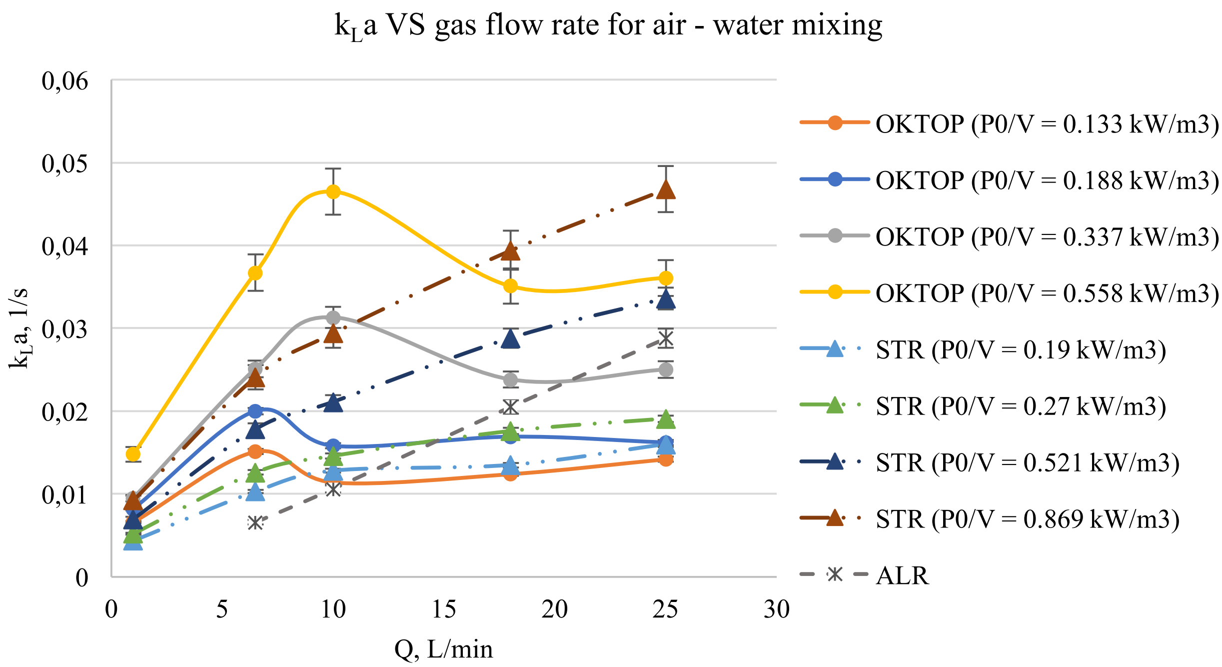

Figure 27. k_La VS gas flow rate for air - water mixing.

The maximum value of the mass transfer coefficient is reached in stirred vessels with the highest impeller speed 650 rpm (0.558 and 0.869 kW/m^3) at gas flow rates 10 and 25 L/min for OKTOP and stirred tank reactors respectively. Using these parameters, ALR can be compared with agitated reactors when the mixing power is 0.337 kW/m^3 for OKTOP and 0.521 kW/m^3 for STR or lower. At the power 0.337 kW/m^3 the optimal gas flow rate for the OKTOP reactor is 10 L/min and for the STR when mixing power is 0.521 kW/m^3 - 25 L/min, the air-lift reactor can be compared with these points when the gas flow rate is 25 L/min. The maximum value of mass transfer coefficient at the impeller speeds 400 and 450 is reached at gas flow rate 6.5 L/min in OKTOP reactor (0.133 and 0.188 kW/m^3) and 25 L/min in stirred tank reactor (0.19 and 0.27 kW/m^3). ALR is competitive when the flow rates are higher than 10 L/min.

7.3.2. Ethanol

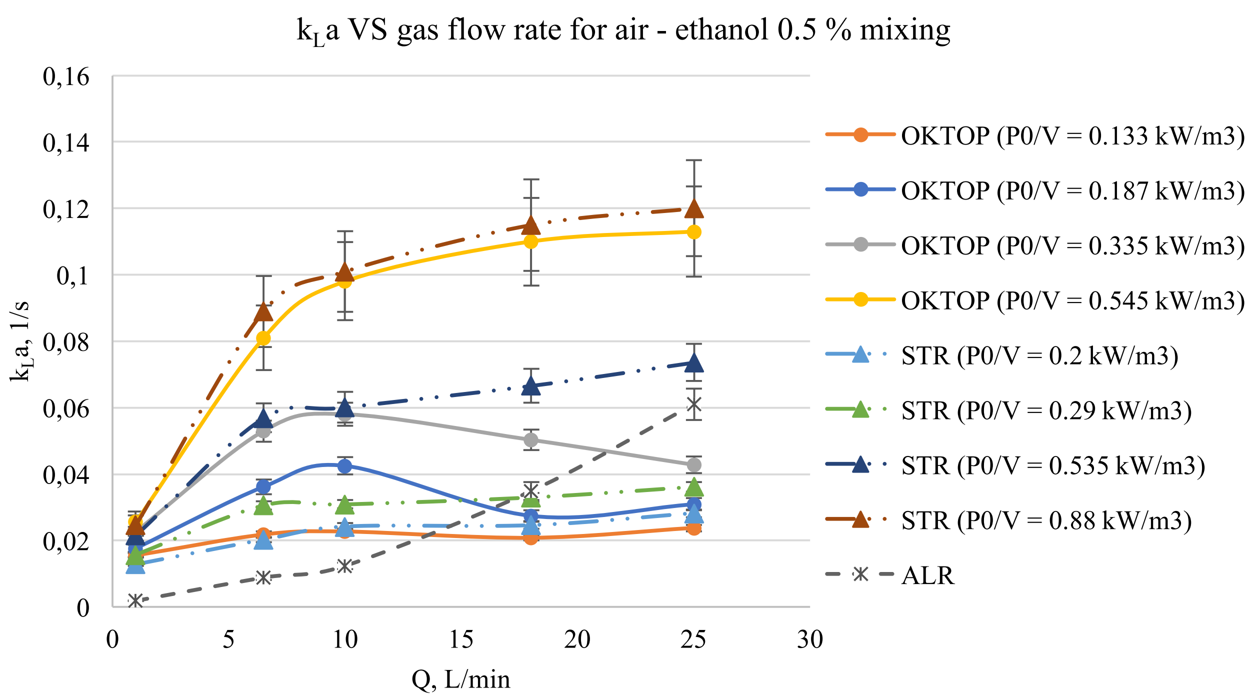

Figure 28. k_La VS gas flow rate for air - ethanol 0.5 % mixing.

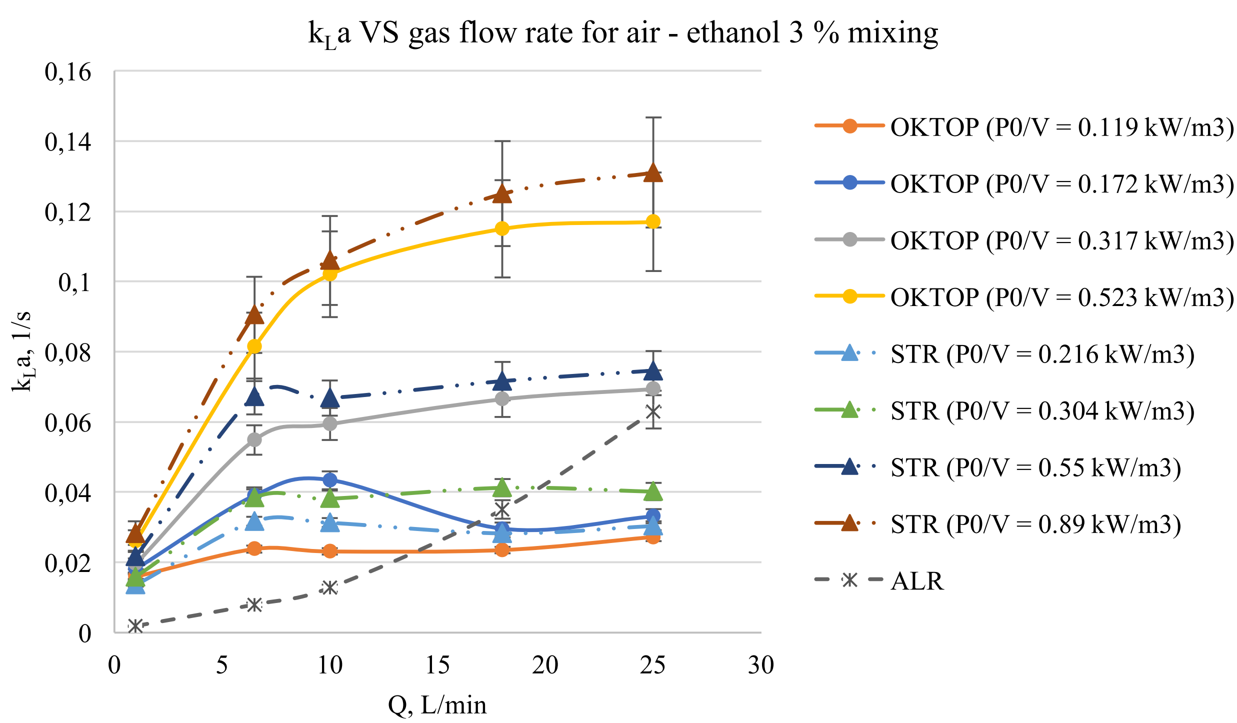

Figure 29. k_La VS gas flow rate for air - ethanol 3 % mixing.

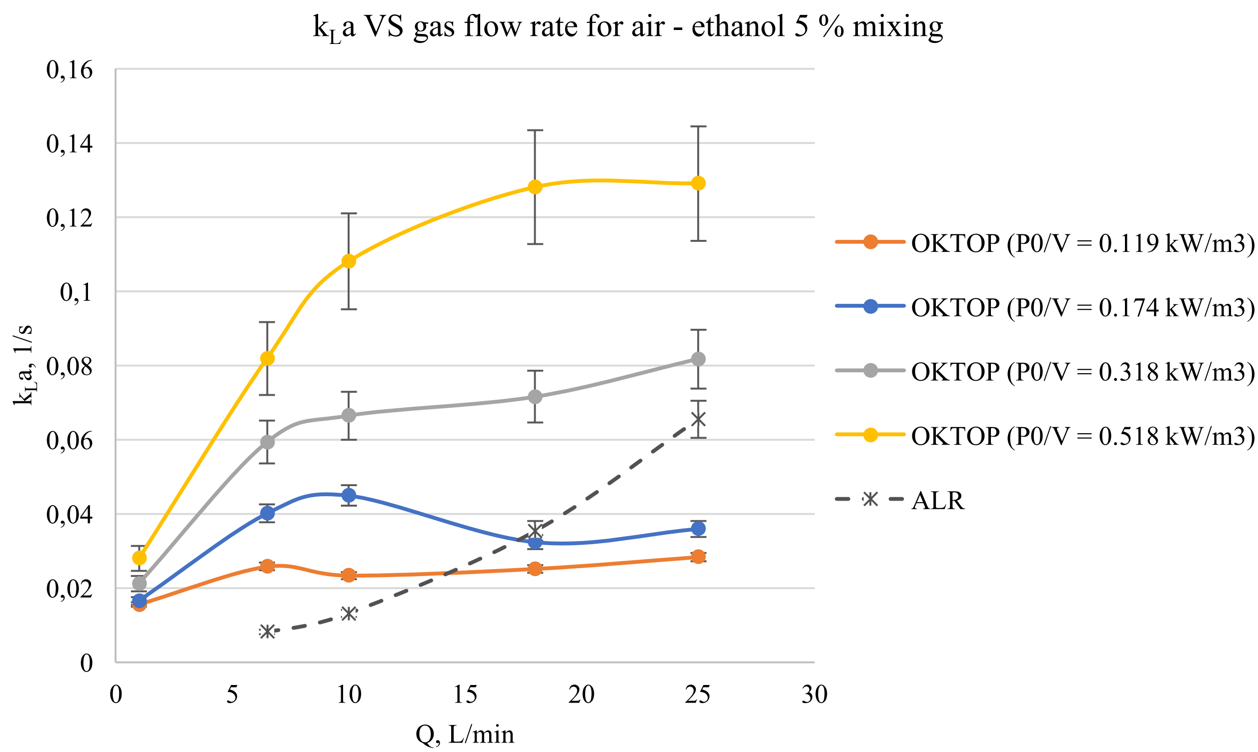

Figure 30. k_La VS gas flow rate for air - ethanol 5 % mixing.

In all the ethanol solutions in stirred vessels the highest level of mess transfer is reached at the impeller speed 650 rpm (the highest value of energy consumption) and gas flow rate 25 L/min. The highest value of mass transfer in ALR is around twice lower than for stirred reactors. STR in all line graph has the highest value of mass transfer. It is interesting to note that in ethanol 0.5 % solution mass transfer in OKTOP reactor with mixing power 0.335 kW/m^3 decreases after flow rate 10 L/min.

As the conclusion can be noted the positive effect of surface tension on mass transfer phenomenon. The lower the surface tension is the higher the value of mass transfer coefficient is.

7.3.3. CMC solutions

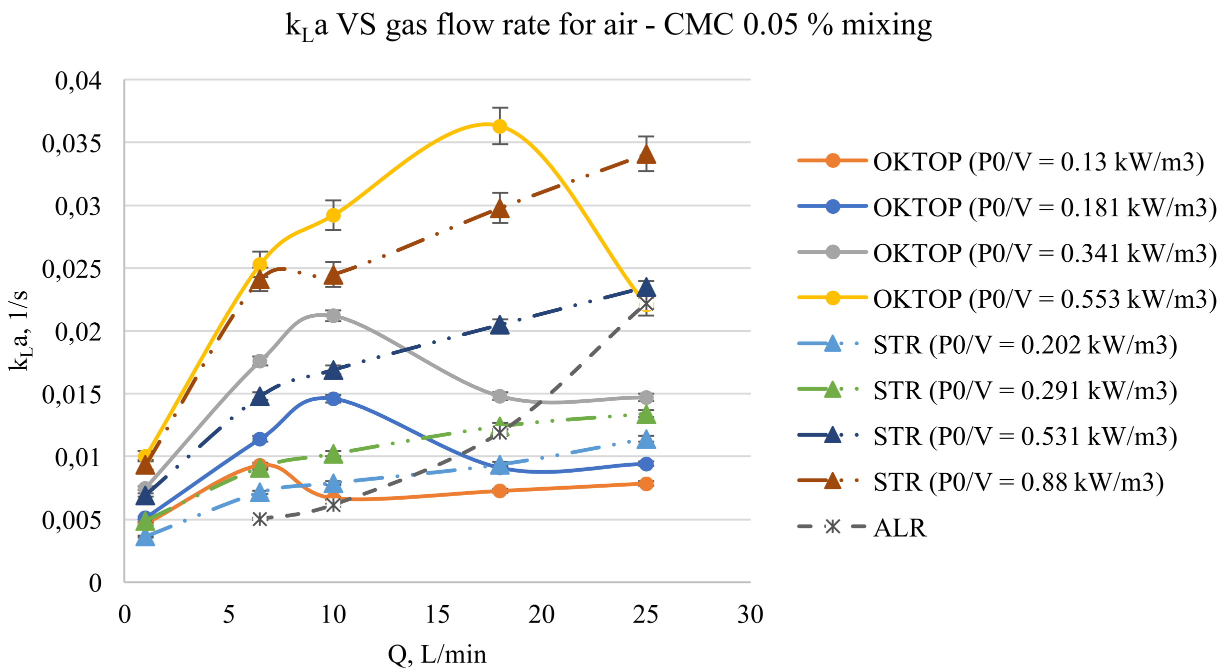

Figure 31. k_La VS gas flow rate for air - CMC 0.05 % mixing.

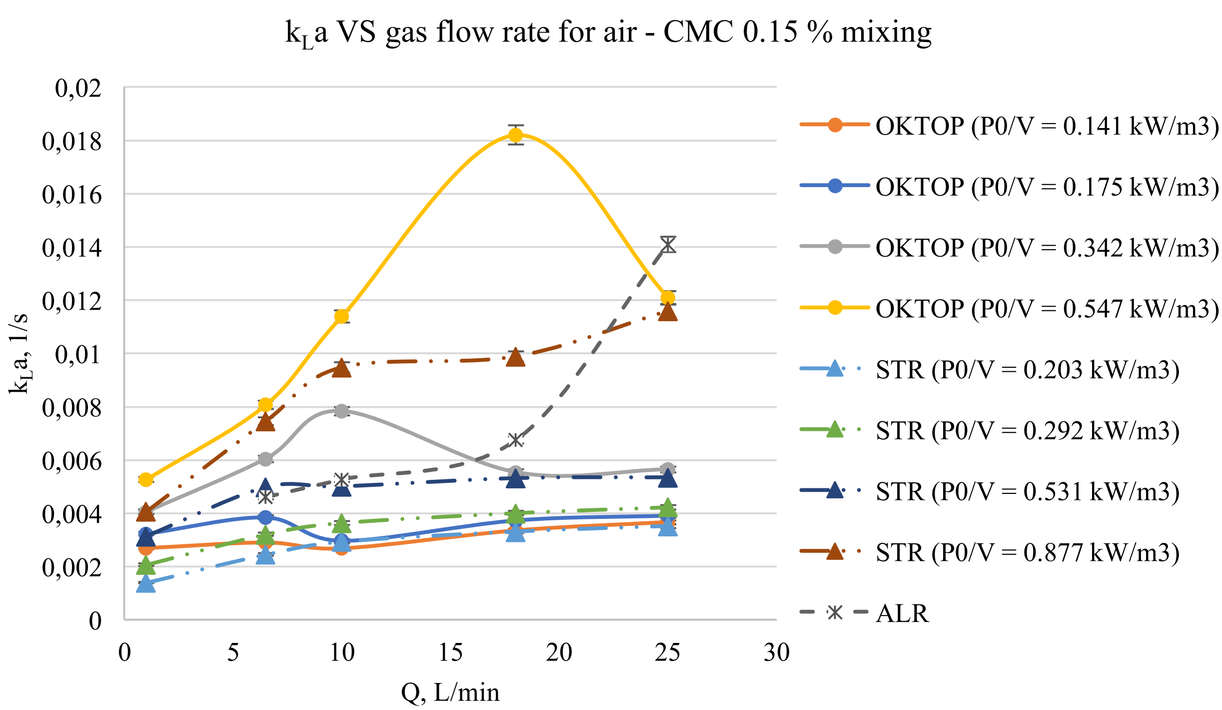

Figure 32. k_La VS gas flow rate for air - CMC 0.15 % mixing.

In the CMC solutions, the highest value of mass transfer coefficient is reached in OKTOP reactor at the impeller speed 650 rpm (0.553 and 0.547 kW/m^3) and gas flow rate 18 L/min. STR has more competitive results in lower concentration of CMC. However, ALR is more competitive in higher concentration of CMC.

The line graphs show negative effect of viscosity on mass transfer coefficient. If viscosity is high the value of mass transfer is relatively low. As it can be seen from the graph, the value of mass transfer in all the reactors for CMC 0.05 % solution is twice higher than for CMC 0.15 %.

7.4. Comparison of the reactors in k_La VS power draw axes

The previous way of the reactors comparison was more viewable for the understanding of mixing efficiency. But it is important to compare reactors between each other taking into account energy consumption of mixing process. The low energy consumption reduces operating costs. For this purpose, for all the reactors was calculated the total power draw (mechanical and gassing power) Example of the calculation is presented in Appendix IV. For the ALR the energy is used only for the gas supply. The comparison of the reactors is shown in Figures 33 - 38.

In order to calculate mixing power in legend, as it was discussed earlier, was used non-gaseous mechanical power draw. It is the highest value of energy consumption of the reactors. For x-axes, gaseous mechanical power and gassing power were used. They are lower as impeller needs less power for air-liquid mixing. The main idea is that higher power is needed for liquid mixing than for air. The more air goes through the solution the lower power draw is. Difference between merely specific power values in the legend and x-axis can be explained by this fact.

7.4.1. Water

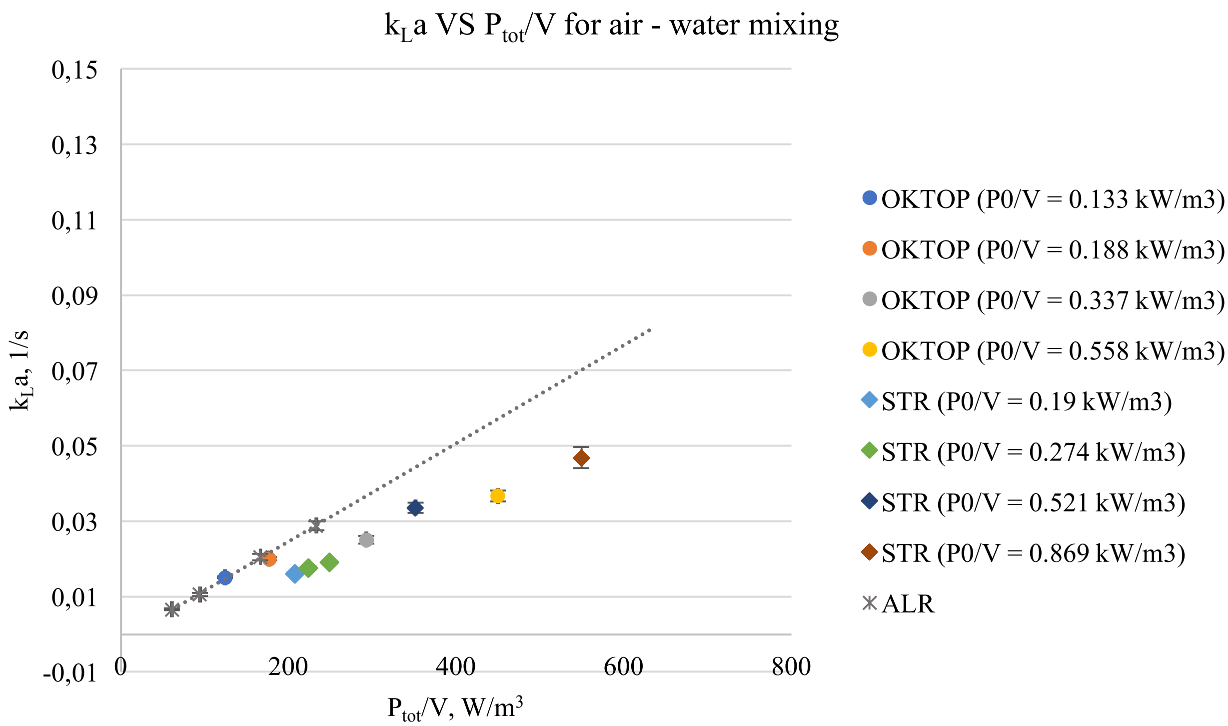

Figure 33. k_La VS power draw for air - water mixing.

The graph demonstrates that ALR has the lowest power draw and relatively high mass transfer. However, OKTOP reactor can be compared with ALR when the power is 0.337 and 0.558 kW/m^3 (impeller speed is 400 and 450 rpm), but the value of mass transfer for the points is lower than for ALR. The values of mass transfer and power draw at impeller speed 650 rpm (0.869 kW/m^3) is the highest compared with other reactors.

7.4.2. Ethanol solutions

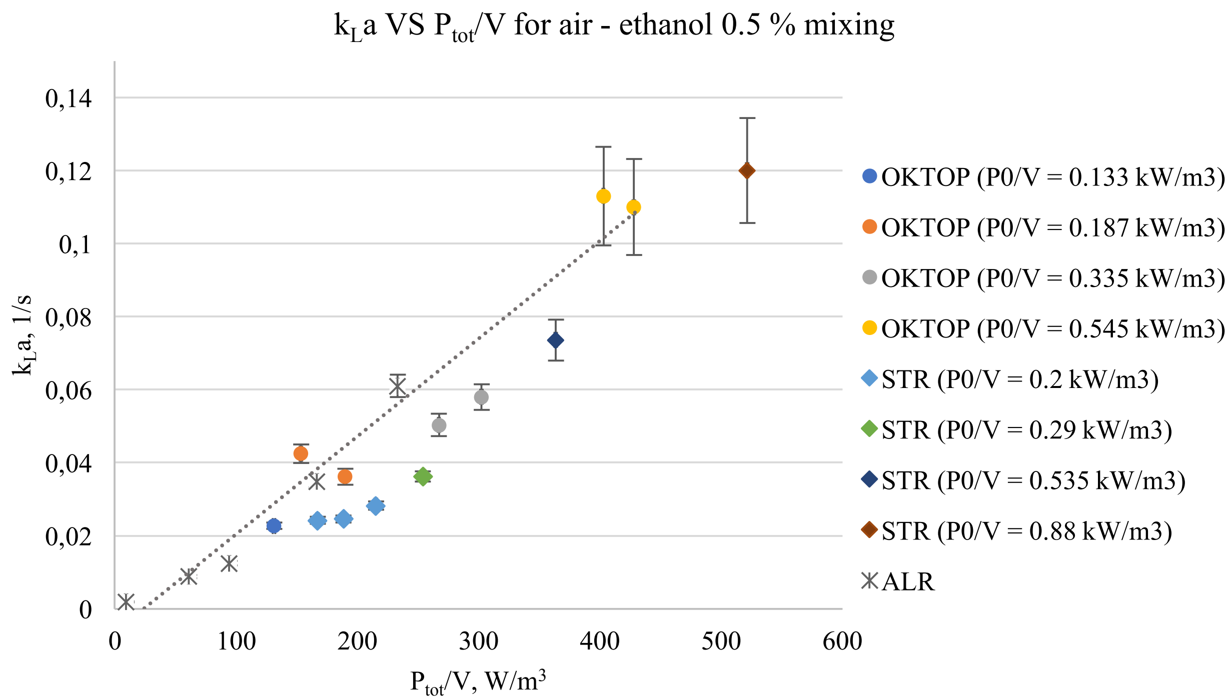

Figure 34. k_La VS power draw for air - ethanol 0.5 % mixing.

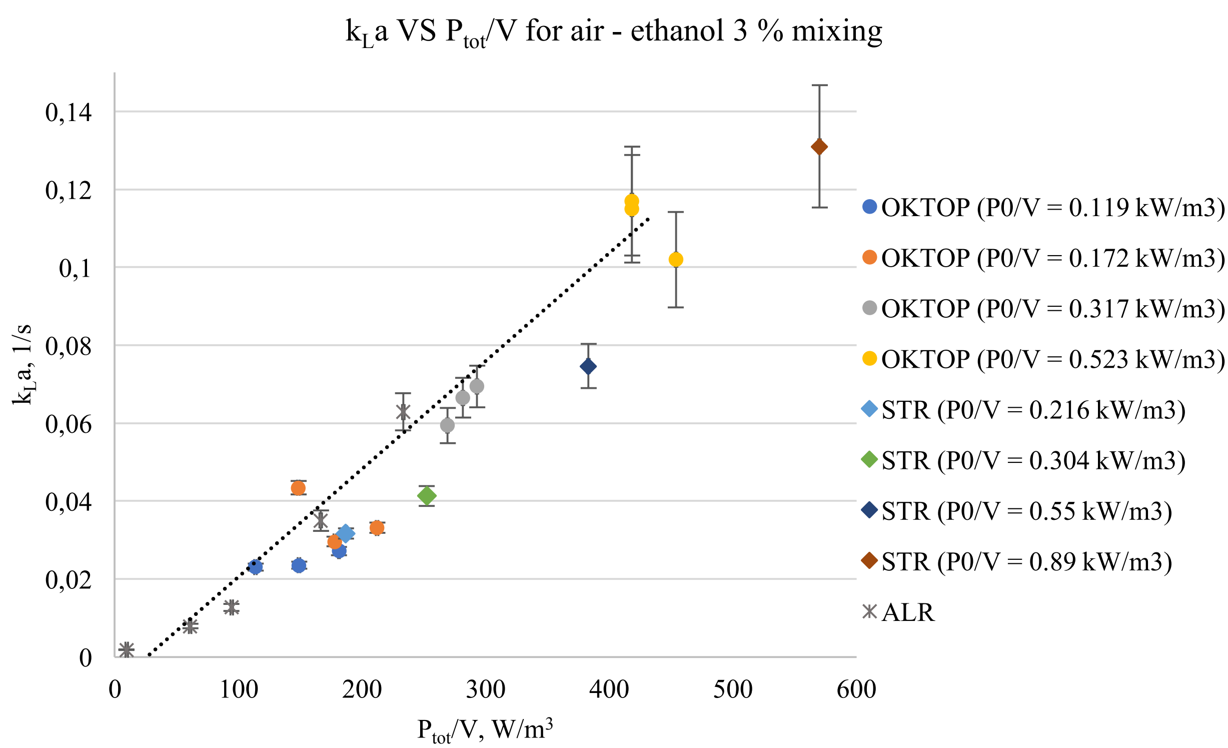

Figure 35. k_La VS power draw for air - ethanol 3 % mixing.

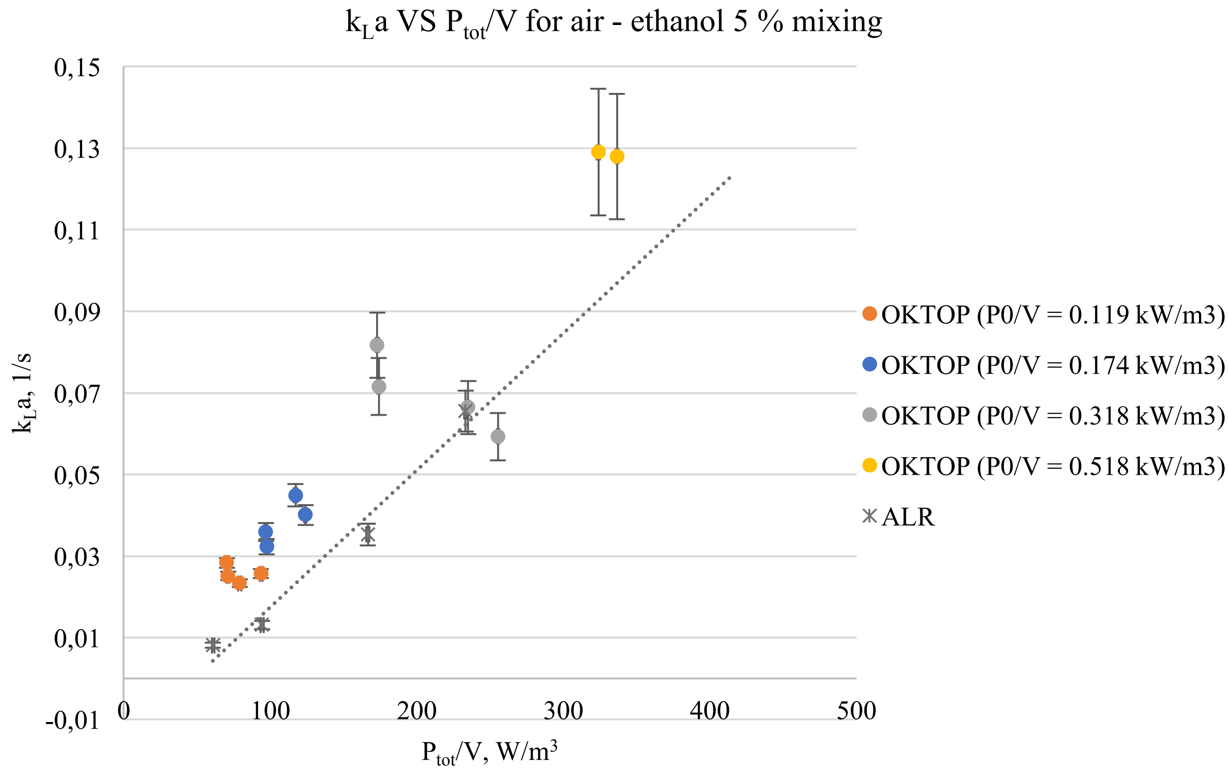

Figure 36. k_La VS power draw for air - ethanol 5 % mixing.

As it can be seen from the graph, in ethanol 0.5 and 3 % the highest value of mass transfer and power draw is reached for STR with gas flow rate 25 L/min and 0.88 and 0.89 kW/m^3. In ethanol 5 % OKTOP reactor has the same dependence at the mixing power 0.518 kW/m^3 (impeller speed 650 rpm) and gas flow rates 18 and 25 L/min. OKTOP reactor has good results in all graphs at the impeller speeds 400 and 450 rpm (0.119 - 0.187 kW/m^3) compared with other reactors. In ethanol 5 % mass transfer at mixing power 0.318 kW/m^3 (impeller speed 550) is higher than in ALR, although power draw is lower.

It can be noted that in low surface tension solutions OKTOP reactor results can be determined as the best compared with other reactors.

7.4.3. CMC solutions

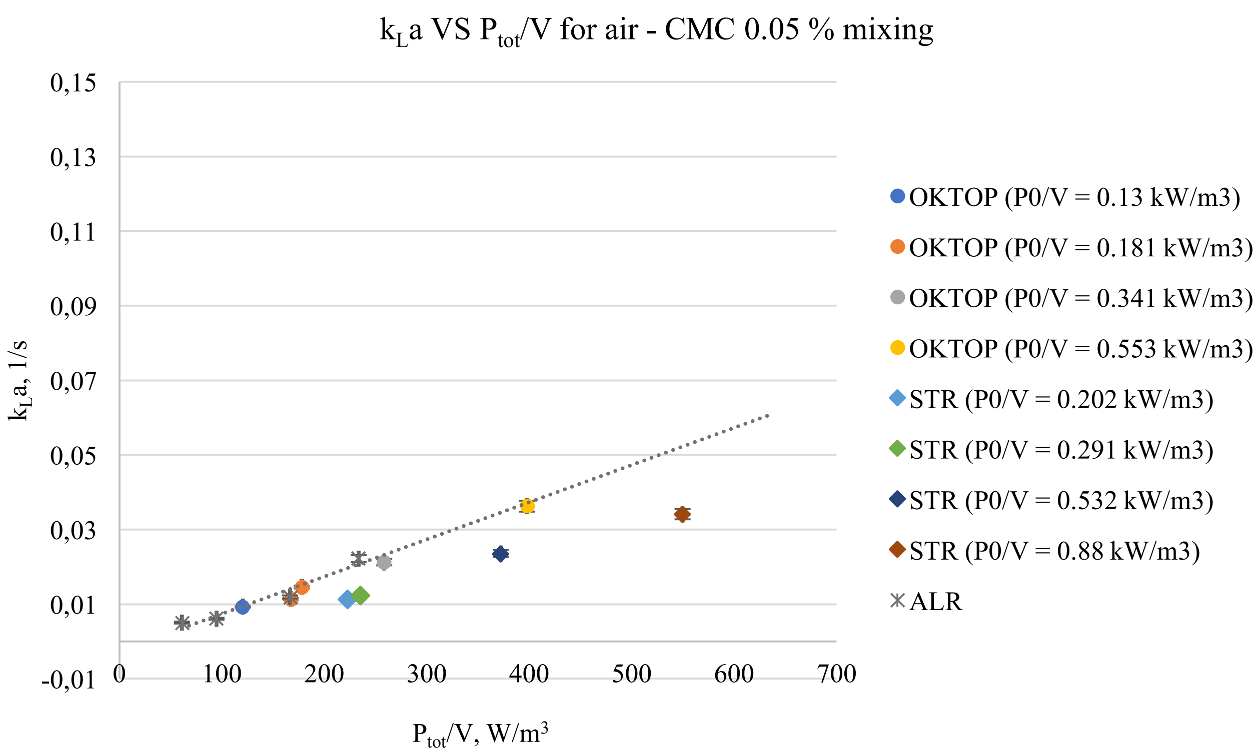

Figure 37. k_La VS power draw for air - CMC 0.05 % mixing.

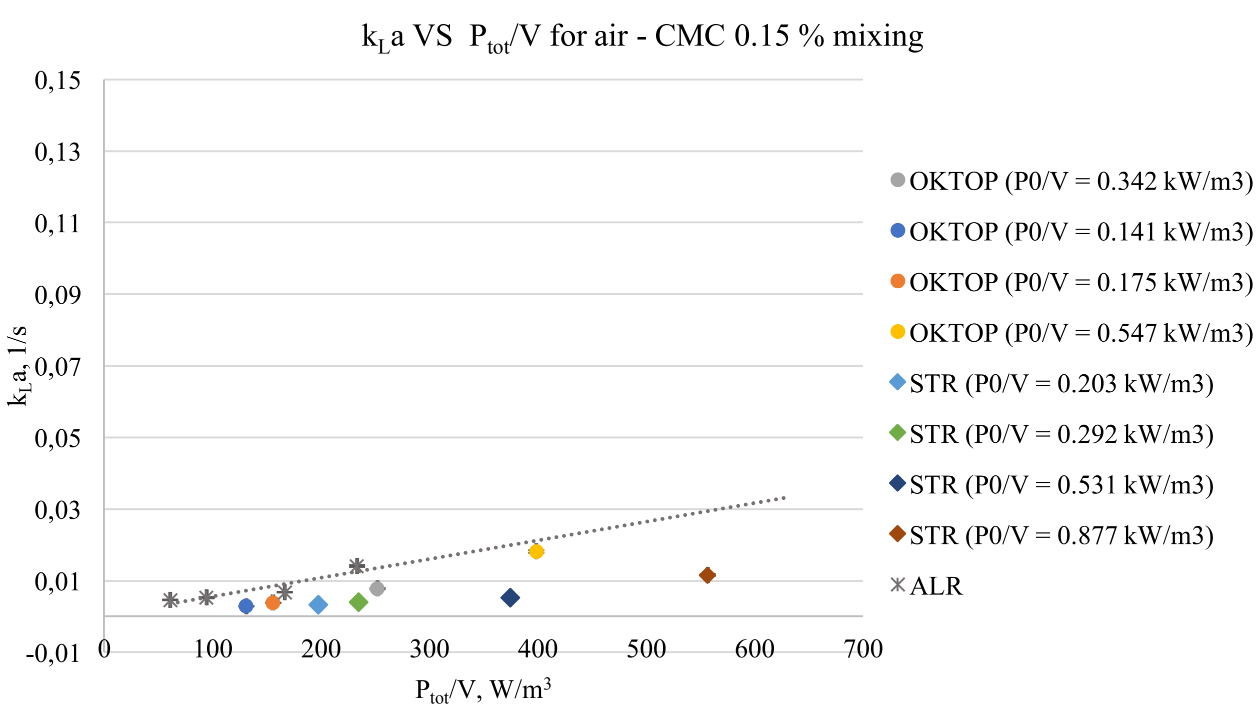

Figure 38. k_La VS power draw for air - CMC 0.15 % mixing.

The highest value of mass transfer coefficient is reached for the OKTOP reactor at the rotation speed 650 rpm (0.547 kW/m^3) and flow rate 18 L/min, but the power draw is twice higher than for ALR. For STR the value of power draw at 650 rpm (0.877 kW/m^3) is the highest. Although value of mass transfer in STR is lower than in ALR and OKTOP. In this line graph, it can be seen that mixing in higher viscosity solution requires higher power. In CMC 0.05 % OKTOP can be used as effectively as ALR. However, when the viscosity grows ALR performs better, taking into account mass transfer and power draw.

7.5. Gas hold-up in the reactors

As the gas hold-up is an important parameter for the gas-liquid mixing processes the analysis of the experimental data related to this parameter is shown in Figures 39 - 44. It is interesting to note how viscosity and surface tension affect the gas hold-up in the reactors.

7.5.1. Water

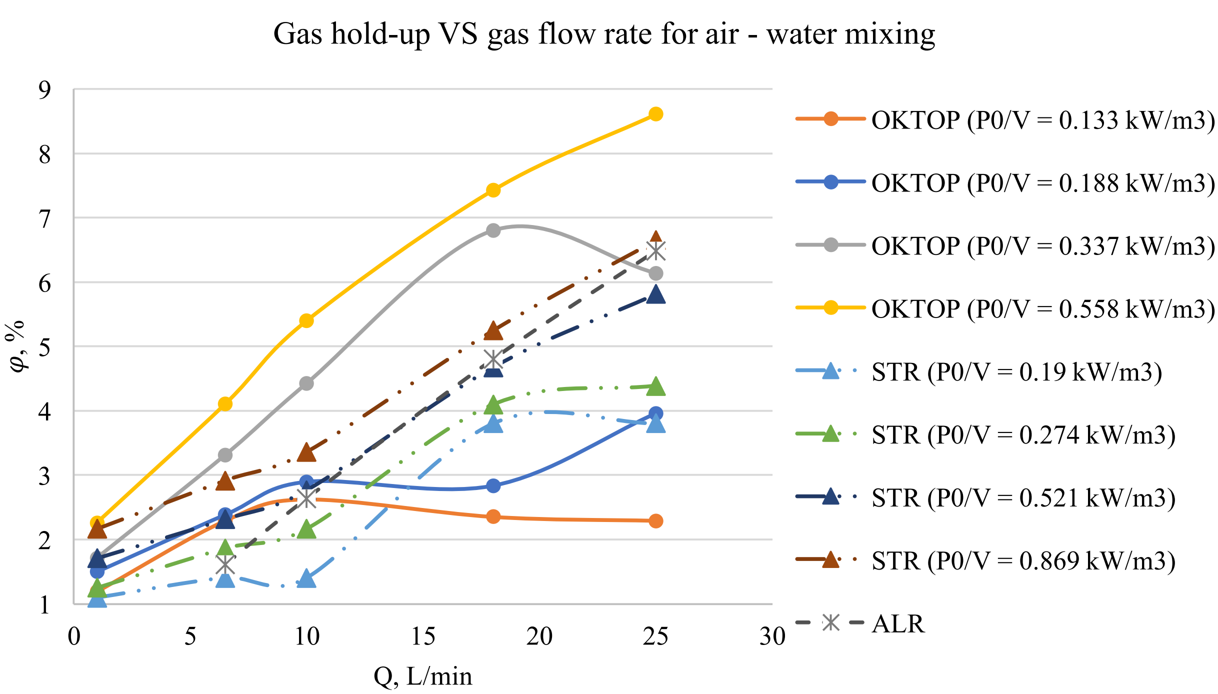

Figure 39. Gas hold-up VS flow rate for air - water mixing.

In the water-air system in OKTOP, the value of gas hold-up is the highest at the mixing power 0.337 and 0.558 kW/m^3 (impeller speeds 550 and 650 rpm) due to the good gas distribution into the reactor as it has a vortex motion principle of gas in the liquid. The low value at the mixing power 0.133 and 0.188 kW/m^3 can be explained due to the flooding effect inside the reactor. The gas hold-up of the ALR has the linear dependence. For STR gas hold-up increase progressively.

7.5.2. Ethanol solutions

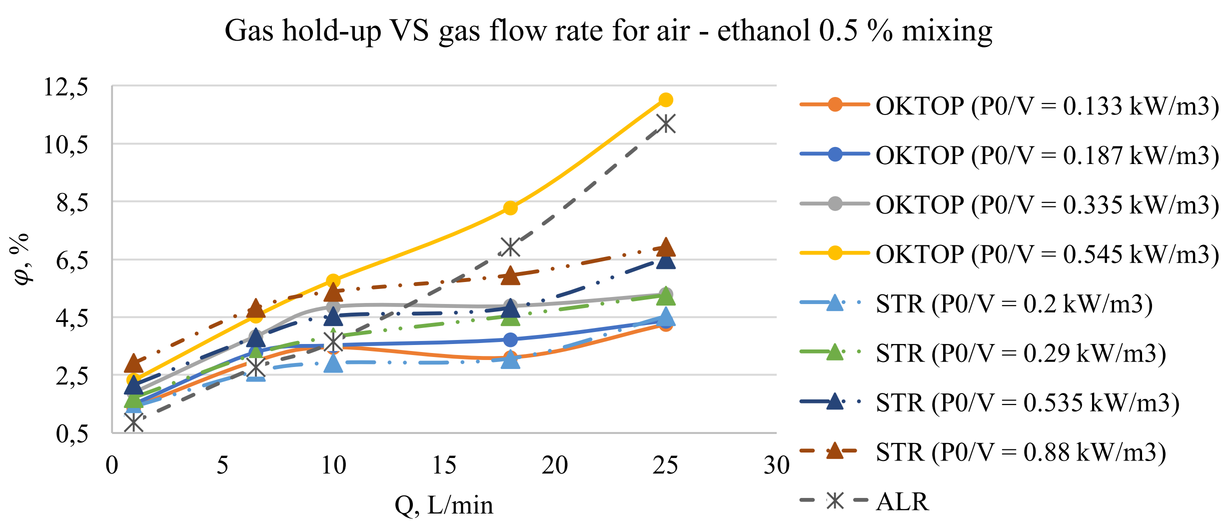

Figure 40. Gas hold-up VS flow rate for air - ethanol 0.05 % mixing.

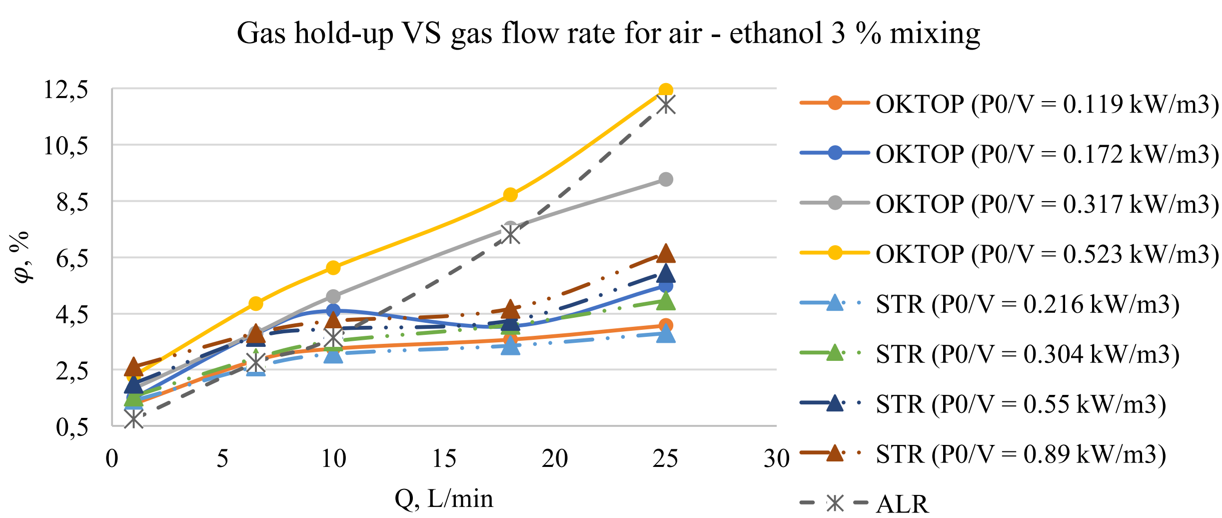

Figure 41. Gas hold-up VS flow rate for air - ethanol 3 % mixing.

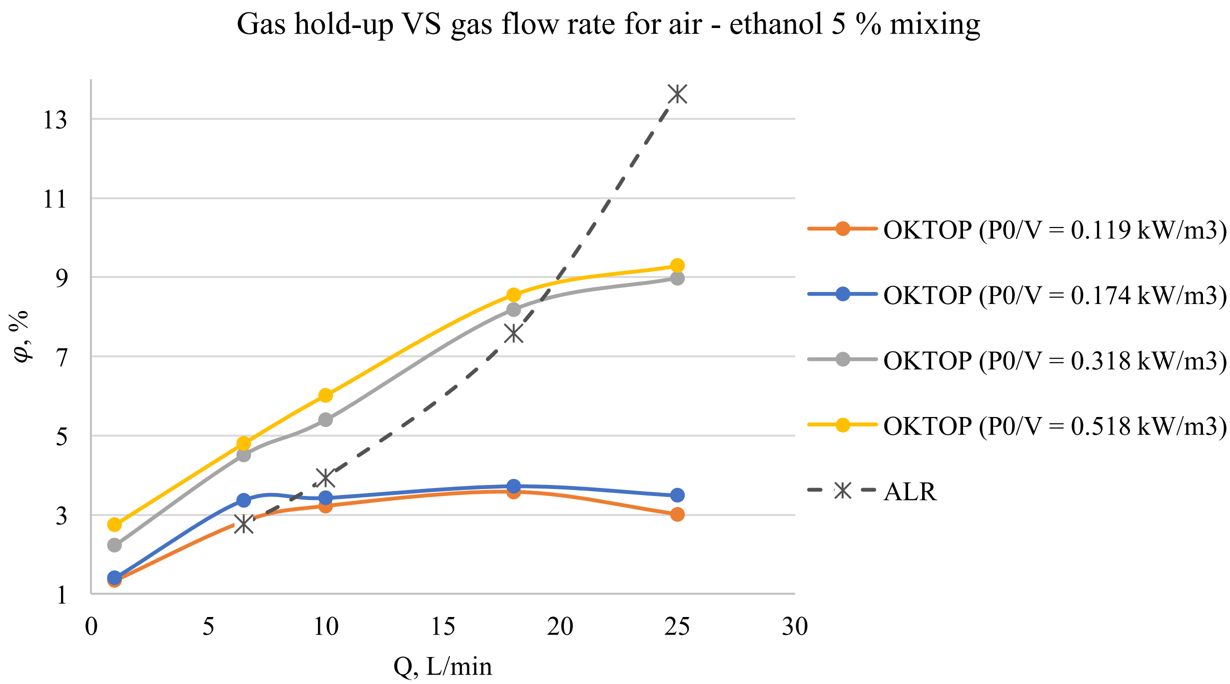

Figure 42. Gas hold-up VS flow rate for air - ethanol 5 % mixing.

In OKTOP the difference between the values of mass transfer coefficients at different gas flow rates at the highest impeller speed and others can be explained be flooding phenomenon. Big amount of gas is going up through the inner tube of it and does not go to the outer. But as it possible to see from the line graph the value of gas hold-up is higher in ethanol solutions than in water. It can be explained due to the lower surface tension in ethanol solution. The value of the gas hold-up has linear dependence with a slight inflection in ALR. For the STR one line is slightly higher than another in all the graphs. In ethanol 5 % for ALR positive effect of the surface tension on gas hold-up is kept. However, for OKTOP reactor picture is different, it can be explained due to replacing molecules of alcohol from solution by air. That is why surface tension can become higher and, as a result, gas hold-up is lower.

7.5.3. CMC solutions

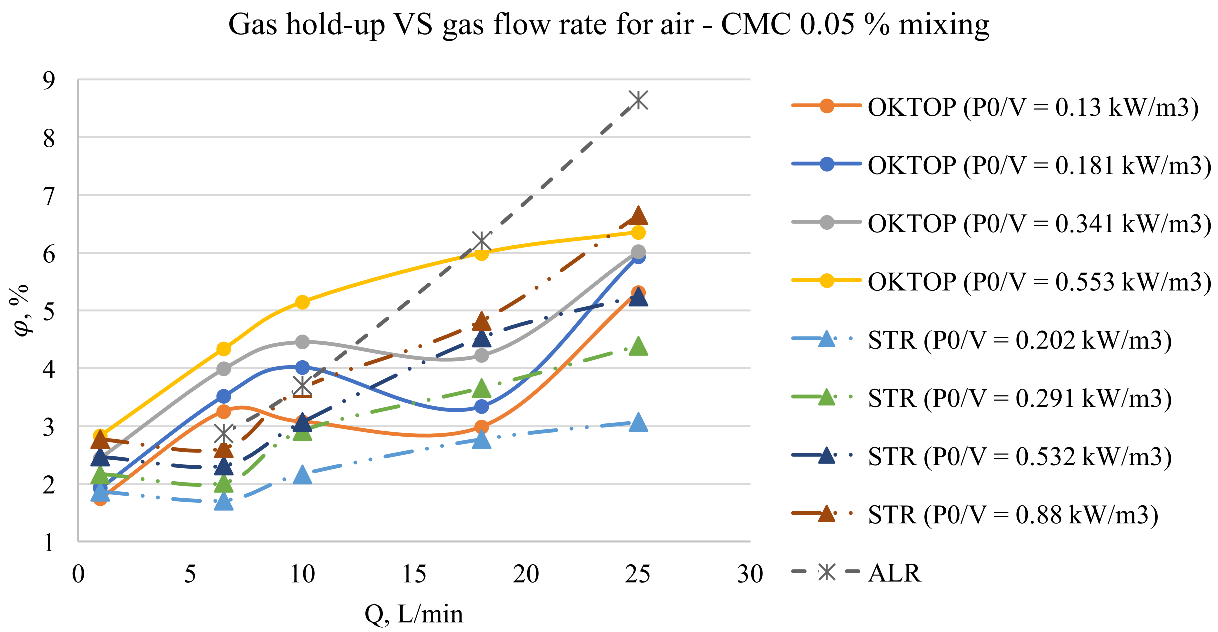

Figure 43. Gas hold-up VS flow rate for air - CMC 0.05 % mixing.

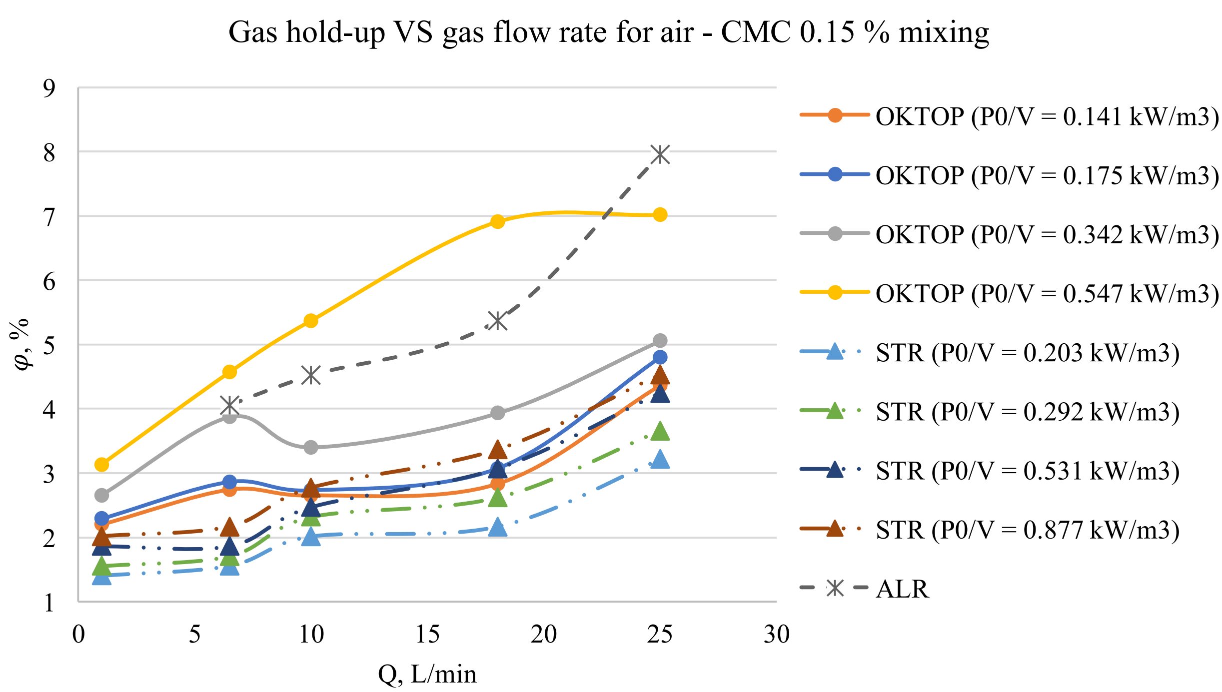

Figure 44. Gas hold-up VS flow rate for air - CMC 0.15 % mixing.

For the ALR at flow rate 25 L/min that gas hold-up value is the highest for both graphs. However, it is possible to note that viscosity makes side effect on the gas hold-up for all the reactors. It is interesting to note that gas hold-up increases slightly at all the impeller speeds for STR. For OKTOP reactor when the mixing power is 0.547 kW/m^3 and gas flow rates are 10 and 25 L/min gas hold-up grows significantly.

CONCLUSIONS

Analysis of volumetric mass transfer, gas hold-up and flooding in the conditions that are close to gas fermentation process was made. Three gas-liquid reactors were studied experimentally and compared at a laboratory scale. The comparison was made with six solutions tested in OKTOP, ALR and STR. The tested fluids were pure water, ethanol 0.5, 3 and 5 %, CMC 0.05 and 0.15 %. Impeller speeds for the analysis were 400, 450, 550 and 650 rpm. The solutions were supplied with air at the following flow rates 1, 6.5, 10, 18 and 25 L/min.

Analysis of viscosity in CMC solutions was made under normal conditions (20 - 25 °C and atmospheric pressure), due to the fact that all the reactors were working under identical operational conditions. The rheology was measured and analyzed.

The dependence of main parameters such as mass transfer, gas hold-up, flooding, bubble size and others on surface tension and viscosity was studied. The positive effect of surface tension reduction and negative effect of viscosity growth on mass transfer, flooding and gas hold-up was observed.

Flooding analysis for OKTOP and STR proves that minimum point of power draw corresponds to maximum value of mass transfer for both reactors.

All the reactors were compared using values of mass transfer, power draw and gas hold-up. STR achieved the highest value of mass transfer in the low viscosity solutions at the impeller speed 650 rpm (~ 0.88 kW/m^3) and gas flow rate 25 L/min, but at high cost of power consumption compared to other reactors. For example, the highest value of mass transfer in ethanol 0.5 % solution is 0.12 1/s at 0.521 kW/m^3. The same relation was observed in water and ethanol 3 %. However, the mass transfer in the CMC solutions at the highest values of the operational conditions was found to be slightly lower than in OKTOP reactor while power draw was 28 % higher.

Ratio between mass transfer and volumetric power draw in ALR makes it the most effective gas-liquid reactor. The dependence of mass transfer and power draw on gas flow rate is almost linear. It is interesting to note that the mass transfer values in water is around twice lower than in the ethanol solutions at the gas flow rate 25 L/min: 0.0288 1/s (water) and 0.0655 1/s (ethanol 5 %). The value of mass transfer in CMC 0.15 % is 0.0141 1/s, which is twice lower than in water and around 50 % times lower than in CMC 0.05 % (0.0222 1/s). For lower flow rates the difference is less significant.

OKTOP reactor provides relatively high value of mass transfer at low energy consumption for all the solutions. The highest efficiency OKTOP reactor reached in ethanol solutions. In ethanol 5 % solution when the gas flow rate is 25 L/min and impeller speed is 550 rpm (0.318 kW/m^3) mass transfer value is 0.0817 1/s (approximately 20 % higher than in ALR) and power draw is 0.173 kW/m^3 (for ALR power draw is 0.233 kW/m^3). In water and CMC solutions value of mass transfer is slightly lower than in ALR at similar power consumption. In water, when the impeller speed and gas flow rate are 650 rpm (0.558 kW/m^3) and 6.5 L/min correspondingly, value of mass transfer is 0.0367 1/s (0.0288 1/s - 22 % higher in ALR) and power draw is 0.450 kW/m^3 (0.233 kW/m^3 - twice higher in ALR).

Gas-liquid mixing process in STR is effective, however, power consumption is high. ALR is conventional technology widely used for gas liquid mixing and it is quite efficient. Mass transfer values, achieved in OKTOP reactor are high and values of power draw are quite low. Gas-liquid mixing in OKTOP reactor is more efficient than in ALR in ethanol solutions.

Gas hold-up in STR in all the solutions has slight growth depending on impeller speed. As for ALR, value of gas hold-up increases when gas flow rate rises. In OKTOP reactor picks of gas hold-up values correspond to maximum values of mass transfer and minimum values of power draw. It proves the dependence between these parameters. At constant gas flow rate, the higher the impeller speed, the bigger the value of gas hold-up is.

The viscosity of microorganism’s solution is close to water. The bacteria produce ethanol and they are tolerant up to 3 % of ethanol content. According to the experimental data OKTOP reactor can be successfully utilized for the gas fermentation. Moreover, ALR reaches high values of mass transfer at high gas flow rates. Therefore, contact time is short and off-gases are not used effectively.

REFERENCES

[1] IBC Finland, "Tackling mass transfer challenges in fermentations.," 2016. [Online]. Available: https://www.ibcfinland.fi/projects/fermatra-tackling-mass-transfer-/. [Accessed 22 January 2017].

[2] Raj SB, Ramaswamy S, Plapp BV, "Yeast alcohol dehydrogenase structure and catalysis.," *Biochemistry. 53: 5791-803.*

[3] Khan academy, "Science," [Online]. Available: https://www.khanacademy.org/science/biology/cellular-respiration-and-fermentation/variations-on-cellular-respiration/a/fermentation-and- anaerobic-respiration. [Accessed 12 February 2017].

[4] B. Sarfraz, "Aerobic and anaerobic fermentation," 2016. [Online]. Available: http://www.slideshare.net/HazemHussein8/aerobic-and-anaerobic-fermentation. [Accessed 12 February 2017].

[5] BBC, "GCSE Bitesize: What is aerobic respiration?," 13 February 2017. [Online]. Available: http://www.bbc.co.uk/schools/gcsebitesize/science/add_aqa/respiration/respirationrev1.shtml.

[6] B. Molitor and others, "Carbon recovery by fermentation of CO-rich off gases - turning steel mills into biorefineries," *Bioresource Technology,* p. 386-396, 9 March 2016.

[7] LanzaTech, "LanzaTech," 2017. [Online]. Available: http://www.lanzatech.com. [Accessed 14 February 2017].

[8] F. Liew and others, "Gas Fermentation—A flexible platform for commercial scale production of low-carbon-fuels and chemicals from waste and renewable Feedstocks," *Frontiers in Microbiology,* vol. 7, 2016.

[9] INEOS AT A GLANCE, 2016. [Online]. Available: http://www.ineos.com/company/ . [Accessed 14 February 2017].

[10] D. v. d. Hoeven, "Gas fermentation: Another promising biobased technology.," 2016. [Online]. Available: http://www.biobasedpress.eu/2016/07/gas-fermentation-another-promising-biobased-technology/. [Accessed 22 January 2017].

[11] L. Q. a. others, "The global carbon budget 1959-2011.," 2012.

[12] Edward L. Paul and others, Handbook of industrial mixing : science and practice, TP156,M5K74, 2003.

[13] N. Kantarci and others, "Bubble column reactors," *Process Biochemistry,* p. 2263-2283, 4 October 2004.

[14] P. Zehner and M. Kraume, "Bubble Columns.," 2000. [Online]. Available: https://www.researchgate.net/publication/228033687_Bubble_Columns. [Accessed 15 February 2017].

[15] J.C. Merchuk, and M. Gluz, "Bioreactors, air-lift reactors," *Encyclopedia of Bioprocess Technology,* p. 320-353, 2002.

[16] "The advantages and disadvantages of airlift Bioreactor," [Online]. Available: http://upotency.blogspot.fi/2010/04/advantages-and-disadvantages-of-airlift.html. [Accessed 15 February 2017].

[17] "Training - evaluation chemical reaction hazards," 2003. [Online]. Available: http://www.safety- s2s.eu/modules.php?name=s2s_wp4&idpart=2&op=v&idp=1492 . [Accessed 5 March 2017].

[18] "Continuous stirred tank reactors," [Online]. Available: http://www.umich.edu/~elements/5e/asyLearn/bits/cstr/index.htm. [Accessed 5 March 2017].

[19] R. Rakoczy and others, "The effects of power characteristics on the heat transfer process in various types of motionless mixing devices.," *Chemical Engineering and Processing: Process Intensification,* 2011.

[20] S. Agrawal, "Bubble dynamics and interface phenomenon.," *Journal of Engineering and Technology Research,* pp. 42-50, 2013.

[21] G.M. Ostrovsky, Processes and apparatus of chemical technologies, Moscow: Goskhimizdat, 1996.

[22] G.B. Tatterson, Fluid Mixing and Gas Dispersion in Agitated Tanks., New York: NY, McGraw-Hill, 1991.

[23] "METHODS OF BUBBLE MEASUREMENTS," 2017. [Online]. Available: http://magde.info/main/texts/MS/Chap4.pdf. [Accessed 21 March 2017].

[24] O. Noraishah and others, "THE HYDRODYNAMICS STUDIES OF BUBBLING PHENOMENA USING HIGH SPEED CAMERA: A VISUAL OBSERVATION.," *Mara Technological University,* 2014.

[25] "GAS HOLDUPS IN FERMENTOR.," January 2008. [Online]. Available: http://fermentationtechnology.blogspot.fi/2008/01/gas-holdups-in- fermentor.html. [Accessed 21 March 2017].

[26] M. Han and others, "Local gas distribution and mass transfer characteristics in an annulus-rising airlift reactor with non- Newtonian fluid.," *Chemical Engineering Journal,* pp. 929-939, 2017.

[27] E. Nauman and C. Collinge, "Measurement of contact time distributions in gas fluidized beds.," *Chemical Engineering Science,* pp. 1317-1326, 1968.

[28] W. Lu, Multiple impeller gas-liquid contactors., Taipei: Gau Lih, 2004.

[29] Bates and others, Ind. Eng. Chem. Process. Des. Dev., 1963, p. 311.

[30] Dickey, Chemical engineering, 1984, pp. 102-110.

[31] V.O. Reykhsfel and others, Equipment for the production of basic organic synthesis and synthetic rubbers., Moscow: Chemistry, 1965.

[32] M. Alvarez-Cuenca and others, "Oxygen mass transfer in bubble columns.," *Chemical Engineering Science,* pp. 1121-1127, 1980.

[33] H. Ghahremani and others, " Measuring surface tension of binary mixtures of water + alcohols from the diffraction pattern of surface ripples.," *Pelagia Research Library*, pp. 212-221, 2011.

Appendix I: Samples of experimental data

Table A-1. Measurements of oxygen concentration temporal history in aerated ethanol (3 w %) solution in OKTOP reactor.

№	τ, s	C, mg/L	t, ℃
1	0	0.1	18.26
2	6	0.1	18.27
3	12	0.11	18.28
4	18	0.1	18.27
5	24	0.1	18.27
6	30	0.1	18.27
7	36	0.1	18.25
8	42	0.1	18.26
9	48	0.1	18.27
10	54	0.1	18.27
11	60	0.41	18.27
12	66	1.81	18.28
13	72	3.65	18.28
14	78	5.27	18.28
15	84	6.47	18.29
16	90	7.29	18.29
17	96	7.86	18.28
18	102	8.21	18.28
19	108	8.45	18.28
20	114	8.59	18.29
21	120	8.68	18.29
22	126	8.73	18.3
23	132	8.77	18.29
24	138	8.79	18.29
25	144	8.8	18.29
26	150	8.81	18.28
27	156	8.82	18.28
28	162	8.83	18.28
29	168	8.83	18.28
30	174	8.84	18.29
31	180	8.84	18.28
32	186	8.84	18.28
33	192	8.83	18.29
34	198	8.83	18.28
35	204	8.84	18.28

Table A-2. Bubble size measurement CMC 0.15 % solution in OKTOP.

bubble size - d, [mm]										
rpm	Q, L/min									
	1		6.5		10		18		25	
	min	max	min	max	min	max	min	max	min	max
400	1	7	1	14	1	18	1	24	1	26
450	1	6	1	13	1	17	1	23	1	26
550	1	5	1	12	1	15	1	22	1	23
650	1	3	1	9	1	12	1	18	1	20

Table A-3. Torque measurement CMC 0.15 % solution in OKTOP.

Torque - M, [mNm]						
rpm	Q, L/min					
	0	1	6.5	10	18	25
400	48.92	38.76	31.22	24.56	24.25	22.78
450	53.87	42.38	34.81	34.25	33.03	28.59
550	86.21	62.29	53.38	46.68	45.39	44.36
650	116.5	90.98	75.7	69.13	60.55	60.27

Table A-4. Gas hold-up measurement CMC 0.15 % solution in OKTOP.

CMC 0.15 % - AIR		**ΔH, mm**								
N, rpm	Q, L/min	1			2			3		
		min	max	eye average	min	max	eye average	min	max	eye average
400	0	-1	1	0	-1	1	0	-1	1	0
	1	5	19	12	6	18	12	5	18	11
	6.5	6	25	16	6	26	16	5	21	13
	10	6	24	15	5	23	14	6	22	14
	18	4	28	15	6	25	15	-4	33	13
	25	6	41	21	3	43	28	6	45	21
450	0	-1	1	0	-1	1	0	-1	1	0
	1	6	18	12	7	20	14	6	17	12
	6.5	6	26	16	7	27	17	6	21	14
	10	5	21	13	8	22	15	4	22	13
	18	3	28	18	4	30	20	2	33	17
	25	14	44	29	11	42	26	8	40	28
550	0	-1	1	0	-1	1	0	-1	1	0
	1	8	22	15	9	21	15	8	18	13
	6.5	10	31	21	12	33	23	11	30	21
	10	7	33	20	8	30	19	6	27	17
	18	5	38	21	7	35	23	5	39	23
	25	9	44	27	10	46	28	12	47	30
650	0	-1	1	0	-1	1	0	-1	1	0
	1	10	25	18	11	25	18	10	21	16
	6.5	13	40	27	14	35	25	13	36	25
	10	17	43	30	16	42	29	17	44	31
	18	19	63	41	19	60	40	14	59	37
	25	18	61	40	20	62	41	18	59	39

Table A-5. Viscosity analysis of CMC 0.15 % solution for share rate 1-30.

Meas. Pts.	Shear Rate	Shear Stress	Viscosity	Speed	Torque
	1/s	Pa	Pa·s	1/min	μNm
1	0.998	0.0681	0.0682	0.773	3.62
2	2	0.132	0.0662	1.55	7.03
3	3	0.191	0.0638	2.32	10.2
4	4	0.247	0.0618	3.1	13.1
5	5	0.3	0.06	3.87	15.9
6	6	0.35	0.0584	4.65	18.6
7	7	0.399	0.057	5.42	21.2
8	8	0.446	0.0558	6.2	23.7
9	9	0.492	0.0547	6.97	26.1
10	10	0.537	0.0537	7.74	28.5
11	11	0.58	0.0527	8.52	30.8
12	12	0.621	0.0518	9.29	33
13	13	0.663	0.051	10.1	35.2
14	14	0.703	0.0502	10.8	37.4
15	15	0.742	0.0495	11.6	39.4
16	16	0.782	0.0489	12.4	41.5
17	17	0.818	0.0481	13.2	43.5
18	18	0.856	0.0476	13.9	45.5
19	19	0.892	0.0469	14.7	47.4
20	20	0.928	0.0464	15.5	49.3
21	21	0.962	0.0458	16.3	51.1
22	22	0.999	0.0454	17	53
23	23	1.03	0.0448	17.8	54.7
24	24	1.07	0.0444	18.6	56.6
25	25	1.1	0.0439	19.4	58.3
26	26	1.13	0.0434	20.1	59.9
27	27	1.16	0.0431	20.9	61.9
28	28	1.19	0.0426	21.7	63.4
29	29	1.22	0.0421	22.5	64.9
30	30	1.26	0.0418	23.2	66.7

Appendix II: Experimental data

Table A-6. OKTOP reactor experimental data.

OKTOP													
	Q, m^3/s	N, rps	k_La, 1/s	P_0, W	P, W	P_{tot}, W/m^3	ε	D, m	V_L, m^3	ρ, kg/m^3	σ, N/m	μ, Pa·s	D_L, m^2/s
Water	0.000017	6.67	0.0066	1.721138667	1.654570667	127.8216753	0.011908992	0.073	0.0135	1000	0.073	0.001002	0.000024
	0.000017	7.5	0.00818	2.500539	2.394093	178.5092155	0.014995941	0.073	0.0135	1000	0.073	0.001002	0.000024
	0.000017	9.167	0.00949	4.604182	4.581731	320.9352844	0.017145353	0.073	0.0135	1000	0.073	0.001002	0.000024
	0.000017	10.83	0.0148	7.584356	6.866604333	523.3028706	0.022629581	0.073	0.0135	1000	0.073	0.001002	0.000024
	0.00011	6.67	0.0151	1.721138667	0.834402667	118.2728167	0.022932466	0.073	0.0135	1000	0.073	0.001002	0.000024
	0.00011	7.5	0.02	2.500539	1.934397	167.188242	0.023839997	0.073	0.0135	1000	0.073	0.001002	0.000024
	0.00011	9.167	0.0251	4.604182	3.582373667	275.3125179	0.033120034	0.073	0.0135	1000	0.073	0.001002	0.000024
	0.00011	10.83	0.0367	7.584356	5.906654	421.4524489	0.041060065	0.073	0.0135	1000	0.073	0.001002	0.000024
	0.00017	6.67	0.0114	1.721138667	0.819749333	130.3482466	0.026251857	0.073	0.0135	1000	0.073	0.001002	0.000024
	0.00017	7.5	0.0158	2.500539	1.287714	155.3022236	0.028950992	0.073	0.0135	1000	0.073	0.001002	0.000024
	0.00017	9.167	0.0313	4.604182	2.919205667	272.1030052	0.04425763	0.073	0.0135	1000	0.073	0.001002	0.000024
	0.00017	10.83	0.0465	7.584356	5.412732	415.0957179	0.054007568	0.073	0.0135	1000	0.073	0.001002	0.000024
	0.0003	6.67	0.0124	1.721138667	0.747738667	169.2882296	0.023537674	0.073	0.0135	1000	0.073	0.001002	0.000024
	0.0003	7.5	0.0169	2.500539	1.136994	190.0050112	0.028352478	0.073	0.0135	1000	0.073	0.001002	0.000024
	0.0003	9.167	0.0238	4.604182	2.536387333	270.1183215	0.067989682	0.073	0.0135	1000	0.073	0.001002	0.000024
	0.0003	10.83	0.0351	7.584356	4.383387667	374.8679997	0.074283598	0.073	0.0135	1000	0.073	0.001002	0.000024
	0.00042	6.67	0.0142	1.721138667	0.676984	198.14548	0.022932466	0.073	0.0135	1000	0.073	0.001002	0.000024
	0.00042	7.5	0.0162	2.500539	1.093662	219.9594571	0.039599542	0.073	0.0135	1000	0.073	0.001002	0.000024
	0.00042	9.167	0.025	4.604182	2.186382	296.9291582	0.061330218	0.073	0.0135	1000	0.073	0.001002	0.000024
	0.00042	10.83	0.0361	7.584356	3.879260667	391.2446524	0.086090294	0.073	0.0135	1000	0.073	0.001002	0.000024

	Q, m^3/s	N, rps	k_La, 1/s	P_0, W	P, W	P_{tot}, W/m^3	ε	D, m	V_L, m^3	ρ, kg/m^3	σ, N/m	μ, Pa·s	D_L, m^2/s
Ethanol 0.5 %	0.000017	6.67	0.0155	1.930053333	1.895722667	136.0363007	0.013763479	0.073	0.0135	1000	0.07056	0.001002	0.000011
	0.000017	7.5	0.0176	2.707308	2.574486	182.847565	0.014995941	0.073	0.0135	1000	0.07056	0.001002	0.000011
	0.000017	9.167	0.0227	4.864383333	4.760763333	333.6253121	0.018980255	0.073	0.0135	1000	0.07056	0.001002	0.000011
	0.000017	10.83	0.0256	7.89867	7.823833333	544.871519	0.023235164	0.073	0.0135	1000	0.07056	0.001002	0.000011
	0.00011	6.67	0.0218	1.930053333	1.474125333	135.9372693	0.029847382	0.073	0.0135	1000	0.07056	0.001002	0.000011
	0.00011	7.5	0.0362	2.707308	2.101602	179.2115222	0.032823433	0.073	0.0135	1000	0.07056	0.001002	0.000011
	0.00011	9.167	0.053	4.864383333	3.779827333	294.9512003	0.038427917	0.073	0.0135	1000	0.07056	0.001002	0.000011
	0.00011	10.83	0.081	7.89867	7.26596	535.3741428	0.0454151	0.073	0.0135	1000	0.07056	0.001002	0.000011
	0.00017	6.67	0.0227	1.930053333	1.058389333	125.9604318	0.035191159	0.073	0.0135	1000	0.07056	0.001002	0.000011
	0.00017	7.5	0.0425	2.707308	1.356951	146.5508916	0.034600315	0.073	0.0135	1000	0.07056	0.001002	0.000011
	0.00017	9.167	0.058	4.864383333	3.368801333	285.2991904	0.048583735	0.073	0.0135	1000	0.07056	0.001002	0.000011
	0.00017	10.83	0.098	7.89867	5.558323333	436.3007077	0.057683119	0.073	0.0135	1000	0.07056	0.001002	0.000011
	0.0003	6.67	0.0208	1.930053333	1.005218667	162.7984795	0.031039997	0.073	0.0135	1000	0.07056	0.001002	0.000011
	0.0003	7.5	0.0274	2.707308	1.272642	181.2414679	0.03725343	0.073	0.0135	1000	0.07056	0.001002	0.000011
	0.0003	9.167	0.0503	4.864383333	2.345841667	255.2552381	0.04887075	0.073	0.0135	1000	0.07056	0.001002	0.000011
	0.0003	10.83	0.11	7.89867	4.517413333	405.0188012	0.082900258	0.073	0.0135	1000	0.07056	0.001002	0.000011
	0.00042	6.67	0.0238	1.930053333	0.90432	193.2291723	0.043677841	0.073	0.0135	1000	0.07056	0.001002	0.000011
	0.00042	7.5	0.0309	2.707308	1.21047	214.3429655	0.042516152	0.073	0.0135	1000	0.07056	0.001002	0.000011
	0.00042	9.167	0.0428	4.864383333	2.204803333	282.9176781	0.052870854	0.073	0.0135	1000	0.07056	0.001002	0.000011
	0.00042	10.83	0.113	7.89867	3.6738	384.227793	0.120261185	0.073	0.0135	1000	0.07056	0.001002	0.000011

	Q, m^3/s	N, rps	k_La, 1/s	P_0, W	P, W	P_{tot}, W/m^3	ε	D, m	V_L, m^3	ρ, kg/m^3	σ, N/m	μ, Pa·s	D_L, m^2/s
Ethanol 3 %	0.000017	6.67	0.0155	1.721138667	1.654570667	119.3812281	0.012837106	0.073	0.0135	1000	0.06287	0.001002	0.000011
	0.000017	7.5	0.0182	2.500539	2.394093	170.3827683	0.014995941	0.073	0.0135	1000	0.06287	0.001002	0.000011
	0.000017	9.167	0.0196	4.604182	4.581731	321.2543545	0.018369383	0.073	0.0135	1000	0.06287	0.001002	0.000011
	0.000017	10.83	0.026	7.584356	6.866604333	478.8318258	0.022932466	0.073	0.0135	1000	0.06287	0.001002	0.000011
	0.00011	6.67	0.0238	1.721138667	0.834402667	91.66381661	0.028352478	0.073	0.0135	1000	0.06287	0.001002	0.000011
	0.00011	7.5	0.039	2.500539	1.934397	167.5254948	0.037841032	0.073	0.0135	1000	0.06287	0.001002	0.000011
	0.00011	9.167	0.0549	4.604182	3.582373667	281.179058	0.038134564	0.073	0.0135	1000	0.06287	0.001002	0.000011
	0.00011	10.83	0.0814	7.584356	5.906654	441.4742534	0.048583735	0.073	0.0135	1000	0.06287	0.001002	0.000011
	0.00017	6.67	0.0231	1.721138667	0.819749333	109.2634992	0.032526649	0.073	0.0135	1000	0.06287	0.001002	0.000011
	0.00017	7.5	0.0434	2.500539	1.287714	141.5369245	0.045992784	0.073	0.0135	1000	0.06287	0.001002	0.000011
	0.00017	9.167	0.0594	4.604182	2.919205667	254.0535912	0.051160651	0.073	0.0135	1000	0.06287	0.001002	0.000011
	0.00017	10.83	0.102	7.584356	5.412732	426.0209245	0.061330218	0.073	0.0135	1000	0.06287	0.001002	0.000011
	0.0003	6.67	0.0235	1.721138667	0.747738667	144.6194706	0.03578128	0.073	0.0135	1000	0.06287	0.001002	0.000011
	0.0003	7.5	0.0296	2.500539	1.136994	171.4646659	0.040476389	0.073	0.0135	1000	0.06287	0.001002	0.000011
	0.0003	9.167	0.0665	4.604182	2.536387333	267.974551	0.075369525	0.073	0.0135	1000	0.06287	0.001002	0.000011
	0.0003	10.83	0.115	7.584356	4.383387667	395.3538843	0.087148714	0.073	0.0135	1000	0.06287	0.001002	0.000011
	0.00042	6.67	0.0272	1.721138667	0.676984	176.960353	0.040768316	0.073	0.0135	1000	0.06287	0.001002	0.000011
	0.00042	7.5	0.0331	2.500539	1.093662	205.6967668	0.054858315	0.073	0.0135	1000	0.06287	0.001002	0.000011
	0.00042	9.167	0.0694	4.604182	2.186382	281.0567668	0.092665437	0.073	0.0135	1000	0.06287	0.001002	0.000011
	0.00042	10.83	0.117	7.584356	3.879260667	397.8070197	0.104265326	0.073	0.0135	1000	0.06287	0.001002	0.000011

	Q, m^3/s	N, rps	k_La, 1/s	P_0, W	P, W	P_{tot}, W/m^3	ε	D, m	V_L, m^3	ρ, kg/m^3	σ, N/m	μ, Pa·s	D_L, m^2/s
Ethanol 5 %	0.000017	6.67	0.016	1.73328	1.674666667	120.7491012	0.013454881	0.073	0.0135	1000	0.05671	0.001002	0.000011
	0.000017	7.5	0.0165	2.523147	2.440722	173.5805035	0.014071883	0.073	0.0135	1000	0.05671	0.001002	0.000011
	0.000017	9.167	0.0212	4.61109	4.538556	318.2587104	0.022326507	0.073	0.0135	1000	0.05671	0.001002	0.000011
	0.000017	10.83	0.028	7.517683333	7.046212333	491.2005265	0.017451647	0.073	0.0135	1000	0.05671	0.001002	0.000011
	0.00011	6.67	0.0257	1.73328	1.042898667	116.4648564	0.028352478	0.073	0.0135	1000	0.05671	0.001002	0.000011
	0.00011	7.5	0.0401	2.523147	1.603284	144.5732702	0.033712691	0.073	0.0135	1000	0.05671	0.001002	0.000011
	0.00011	9.167	0.0593	4.61109	3.378012	266.9683047	0.045125995	0.073	0.0135	1000	0.05671	0.001002	0.000011
	0.00011	10.83	0.0819	7.517683333	6.583585667	488.0423507	0.048009185	0.073	0.0135	1000	0.05671	0.001002	0.000011
	0.00017	6.67	0.0233	1.73328	0.997264	121.325311	0.032229684	0.073	0.0135	1000	0.05671	0.001002	0.000011
	0.00017	7.5	0.0449	2.523147	1.512381	156.8506214	0.034304621	0.073	0.0135	1000	0.05671	0.001002	0.000011
	0.00017	9.167	0.0664	4.61109	3.101692	266.4582765	0.054007568	0.073	0.0135	1000	0.05671	0.001002	0.000011
	0.00017	10.83	0.108	7.517683333	5.583495667	437.6171501	0.060211044	0.073	0.0135	1000	0.05671	0.001002	0.000011
	0.0003	6.67	0.0251	1.73328	0.889666667	154.0889397	0.03578128	0.073	0.0135	1000	0.05671	0.001002	0.000011
	0.0003	7.5	0.0323	2.523147	1.24815	178.8119282	0.03725343	0.073	0.0135	1000	0.05671	0.001002	0.000011
	0.0003	9.167	0.0715	4.61109	2.27964	249.9491696	0.081831959	0.073	0.0135	1000	0.05671	0.001002	0.000011
	0.0003	10.83	0.128	7.517683333	4.474552333	401.3224339	0.085560164	0.073	0.0135	1000	0.05671	0.001002	0.000011
	0.00042	6.67	0.0283	1.73328	0.880456	190.5467684	0.034895827	0.073	0.0135	1000	0.05671	0.001002	0.000011
	0.00042	7.5	0.0359	2.523147	1.237788	215.1903546	0.030145811	0.073	0.0135	1000	0.05671	0.001002	0.000011
	0.00042	9.167	0.0817	4.61109	2.265248333	286.0496879	0.089784067	0.073	0.0135	1000	0.05671	0.001002	0.000011
	0.00042	10.83	0.129	7.517683333	4.301747667	426.4979179	0.092926476	0.073	0.0135	1000	0.05671	0.001002	0.000011

	Q, m^3/s	N, rps	k_La, 1/s	P_0, W	P, W	P_{tot}, W/m^3	ε	D, m	V_L, m^3	ρ, kg/m^3	σ, N/m	μ, Pa·s	D_L, m^2/s
CMC 0.05 %	0.000017	6.67	0.00462	1.882744	1.46952	106.6573534	0.017451647	0.073	0.0135	1000	0.073	0.00867	0.0000197
	0.000017	7.5	0.00511	2.631477	2.113848	151.0937672	0.019285406	0.073	0.0135	1000	0.073	0.00814	0.0000197
	0.000017	9.167	0.00749	4.949582	3.608278667	254.1579511	0.024444081	0.073	0.0135	1000	0.073	0.00786	0.0000197
	0.000017	10.83	0.01	8.026572667	6.386969333	445.7917902	0.028352478	0.073	0.0135	1000	0.073	0.00735	0.0000197
	0.00011	6.67	0.00931	1.882744	1.157613333	114.2016443	0.032526649	0.073	0.0135	1000	0.073	0.00853	0.0000197
	0.00011	7.5	0.0114	2.631477	1.79451	158.1255524	0.035191159	0.073	0.0135	1000	0.073	0.00814	0.0000197
	0.00011	9.167	0.0176	4.949582	3.130475333	250.2610926	0.039892002	0.073	0.0135	1000	0.073	0.00769	0.0000197
	0.00011	10.83	0.0253	8.026572667	5.484847333	412.6315753	0.043387683	0.073	0.0135	1000	0.073	0.00737	0.0000197
	0.00017	6.67	0.00667	1.882744	1.072205333	127.0566603	0.030742119	0.073	0.0135	1000	0.073	0.00827	0.0000197
	0.00017	7.5	0.0146	2.631477	1.685709	169.3672581	0.040184285	0.073	0.0135	1000	0.073	0.00818	0.0000197
	0.00017	9.167	0.0212	4.949582	2.769532333	244.1136948	0.04454726	0.073	0.0135	1000	0.073	0.00771	0.0000197
	0.00017	10.83	0.0292	8.026572667	5.129713333	406.8847983	0.051446114	0.073	0.0135	1000	0.073	0.00737	0.0000197
	0.0003	6.67	0.00725	1.882744	1.04876	166.0543905	0.029847382	0.073	0.0135	1000	0.073	0.00814	0.0000197
	0.0003	7.5	0.0091	2.631477	1.429485	192.3112871	0.033416453	0.073	0.0135	1000	0.073	0.00801	0.0000197
	0.0003	9.167	0.0148	4.949582	2.733265333	282.2271721	0.042225288	0.073	0.0135	1000	0.073	0.00781	0.0000197
	0.0003	10.83	0.0363	8.026572667	4.103090333	376.6978618	0.059930834	0.073	0.0135	1000	0.073	0.00744	0.0000197
	0.00042	6.67	0.00785	1.882744	0.983866667	199.0694341	0.053155288	0.073	0.0135	1000	0.073	0.00799	0.0000197
	0.00042	7.5	0.00942	2.631477	1.333872	223.2077329	0.059369911	0.073	0.0135	1000	0.073	0.00787	0.0000197
	0.00042	9.167	0.0147	4.949582	2.429313333	298.7554111	0.060211044	0.073	0.0135	1000	0.073	0.00767	0.0000197
	0.00042	10.83	0.0221	8.026572667	4.088803333	413.2029973	0.063560589	0.073	0.0135	1000	0.073	0.00737	0.0000197

	Q, m^3/s	N, rps	k_La, 1/s	P_0, W	P, W	P_{tot}, W/m^3	ε	D, m	V_L, m^3	ρ, kg/m^3	σ, N/m	μ, Pa·s	D_L, m^2/s
CMC 0.15 %	0.000017	6.67	0.0027	2.048117333	1.622752	117.2250775	0.022023246	0.073	0.0135	1000	0.073	0.0344	0.0000197
	0.000017	7.5	0.00324	2.537277	1.996098	142.9730775	0.022932466	0.073	0.0135	1000	0.073	0.0331	0.0000197
	0.000017	9.167	0.00405	4.962822333	3.585827667	252.6096063	0.026552501	0.073	0.0135	1000	0.073	0.0298	0.0000197
	0.000017	10.83	0.00527	7.925883333	6.189672667	432.1851235	0.031337693	0.073	0.0135	1000	0.073	0.0267	0.0000197
	0.00011	6.67	0.00291	2.048117333	1.307077333	124.5095064	0.027453323	0.073	0.0135	1000	0.073	0.0341	0.0000197
	0.00011	7.5	0.00385	2.537277	1.639551	147.4387248	0.028651828	0.073	0.0135	1000	0.073	0.0329	0.0000197
	0.00011	9.167	0.00605	4.962822333	3.072908667	246.2909777	0.038721091	0.073	0.0135	1000	0.073	0.0299	0.0000197
	0.00011	10.83	0.00808	7.925883333	5.150123333	389.5471616	0.045704029	0.073	0.0135	1000	0.073	0.0272	0.0000197
	0.00017	6.67	0.00269	2.048117333	1.028245333	124.0249362	0.026552501	0.073	0.0135	1000	0.073	0.0341	0.0000197
	0.00017	7.5	0.00298	2.537277	1.613175	164.3649132	0.027348807	0.073	0.0135	1000	0.073	0.0323	0.0000197
	0.00017	9.167	0.00784	4.962822333	2.687212	238.4364305	0.034008747	0.073	0.0135	1000	0.073	0.0301	0.0000197
	0.00017	10.83	0.0114	7.925883333	4.703144333	377.4662466	0.053723645	0.073	0.0135	1000	0.073	0.0272	0.0000197
	0.0003	6.67	0.00336	2.048117333	1.015266667	163.7445055	0.028352478	0.073	0.0135	1000	0.073	0.0323	0.0000197
	0.0003	7.5	0.00374	2.537277	1.555713	201.0166664	0.030742119	0.073	0.0135	1000	0.073	0.0311	0.0000197
	0.0003	9.167	0.00554	4.962822333	2.612951	273.9296319	0.039306904	0.073	0.0135	1000	0.073	0.0291	0.0000197
	0.0003	10.83	0.0182	7.925883333	4.119418333	377.8239307	0.069090417	0.073	0.0135	1000	0.073	0.0272	0.0000197
	0.00042	6.67	0.00367	2.048117333	0.953722667	196.9905375	0.043677841	0.073	0.0135	1000	0.073	0.0311	0.0000197
	0.00042	7.5	0.00392	2.537277	1.346589	224.0847674	0.048009185	0.073	0.0135	1000	0.073	0.0304	0.0000197
	0.00042	9.167	0.00565	4.962822333	2.553657333	307.3308593	0.05058921	0.073	0.0135	1000	0.073	0.0286	0.0000197
	0.00042	10.83	0.0121	7.925883333	4.100369	414.0006295	0.070188554	0.073	0.0135	1000	0.073	0.0268	0.0000197

Table A-7. STR experimental data.

STR														
	Q, m^3/s	N, rps	k_La, 1/s	P_0, W	P, W	P_{tot}, W/m^3	ε	D, m	V_L, m^3	ρ, kg/m^3	σ, N/m	μ, Pa·s	D_L, m^2/s
Water	0.000017	6.67	0.00436	2.467621333	2.369234667	186.6381978	0.010960128	0.073	0.013	1000	0.073	0.001002	0.000024
	0.000017	7.5	0.00522	3.565941	3.448662	269.6710696	0.012506279	0.073	0.013	1000	0.073	0.001002	0.000024
	0.000017	9.167	0.00697	6.770991333	6.385294667	495.5658901	0.017115862	0.073	0.013	1000	0.073	0.001002	0.000024
	0.000017	10.83	0.00922	11.294894	10.75062733	831.3607103	0.021682611	0.073	0.013	1000	0.073	0.001002	0.000024
	0.00011	6.67	0.0103	2.467621333	1.641592	154.6781606	0.014047603	0.073	0.013	1000	0.073	0.001002	0.000024
	0.00011	7.5	0.0126	3.565941	2.436012	215.7873914	0.018642842	0.073	0.013	1000	0.073	0.001002	0.000024
	0.00011	9.167	0.0178	6.770991333	4.928858	407.544776	0.023195445	0.073	0.013	1000	0.073	0.001002	0.000024
	0.00011	10.83	0.0241	11.294894	8.954547333	717.2131862	0.02920028	0.073	0.013	1000	0.073	0.001002	0.000024
	0.00017	6.67	0.0128	2.467621333	1.458216	156.0642342	0.014047603	0.073	0.013	1000	0.073	0.001002	0.000024
	0.00017	7.5	0.0146	3.565941	2.250438	217.0043881	0.021682611	0.073	0.013	1000	0.073	0.001002	0.000024
	0.00017	9.167	0.0211	6.770991333	4.405577	382.7843112	0.027706004	0.073	0.013	1000	0.073	0.001002	0.000024
	0.00017	10.83	0.0294	11.294894	7.797980667	643.7384394	0.033655679	0.073	0.013	1000	0.073	0.001002	0.000024
	0.0003	6.67	0.0135	2.467621333	1.329685333	179.743086	0.038070369	0.073	0.013	1000	0.073	0.001002	0.000024
	0.0003	7.5	0.0176	3.565941	1.906608	224.1217527	0.040991155	0.073	0.013	1000	0.073	0.001002	0.000024
	0.0003	9.167	0.0288	6.770991333	3.508688333	347.3587014	0.046779836	0.073	0.013	1000	0.073	0.001002	0.000024
	0.0003	10.83	0.0394	11.294894	6.362477333	566.8809322	0.052499053	0.073	0.013	1000	0.073	0.001002	0.000024
	0.00042	6.67	0.016	2.467621333	1.288237333	207.5386179	0.038070369	0.073	0.013	1000	0.073	0.001002	0.000024
	0.00042	7.5	0.0191	3.565941	1.827009	248.9825923	0.043894257	0.073	0.013	1000	0.073	0.001002	0.000024
	0.00042	9.167	0.0336	6.770991333	3.16041	351.5519	0.058150051	0.073	0.013	1000	0.073	0.001002	0.000024
	0.00042	10.83	0.0468	11.294894	5.736570667	549.7181051	0.066501282	0.073	0.013	1000	0.073	0.001002	0.000024

	Q, m^3/s	**N, rps**	**k_La, 1/s**	**P_0, W**	**P, W**	**P_{tot}, W/m^3**	**ε**	**D, m**	**V_L, m^3**	**ρ, kg/m^3**	**σ, N/m**	**μ, Pa·s**	**D_L, m^2/s**
Ethanol 0.5 %	0.000017	6.67	0.0129	2.603269333	2.511162667	197.5557363	0.014047603	0.073	0.013	1000	0.07056	0.001002	0.000011
	0.000017	7.5	0.0157	3.767058	3.639888	284.3807619	0.017115862	0.073	0.013	1000	0.07056	0.001002	0.000011
	0.000017	9.167	0.0216	6.95981	6.64895	515.8470696	0.021682611	0.073	0.013	1000	0.07056	0.001002	0.000011
	0.000017	10.83	0.0246	11.43640333	11.04861333	854.2827103	0.02920028	0.073	0.013	1000	0.07056	0.001002	0.000011
	0.00011	6.67	0.0203	2.603269333	1.732024	161.6344683	0.02620712	0.073	0.013	1000	0.07056	0.001002	0.000011
	0.00011	7.5	0.0306	3.767058	2.592855	227.8522375	0.032175097	0.073	0.013	1000	0.07056	0.001002	0.000011
	0.00011	9.167	0.0569	6.95981	5.088893333	419.8551862	0.038070369	0.073	0.013	1000	0.07056	0.001002	0.000011
	0.00011	10.83	0.089	11.43640333	8.55179	686.2318529	0.048216103	0.073	0.013	1000	0.07056	0.001002	0.000011
	0.00017	6.67	0.0242	2.603269333	1.603912	167.2716189	0.02920028	0.073	0.013	1000	0.07056	0.001002	0.000011
	0.00017	7.5	0.0309	3.767058	2.314494	221.9317727	0.038070369	0.073	0.013	1000	0.07056	0.001002	0.000011
	0.00017	9.167	0.0601	6.95981	4.514953667	391.1979009	0.045339227	0.073	0.013	1000	0.07056	0.001002	0.000011
	0.00017	10.83	0.101	11.43640333	7.7558	640.4937727	0.053918151	0.073	0.013	1000	0.07056	0.001002	0.000011
	0.0003	6.67	0.0246	2.603269333	1.446074667	188.6961117	0.030689971	0.073	0.013	1000	0.07056	0.001002	0.000011
	0.0003	7.5	0.033	3.767058	2.043669	234.6649066	0.045339227	0.073	0.013	1000	0.07056	0.001002	0.000011
	0.0003	9.167	0.0666	6.95981	3.630729667	356.7464963	0.048216103	0.073	0.013	1000	0.07056	0.001002	0.000011
	0.0003	10.83	0.115	11.43640333	6.3271	564.1595989	0.059552284	0.073	0.013	1000	0.07056	0.001002	0.000011
	0.00042	6.67	0.0282	2.603269333	1.390810667	215.4288744	0.045339227	0.073	0.013	1000	0.07056	0.001002	0.000011
	0.00042	7.5	0.0362	3.767058	1.893891	254.1273615	0.052499053	0.073	0.013	1000	0.07056	0.001002	0.000011
	0.00042	9.167	0.0736	6.95981	3.317567	363.6409	0.06511971	0.073	0.013	1000	0.07056	0.001002	0.000011
	0.00042	10.83	0.12	11.43640333	5.371912	521.6674384	0.069252212	0.073	0.013	1000	0.07056	0.001002	0.000011

	Q, m^3/s	N, rps	k_La, 1/s	P_0, W	P, W	P_{tot}, W/m^3	ε	D, m	V_L, m^3	ρ, kg/m^3	σ, N/m	μ, Pa·s	D_L, m^2/s
Ethanol 3 %	0.000017	6.67	0.0136	2.803392	2.548424	200.4219927	0.014047603	0.073	0.013	1000	0.06287	0.001002	0.000011
	0.000017	7.5	0.0159	3.954516	3.865026	301.6990696	0.015584124	0.073	0.013	1000	0.06287	0.001002	0.000011
	0.000017	9.167	0.0216	7.153234	6.992047333	542.2391721	0.020165084	0.073	0.013	1000	0.06287	0.001002	0.000011
	0.000017	10.83	0.0283	11.56974867	11.20236867	866.1100442	0.02620712	0.073	0.013	1000	0.06287	0.001002	0.000011
	0.00011	6.67	0.0317	2.803392	2.062352	187.0443145	0.02620712	0.073	0.013	1000	0.06287	0.001002	0.000011
	0.00011	7.5	0.0385	3.954516	3.017226	260.4961606	0.02920028	0.073	0.013	1000	0.06287	0.001002	0.000011
	0.00011	9.167	0.0672	7.153234	6.001900667	490.0865196	0.036603294	0.073	0.013	1000	0.06287	0.001002	0.000011
	0.00011	10.83	0.0905	11.56974867	9.868915333	787.5491862	0.038070369	0.073	0.013	1000	0.06287	0.001002	0.000011
	0.00017	6.67	0.0313	2.803392	1.831248	184.7590035	0.030689971	0.073	0.013	1000	0.06287	0.001002	0.000011
	0.00017	7.5	0.0382	3.954516	2.560356	240.8442342	0.035131738	0.073	0.013	1000	0.06287	0.001002	0.000011
	0.00017	9.167	0.0668	7.153234	4.879350667	419.2284394	0.039532983	0.073	0.013	1000	0.06287	0.001002	0.000011
	0.00017	10.83	0.106	11.56974867	8.521855333	699.421106	0.042444906	0.073	0.013	1000	0.06287	0.001002	0.000011
	0.0003	6.67	0.0283	2.803392	1.635312	203.2528297	0.033655679	0.073	0.013	1000	0.06287	0.001002	0.000011
	0.0003	7.5	0.0413	3.954516	2.27493	252.4542143	0.040991155	0.073	0.013	1000	0.06287	0.001002	0.000011
	0.0003	9.167	0.0716	7.153234	4.223090667	402.3127271	0.042444906	0.073	0.013	1000	0.06287	0.001002	0.000011
	0.0003	10.83	0.125	11.56974867	7.229222	633.5535989	0.046779836	0.073	0.013	1000	0.06287	0.001002	0.000011
	0.00042	6.67	0.0304	2.803392	1.593445333	231.0161564	0.038070369	0.073	0.013	1000	0.06287	0.001002	0.000011
	0.00042	7.5	0.0402	3.954516	2.221236	279.3077461	0.049648049	0.073	0.013	1000	0.06287	0.001002	0.000011
	0.00042	9.167	0.0746	7.153234	3.572587333	383.2578487	0.059552284	0.073	0.013	1000	0.06287	0.001002	0.000011
	0.00042	10.83	0.131	11.56974867	6.004622	570.3374384	0.066501282	0.073	0.013	1000	0.06287	0.001002	0.000011

	Q, m^3/s	N, rps	k_La, 1/s	P_0, W	P, W	P_{tot}, W/m^3	ε	D, m	V_L, m^3	ρ, kg/m^3	σ, N/m	μ, Pa·s	D_L, m^2/s
CMC 0.05 %	0.000017	6.67	0.00363	2.632157333	2.598664	204.286608	0.018642842	0.073	0.013	1000	0.073	0.00804	0.0000197
	0.000017	7.5	0.00489	3.780717	3.705357	289.4168388	0.021682611	0.073	0.013	1000	0.073	0.00769	0.0000197
	0.000017	9.167	0.00693	6.912029667	6.652979667	516.157044	0.024703607	0.073	0.013	1000	0.073	0.00727	0.0000197
	0.000017	10.83	0.00933	11.43436233	10.937719	845.7523773	0.027706004	0.073	0.013	1000	0.073	0.00708	0.0000197
	0.00011	6.67	0.00714	2.632157333	1.742490667	162.4395965	0.017115862	0.073	0.013	1000	0.073	0.00835	0.0000197
	0.00011	7.5	0.00912	3.780717	2.678577	234.4462375	0.020165084	0.073	0.013	1000	0.073	0.00795	0.0000197
	0.00011	9.167	0.0148	6.912029667	5.185029667	427.2502888	0.023195445	0.073	0.013	1000	0.073	0.0074	0.0000197
	0.00011	10.83	0.0241	11.43436233	8.386469	673.5148529	0.02620712	0.073	0.013	1000	0.073	0.00715	0.0000197
	0.00017	6.67	0.00788	2.632157333	1.637405333	169.8480291	0.021682611	0.073	0.013	1000	0.073	0.00828	0.0000197
	0.00017	7.5	0.0102	3.780717	2.381847	227.1127727	0.02920028	0.073	0.013	1000	0.073	0.00791	0.0000197
	0.00017	9.167	0.0169	6.912029667	4.597849667	397.5745163	0.030689971	0.073	0.013	1000	0.073	0.00742	0.0000197
	0.00017	10.83	0.0245	11.43436233	7.855809	648.1867727	0.036603294	0.073	0.013	1000	0.073	0.00701	0.0000197
	0.0003	6.67	0.00935	2.632157333	1.563301333	197.7135476	0.027706004	0.073	0.013	1000	0.073	0.00802	0.0000197
	0.0003	7.5	0.0124	3.780717	2.043669	234.6649066	0.036603294	0.073	0.013	1000	0.073	0.00785	0.0000197
	0.0003	9.167	0.0205	6.912029667	4.062479667	389.9580348	0.045339227	0.073	0.013	1000	0.073	0.00747	0.0000197
	0.0003	10.83	0.0298	11.43436233	6.644815667	588.5992656	0.048216103	0.073	0.013	1000	0.073	0.0072	0.0000197
	0.00042	6.67	0.0114	2.632157333	1.477474667	222.0953359	0.030689971	0.073	0.013	1000	0.073	0.00795	0.0000197
	0.00042	7.5	0.0134	3.780717	2.029068	264.5255923	0.043894257	0.073	0.013	1000	0.073	0.00789	0.0000197
	0.00042	9.167	0.0235	6.912029667	3.423489667	371.7887974	0.052499053	0.073	0.013	1000	0.073	0.00743	0.0000197
	0.00042	10.83	0.0341	11.43436233	5.733169	549.4564384	0.066501282	0.073	0.013	1000	0.073	0.00722	0.0000197

	Q, m³/s	N, rps	kLa, 1/s	P_0, W	P, W	P_{tot}, W/m³	ε	D, m	V_L, m³	ρ, kg/m³	σ, N/m	μ, Pa·s	D_L, m²/s
CMC 0.15 %	0.000017	6.67	0.0014	2.642205333	2.692864	211.5327619	0.014047603	0.073	0.013	1000	0.073	0.0314	0.0000197
	0.000017	7.5	0.00207	3.793434	3.881511	302.9671465	0.015584124	0.073	0.013	1000	0.073	0.0291	0.0000197
	0.000017	9.167	0.00314	6.903970333	6.685792667	518.6811209	0.018642842	0.073	0.013	1000	0.073	0.0262	0.0000197
	0.000017	10.83	0.00406	11.407149	10.813218	836.1753773	0.020165084	0.073	0.013	1000	0.073	0.0236	0.0000197
	0.00011	6.67	0.00245	2.642205333	1.762168	163.9532375	0.015584124	0.073	0.013	1000	0.073	0.0327	0.0000197
	0.00011	7.5	0.00321	3.793434	2.597094	228.1783145	0.017115862	0.073	0.013	1000	0.073	0.0308	0.0000197
	0.00011	9.167	0.00498	6.903970333	5.164881333	425.700417	0.018642842	0.073	0.013	1000	0.073	0.0272	0.0000197
	0.00011	10.83	0.00746	11.407149	8.299386333	666.8161862	0.021682611	0.073	0.013	1000	0.073	0.0249	0.0000197
	0.00017	6.67	0.00293	2.642205333	1.604330667	167.303824	0.020165084	0.073	0.013	1000	0.073	0.0326	0.0000197
	0.00017	7.5	0.00364	3.793434	2.333805	223.4172342	0.023195445	0.073	0.013	1000	0.073	0.031	0.0000197
	0.00017	9.167	0.00501	6.903970333	5.119403667	437.6940548	0.024703607	0.073	0.013	1000	0.073	0.0272	0.0000197
	0.00017	10.83	0.00948	11.407149	8.242918667	677.9644394	0.027706004	0.073	0.013	1000	0.073	0.0248	0.0000197
	0.0003	6.67	0.00331	2.642205333	1.56372	197.7457527	0.021682611	0.073	0.013	1000	0.073	0.0315	0.0000197
	0.0003	7.5	0.00401	3.793434	2.048379	235.0272143	0.02620712	0.073	0.013	1000	0.073	0.0306	0.0000197
	0.0003	9.167	0.00532	6.903970333	4.059025667	389.6923425	0.030689971	0.073	0.013	1000	0.073	0.0276	0.0000197
	0.0003	10.83	0.00989	11.407149	6.649578	588.9655989	0.033655679	0.073	0.013	1000	0.073	0.0255	0.0000197
	0.00042	6.67	0.00352	2.642205333	1.546136	227.3769769	0.032175097	0.073	0.013	1000	0.073	0.0306	0.0000197
	0.00042	7.5	0.00423	3.793434	2.08182	268.5834384	0.036603294	0.073	0.013	1000	0.073	0.0298	0.0000197
	0.00042	9.167	0.00535	6.903970333	3.464362	374.9328231	0.042444906	0.073	0.013	1000	0.073	0.0277	0.0000197
	0.00042	10.83	0.0116	11.407149	5.826374667	556.6261051	0.045339227	0.073	0.013	1000	0.073	0.0258	0.0000197

Table A-8. ALR experimental data.

ALR								
	Q, m^3/s	**Ug, m/s**	**k_La, 1/s**	**ε**	**V_L, m^3**	**ρ, kg/m^3**	**σ, N/m**	**μ, Pa·s**
Water	0.00011	0.006227884	0.00656	0.016136244	0.014	1000	0.073	0.001002
	0.00017	0.009624912	0.0106	0.026408242	0.014	1000	0.073	0.001002
	0.0003	0.016985138	0.0205	0.048039982	0.014	1000	0.073	0.001002
	0.00042	0.023779193	0.0288	0.064886054	0.014	1000	0.073	0.001002
Ethanol 0.5 %	0.000017	0.000962491	0.00187	0.008753942	0.014	1000	0.07056	0.001002
	0.00011	0.006227884	0.00886	0.027602628	0.014	1000	0.07056	0.001002
	0.00017	0.009624912	0.0124	0.036467967	0.014	1000	0.07056	0.001002
	0.0003	0.016985138	0.0349	0.069278117	0.014	1000	0.07056	0.001002
	0.00042	0.023779193	0.061	0.112027273	0.014	1000	0.07056	0.001002
Ethanol 3 %	0.000017	0.000962491	0.00181	0.007512774	0.014	1000	0.06287	0.001002
	0.00011	0.006227884	0.00791	0.027602628	0.014	1000	0.06287	0.001002
	0.00017	0.009624912	0.0127	0.036467967	0.014	1000	0.06287	0.001002
	0.0003	0.016985138	0.035	0.073087467	0.014	1000	0.06287	0.001002
	0.00042	0.023779193	0.0629	0.119425897	0.014	1000	0.06287	0.001002
Ethanol 5 %	0.00011	0.006227884	0.00811	0.027602628	0.014	1000	0.05671	0.001002
	0.00017	0.009624912	0.0131	0.039387266	0.014	1000	0.05671	0.001002
	0.0003	0.016985138	0.0353	0.075789396	0.014	1000	0.05671	0.001002
	0.00042	0.023779193	0.0655	0.13621903	0.014	1000	0.05671	0.001002
CMC 0.05 %	0.00011	0.006227884	0.00504	0.028794087	0.014	1000	0.073	0.00966
	0.00017	0.009624912	0.00614	0.037053245	0.014	1000	0.073	0.00924
	0.0003	0.016985138	0.0119	0.062119902	0.014	1000	0.073	0.00876
	0.00042	0.023779193	0.0222	0.086441404	0.014	1000	0.073	0.00825
CMC 0.15 %	0.00011	0.006227884	0.00462	0.040550039	0.014	1000	0.073	0.0421
	0.00017	0.009624912	0.00528	0.045173116	0.014	1000	0.073	0.0392
	0.0003	0.016985138	0.00676	0.053722377	0.014	1000	0.073	0.0357
	0.00042	0.023779193	0.0141	0.079545739	0.014	1000	0.073	0.0336

Appendix III: Flooding OKTOP and STR

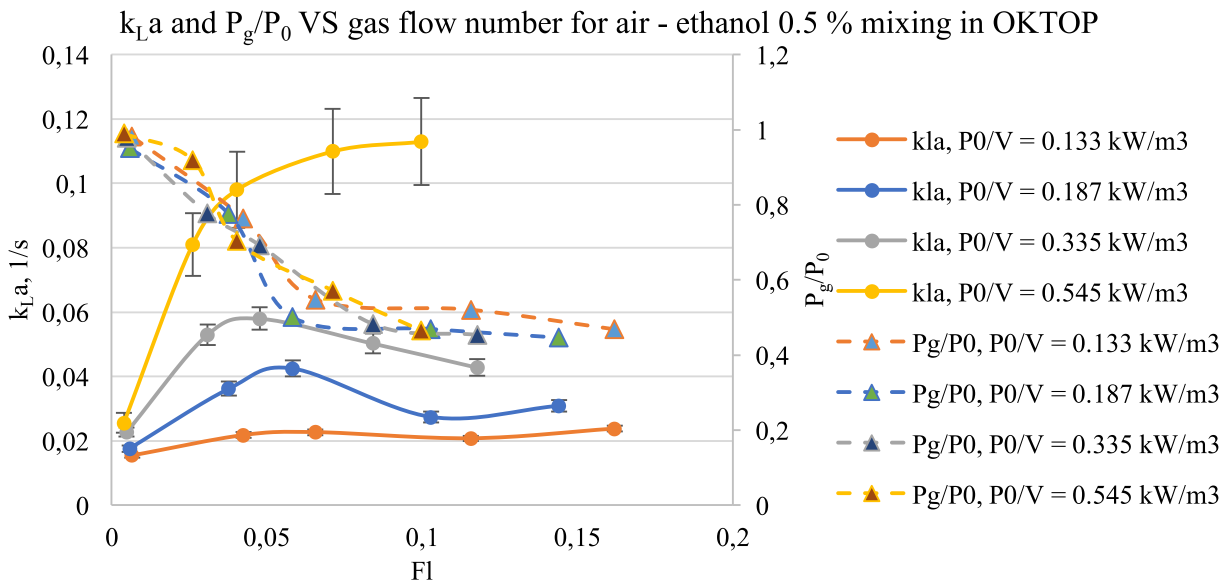

Figure A-1. Flooding for air - ethanol 0.5 % mixing in OKTOP.

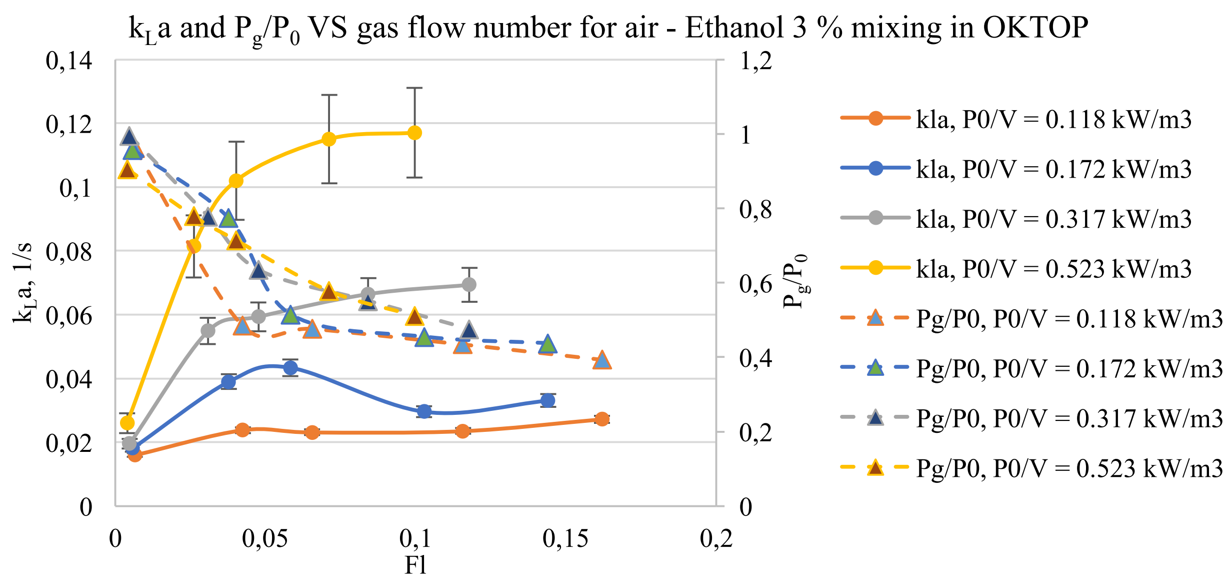

Figure A-2. Flooding for air - ethanol 3% mixing in OKTOP.

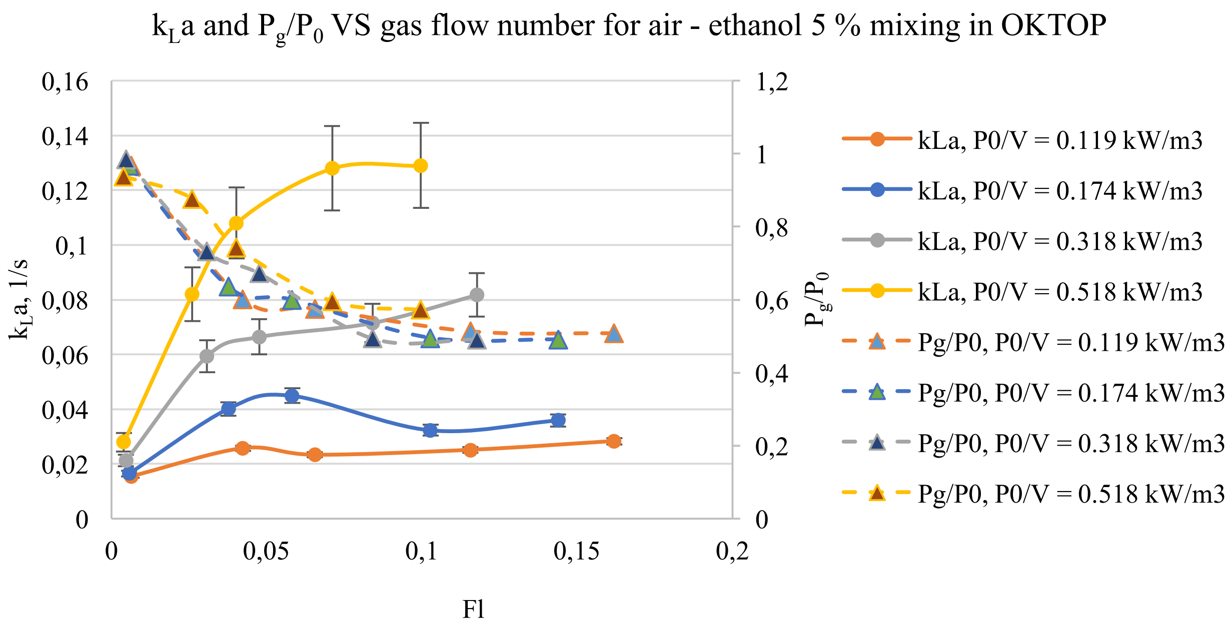

Figure A-3. Flooding for air - ethanol 5 % mixing in OKTOP.

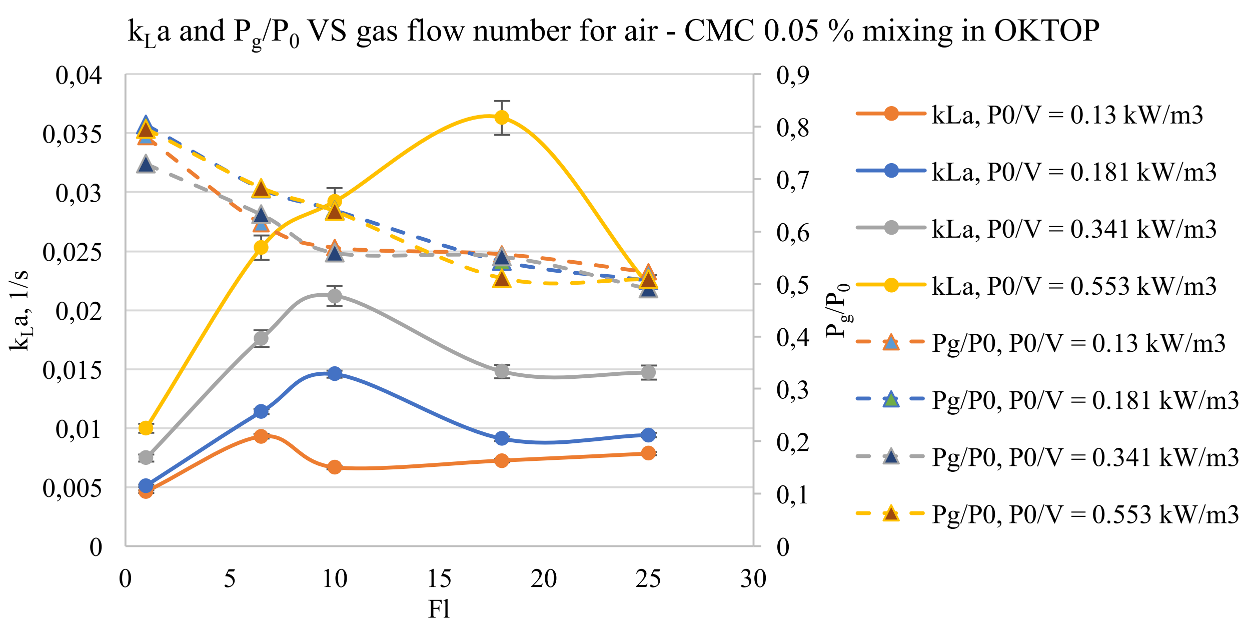

Figure A-4. Flooding for air - CMC 0.05 % mixing in OKTOP.

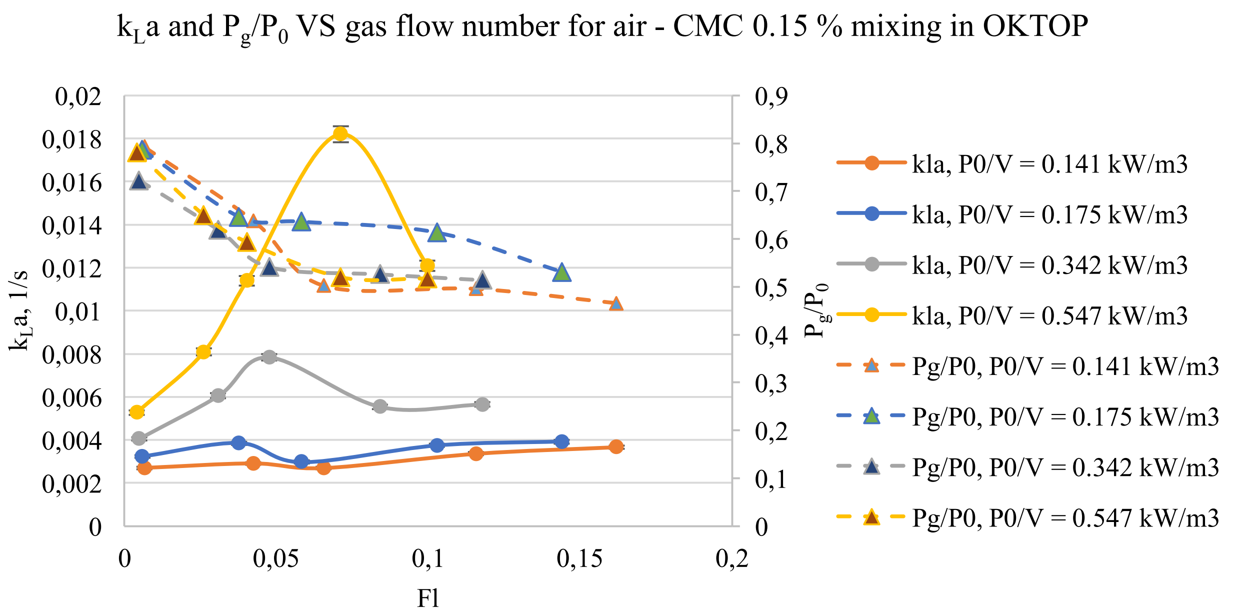

Figure A-5. Flooding for air - CMC 0.15 % mixing in OKTOP.

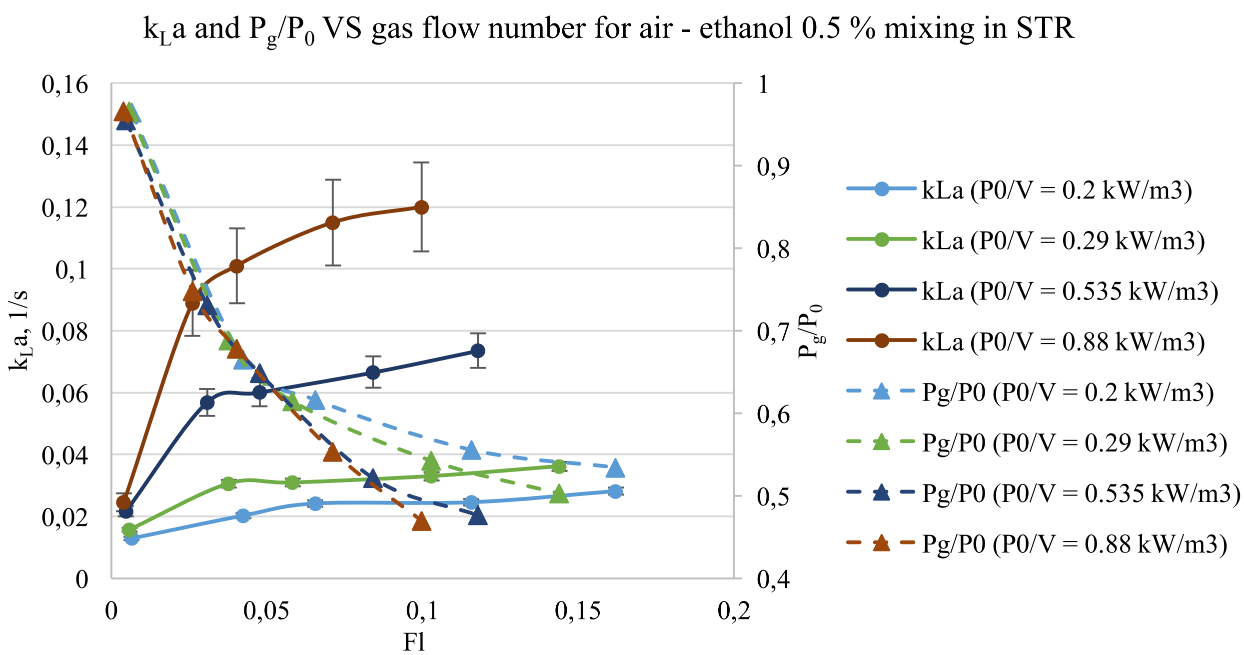

Figure A-6. Flooding for air - ethanol 0.5 % mixing in STR.

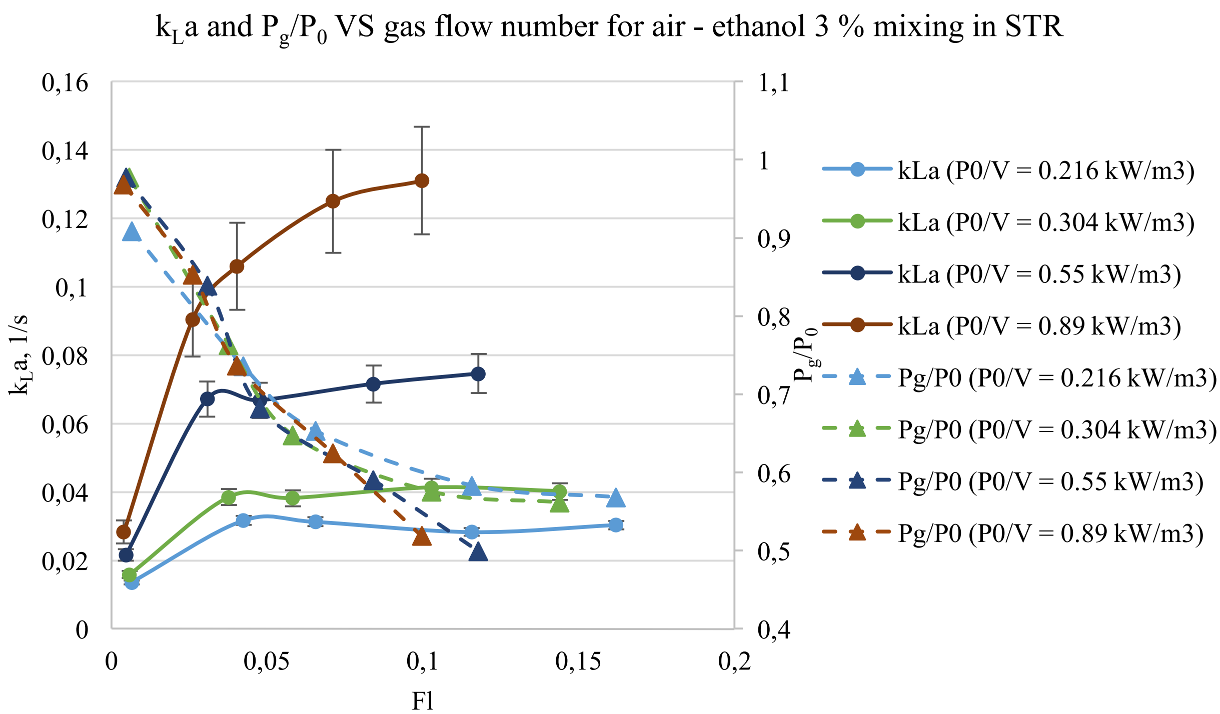

Figure A-7. Flooding for air - ethanol 3 % mixing in STR.

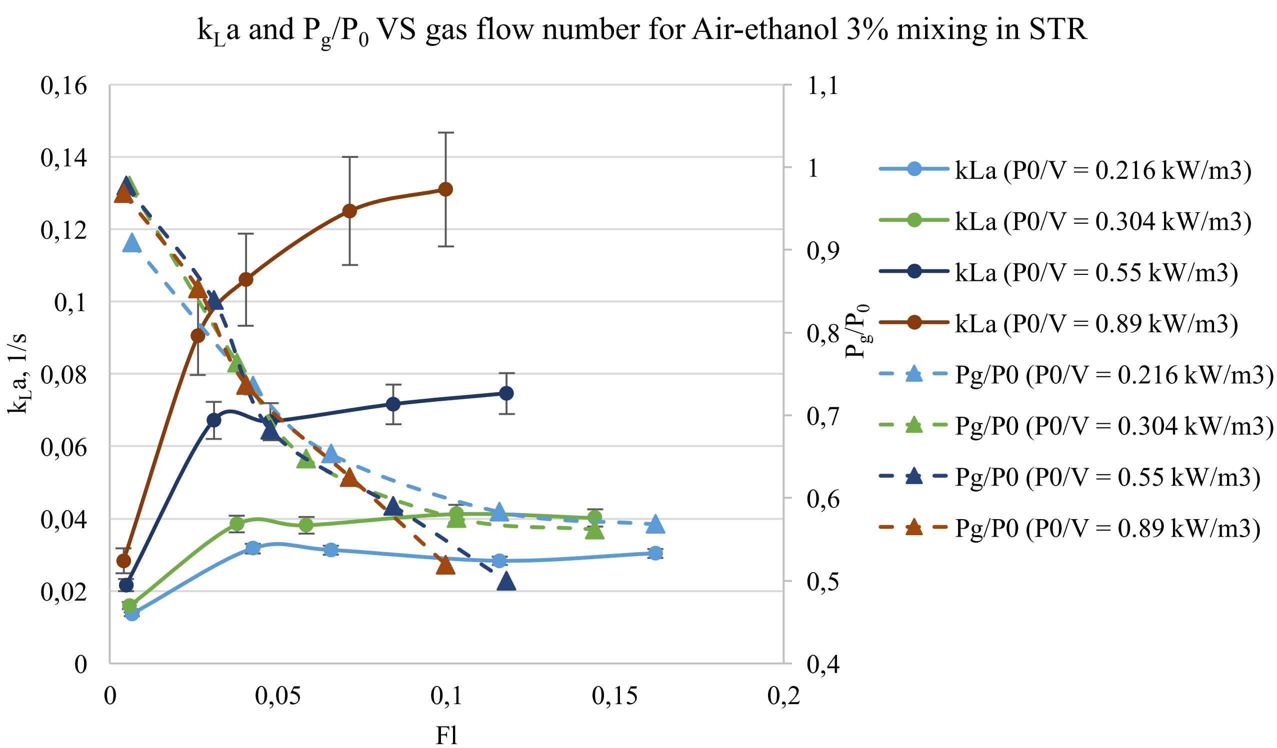

Figure A-8. Flooding for air - CMC 0.05 % mixing in STR.

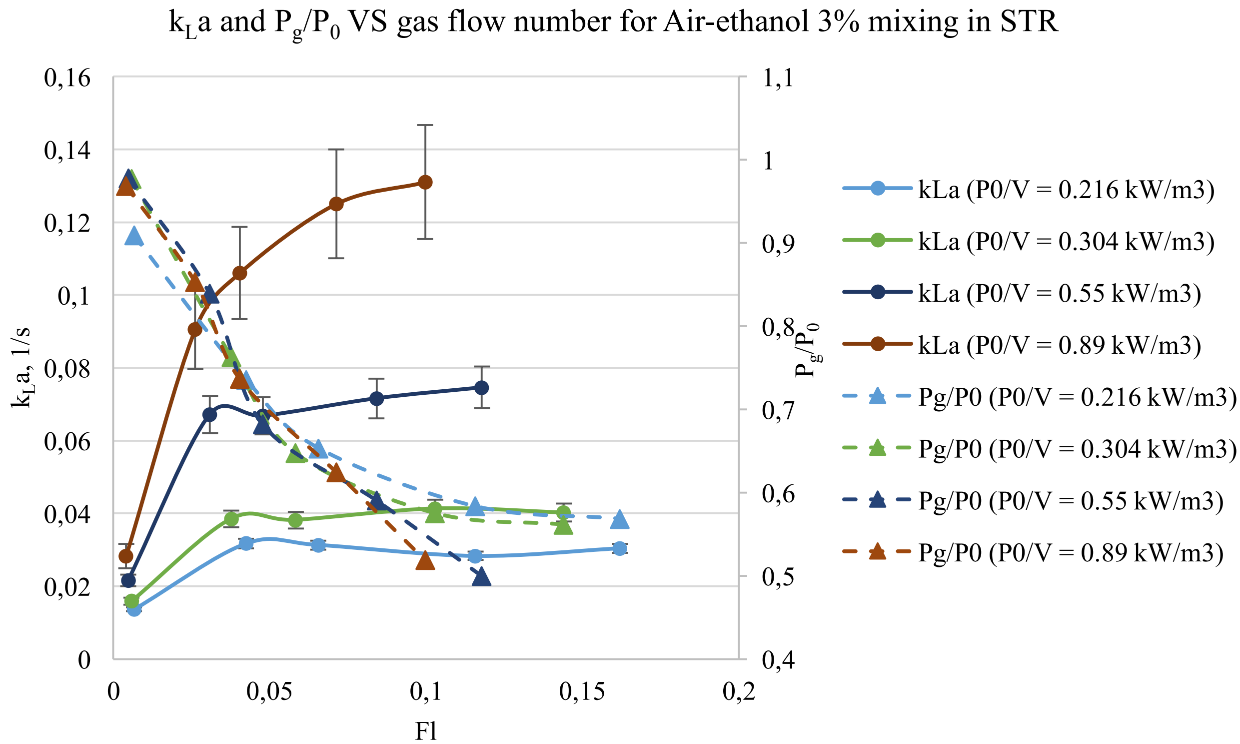

Figure A-9. Flooding for air - CMC 0.15 % mixing in STR.

Appendix IV: Calculations examples

OKTOP mixing power for water solution with impeller speed 400 rpm was determined using equation (32):

$$\frac{P}{V} = \frac{1.93}{0.0135} = 133\frac{W}{m^3} = 0.133\frac{kW}{m^3},$$

where 1.93 W - measured non-aerated power draw; 0.0135 m^3 - reactor volume.

Flooding in OKTOP reactor for water solution with impeller speed 400 rpm and gas flow rate 1 L/min was determined:

$$Fl = \frac{0.000017}{6.67 \cdot 0.073^3} = 0.00655,$$

where 0.000017 m^3/s - volumetric gas flow rate; 6.67 rps - impeller rotation speed; 0.073 m - impeller diameter.

Total power input in OKTOP reactor for water solution with impeller speed 400 rpm and gas flow rate 1 L/min was determined using equation (17), but P_{tot} was divided on volume:

$$\frac{P_{tot}}{V} = \frac{1.776}{0.0135} + \frac{0.000017}{0.1^2 \cdot 3.14} \cdot 1000 \cdot 9.81 = 136.9\frac{W}{m^3},$$

where 1.776 W - measured aerated power; 0.1 m - radius of reactor; 1000 kg/m^3 - liquid density.

Appendix V: Rheology of CMC solutions

Table A-9. CMC solutions rheology.

Reactor	γ, 1/s	μ, N·m
CMC 0.05 %		
ARL	29.24516869	0.0112
	82.13166032	0.00912
	104.4864	0.00861
	143.0444237	0.00814
	172.2981246	0.00789
OKTOP	111.7706051	0.00867
	135.5104773	0.00814
	180.6646321	0.00786
	246.5029891	0.00735
	116.0757951	0.00853
	138.9625516	0.00814
	179.127503	0.00769
	236.1880982	0.00737
	123.1288135	0.00827
	144.3419272	0.00818
	176.6807167	0.00771
	234.3633276	0.00737
	142.7736994	0.00814
	154.8476998	0.00801
	191.4397852	0.00781
	224.5825267	0.00744
	157.8336993	0.00799
	168.1460568	0.00787
	197.5608167	0.00767
	236.3689187	0.00737
STR	150.9320659	0.00804
	182.9226932	0.00769
	251.7852745	0.00727
	330.7782131	0.00708
	134.2558628	0.00835
	163.9050328	0.00795
	227.6294407	0.0074
	292.3269161	0.00715
	138.326054	0.00828
	161.7792984	0.00791
	219.3534058	0.00742
	286.6595636	0.00701
	151.6878392	0.00802
	166.1344316	0.00785
	218.2232418	0.00747
	272.8704279	0.0072
	162.7137009	0.00795
	178.3813397	0.00789
	213.7712823	0.00743
	263.7652744	0.00722

Reactor	γ, 1/s	μ, N·m
CMC 0.15 %		
ARL	13.3032083	0.051
	40.27173216	0.0386
	52.13707008	0.0357
	73.02477276	0.0322
	89.15627752	0.0302
OKTOP	59.276105	0.0344
	66.68569232	0.0331
	93.46879932	0.0298
	128.5317582	0.0267
	61.43424901	0.0341
	67.91349544	0.0329
	92.07479608	0.0299
	120.8514251	0.0272
	61.2923096	0.0341
	72.43579084	0.0323
	90.32148832	0.0301
	118.6139571	0.0272
	72.2734794	0.0323
	81.62282884	0.0311
	98.07098181	0.0291
	118.6806174	0.0272
	80.64908739	0.0311
	87.05596107	0.0304
	104.9978846	0.0286
	125.2957362	0.0268
STR	78.96459552	0.0314
	97.67758771	0.0291
	134.3163468	0.0262
	178.2621978	0.0236
	68.59206585	0.0327
	83.17714557	0.0308
	119.9387439	0.0272
	156.2646925	0.0249
	69.83449754	0.0326
	82.54160069	0.031
	122.2096536	0.0272
	158.0471487	0.0248
	77.77530162	0.0315
	85.81520779	0.0306
	114.8306247	0.0276
	146.0479111	0.0255
	84.96198522	0.0306
	93.33871809	0.0298
	112.908413	0.0277
	141.8383077	0.0258